学位論文

Physiological studies on neuromodulation of sensory system by peptidergic neurons

(感覚情報処理回路におけるペプチドニューロンを介した神経修飾機構の研究)

平成 27 年 12 月博士（理学）申請

東京大学大学院理学系研究科

生物科学専攻

馬谷　千恵

Table of Contents

Abbreviations ---------- p. 1

Abstract ---------- p. 2

General introduction ---------- p. 5

Chapter 1 ---------- p. 11
Analysis on a novel modulator of firing activities in TN-GnRH3 neurons

Chapter 2 ---------- p. 42
Synaptically induced high frequency firing and neuropeptide release of TN-GnRH3 neurons

Chapter 3 ---------- p. 76
GnRH3-induced neuromodulation in optic tectum, where axon of TN-GnRH3 neurons project

General discussion ---------- p. 111

Acknowledgements ---------- p. 122

Reference ---------- p. 123

Abbreviations

TN-GnRH3 neuron terminal nerve – gonadotropin releasing hormone 3 neuron

RFRP RFamide related peptide

NPFF neuropeptide FF

GABA γ-aminobutyric acid

ACh acetylcholine

TRPC channel Transient Receptor Potential-Canonical channel

SPV stratum periventriculare of optic tectum

ACSF artificial cerebrospinal fluid

Abstract

Animals change their behavior in response to sensory cues in the environment as well as their physiological status of their own. However, the neural mechanisms on how such information from the environment and the intrinsic physiological status of the animal are integrated and modulate their behaviors still remain unknown. It is generally accepted that such changes in behaviors are induced by modulations of neural activities in the brain. Although neural activities are modulated by various molecules, neuropeptides have been suggested to play important roles in such modulation. Therefore, I assumed that peptidergic neurons may play a key role in the integration of information from the environment and the physiological status, and the regulation of such changes in behaviors accordingly. To analyze the mechanisms of such behavioral modulation, I focused on the terminal nerve gonadotropin releasing hormone neurons (TN-GnRH3) neurons. The TN-GnRH3 neurons have been suggested to show many characteristic morphological and physiological properties relevant for a neuromodulator; they show spontaneous regular pacemaker activity and project widely in the brain. In the present thesis, I aimed at understanding neuromodulatory functions of TN-GnRH3 neurons in the following three chapters. First, in Chapter 1, I examined inputs to the TN-GnRH3 neurons and found a novel modulator of spontaneous activity, RFRP. I showed that RFRP suppresses the frequency of pacemaker activities of TN-GnRH3 neurons directly via multiple ion channels and thus may modify neuromodulatory actions of the TN-GnRH3 neurons. Second, in Chapter 2, I found that the TN-GnRH3 neurons in

both adult and juvenile are capable of firing at high frequency and thus of releasing neuropeptide such as GnRH3 in response to glutamatergic and GABAergic synaptic inputs, both of which are excitatory to the TN-GnRH3 neurons. This can be the basis for the trigger of effective GnRH3 neuromodulatory peptide release. Finally, in Chapter 3, I examined the output of TN-GnRH3 neurons to know how the GnRH3 peptides, which is expressed in TN-GnRH3 neurons, modulate neurons in the target brain region. I demonstrated that GnRH3 modulates the retino-tectal neurotransmission in the optic tectum, which is important for visual processing. Here, GnRH3 was suggested to induce neuromodulation by suppressing postsynaptic neuron for the retino-tectal neurotransmission in the optic tectum via activating a kind of K^+ channels, called BK channel.

Thus, in my thesis I have demonstrated 1) a novel type of modulation by RFRP of spontaneous firing activities of TN-GnRH3 neuron, which is important for their neuromodulatory functions, 2) the mechanism of synaptically evoked high-frequency firing of TN-GnRH3 neuron that should be sufficient for triggering the neuromodulatory GnRH3 peptide release, and 3) the mechanisms of subsequent GnRH3-induced neuromodulation in the target brain region. From the results of the present thesis, the TN-GnRH3 peptidergic neurons are suggested to play an important role in the integration of sensory information from the environment and the intrinsic physiological status of the animal, modulate neural activities in the target brain regions, and bring about adaptive changes in behaviors.

General introduction

Animals change their behavior in response to sensory cues in the environment as well as the physiological status of their own. For example, various behaviors are modulated by stress (de Kloet et al. 2005), and some social behaviors such as schooling and sexual behaviors (Iwamatsu 2006) are modulated by various sensory cues in the environment, such as the temperature, day length, and so on. However, the neural mechanisms on how such information from the environment and the intrinsic physiological status of the animal are integrated and modulate their behaviors still remain debatable. It is generally accepted that such behavioral changes are induced by modulations of neural activities in the brain (generally called "neuromodulation"). Although neural activities are known to be modulated by various molecules (generally called "neuromodulators"), it has been proposed by various literature that neuropeptides play important roles in such "neuromodulation" (Argiolas and Melis 2013; Dornan and Malsbury 1989; van den Pol 2012). In the processes of such modulations, especially, physiological mechanism of neuromodulation through neuropeptide remains unknown.

To analyze the neural mechanisms of behavioral modulation through peptidergic neurons, I focused on the terminal nerve gonadotropin releasing hormone neurons (TN-GnRH3) neurons. The reasons are the following: 1) TN-GnRH3 neurons show spontaneous pacemaker activities in low frequency and fire in synchrony with each other through gap junctions and auto/paracrine release of neuropeptide (GnRH3, NPFF) (Abe and Oka 2011; Karigo and Oka 2013). 2) Each TN-

GnRH3 neuron projects broadly to brain regions related to behaviors and sensory system. Thus, TN-GnRH3 neurons may modulate multiple neural activities extensively at the same time (Abe and Oka 2011; Karigo and Oka 2013). 3) TN-GnRH3 neurons have been rather well studied as a peptidergic neuromodulator in their projection areas. For example, GnRH3 peptide has been suggested to show neuromodulatory effects on the olfactory receptor neurons and the synaptic transmission in the olfactory bulb (Eisthen et al. 2000; Kawai et al. 2010). 4) TN-GnRH3 neurons receive various inputs from sensory processing areas such as olfactory, visual, and somatosensory (Yamamoto et al., 2000). Based on these previous studies, I assumed that TN-GnRH3 neuron is an excellent model for the study of functions of the "peptidergic modulatory neurons". I hypothesized that the TN-GnRH3 neurons receive multimodal sensory information from the environment and the intrinsic physiological status, which changes the spontaneous activity of the TN-GnRH3 neurons and release GnRH3 peptides accordingly. The GnRH3 peptide thus released modulates activities of neurons in the target brain regions including sensory information processing areas such as the optic tectum, olfactory bulb, etc., and finally changes the behavioral pattern generator circuit. Thus, animals can change their behavior adaptively in response to sensory cues in the environment as well as the physiological status of their own by the neural mechanisms, and the TN-GnRH3 neurons play pivotal roles during this process (Fig. 0).

In the present thesis, I aimed at comprehensive understanding of the mechanisms of

neuromodulation by TN-GnRH3 neuron in the brain, which is one of peptidergic neurons that can induce modulation of behaviors depending on surrounding environment and physiological status. I chose teleost animal models in my thesis because of the wealth of literature on TN-GnRH3 neurons in teleost fishes and their advantage for experiments in which we can keep the neural circuit almost intact by using the whole-brain in vitro preparations. Toward this goal, I organized my thesis in the following three Chapters. In Chapter 1, I focused on the neural inputs to the TN-GnRH3 neurons that should change their spontaneous pacemaker activities, which are important for their neuromodulatory functions, and found a novel inhibitory peptidergic neuromodulator, RFRP. I examined the mechanisms of its action in detail by electrophysiological methods. In Chapter 2, I analyzed the relationship between neural activities and neuropeptide release of TN-GnRH3 neurons and found that the TN-GnRH3 neurons in both adult and juvenile medaka are capable of firing at high frequency and thus of releasing neuropeptide in response to various synaptic inputs, such as glutamate and GABA. Finally, In Chapter 3, I examined the output of TN-GnRH3 neurons in the target brain region, the optic tectum, to understand how GnRH3 peptides, which is expressed in TN-GnRH3 neurons, modulate neurons in the target brain regions. I showed that GnRH3 modulates retino-tectal neurotransmission in the optic tectum, which is important for visual processing.

Figure legend

Figure 0 Working hypothesis for the present study. The TN-GnRH3 neurons receive multimodal sensory information from the environment and the intrinsic physiological status and release GnRH3 peptides accordingly, modulate activities of neurons in the target brain regions including behavior pattern generator circuit, and finally induce changes in behaviors.

Figure 0

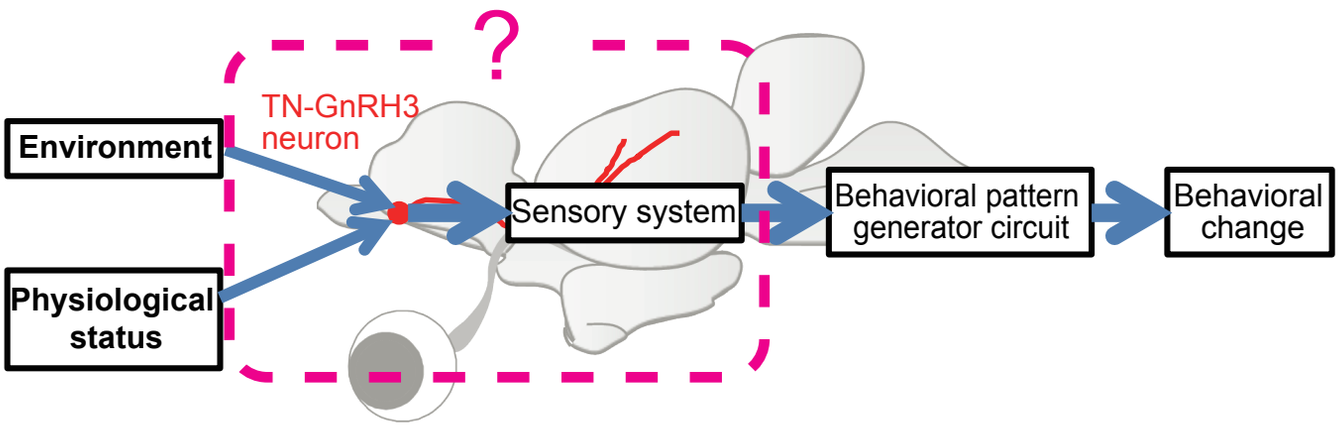
?
TN-GnRH3
neuron
Environment
Physiological
status
Sensory system
Behavioral pattern
generator circuit
Behavioral
change

Chapter 1

A novel modulator of spontaneous firing activities of TN-GnRH3 neurons

Abstract

The terminal nerve gonadotropin-releasing hormone 3 (TN-GnRH3) neurons receive various sensory and other information from a variety of neurons and express GnRH3 peptides, which are suggested to modulate neural activities in wide areas of the brain. GnRH3 has been suggested to be released, depending on the spontaneous firing activities of TN-GnRH3 neurons. Therefore, to understand the neuromodulatory action of TN-GnRH3 neuron, it is important to know the regulatory mechanisms of the spontaneous firing activities of TN-GnRH3 neurons. Previous studies have identified several different neural inputs to TN-GnRH3 neurons: excitatory modulators, GnRH3 (autocrine/ paracrine), glutamate and GABA (synaptic), or inhibitory modulators, NPFF (autocrine/ paracrine) and ACh (synaptic). In Chapter 1, I newly found that neuropeptide RFRP functions as an inhibitory synaptic modulator.

RFamide-related peptide (RFRP) is a member of the RF amide (Arg-Phe-amide) family of peptides. Neuroanatomical evidence has demonstrated that RFRP neurons in the hypothalamus project to the close vicinity of TN-GnRH3 neurons in medaka. Therefore, RFRP was suggested to be a candidate new neuromodulator of TN-GnRH3 neurons. In the present study, I examined the effects of RFRP peptide on the firing activity of TN-GnRH3 neurons by using whole cell patch clamp recording. I showed that RFRP inhibits the firing activities of TN-GnRH3 neurons by changing conductances for K^+ and Na^+, which may arise from the closure of TRPC channels and the opening of voltage-independent (leak) K^+ channels. This novel pathway may be considered

as a negative regulator of reproductive behaviors.

Introduction

The TN-GnRH3 neurons receive various sensory information such as physiological status of the animal (Kawai et al. 2013; Yamamoto and Ito 2000) and express GnRH3 peptide (Oka and Matsushima 1993). Previous studies have suggested that the quantity of GnRH3 peptide released in the brain is closely related to the firing rate of the TN-GnRH3 neurons (Ishizaki et al. 2004). GnRH peptide has been reported to modulate the opening of ion channels such as K^+ channels in the dorsal root ganglia (Adams and Brown 1980) and the activity of voltage-gated sodium currents in the olfactory epithelium (Eisthen et al. 2000), as well as ionotropic glutamate receptors in the hippocampus (Yang et al. 1999). Taken together, these cellular physiological and behavioral studies suggest that the firing rate of TN-GnRH3 neurons regulates the release of GnRH3 peptide, changings the excitability of the target neurons and therefore modulating animal's behavior by controlling motivational or arousal state (Abe and Oka 2006; Oka 2002).

Previous studies have identified several neural inputs that modulate spontaneous firing of TN-GnRH3 neurons: excitatory modulators, GnRH3 (autocrine/ paracrine) (Abe and Oka 2000), glutamate (Kiya and Oka 2003), and GABA (synaptic) (Nakane and Oka 2010), or inhibitory modulators, neuropeptide FF (NPFF) (autocrine/ paracrine) (Saito et al. 2010), and ACh (synaptic) (Kawai et al. 2013). In Chapter 1, I newly found that neuropeptide RFRP functions as an inhibitory synaptic modulator.

RFRP is a member of the RF amide (Arg-Phe-amide) family of peptides. Neuroanatomical

evidence has demonstrated that RFRP neurons in the hypothalamus project to the close vicinity of TN-GnRH3 neurons in medaka (Matsumoto et al. 2006). The metastin (=kisspeptin) immunoreactive neurons and fibers described therein were recently identified as RFRP-immunoreactive. However, it has not been clarified yet whether RFRP affects the activity of non-hypophysiotropic or modulatory GnRH neurons such as TN-GnRH3 neurons. In the present Chapter, I examined the effects of RFRP peptide on the pacemaker activity of TN-GnRH3 neurons by using whole cell patch clamp recording. I showed that RFRP inhibits the pacemaker activities of TN-GnRH3 neurons by changing K^+ and Na^+ conductances, which may arise from the closure of TRPC channels and the opening of voltage-independent (leak) K^+ channels.

Material and Methods

Adult male and female dwarf gouramis (*Trichogaster lalius*; n = 200 fish), ~4 cm in standard length, were purchased from a local dealer. Each aquarium containing ~20 fish was maintained at 27°C on a 14:10 light:dark cycle. The fish were fed with worms daily. All procedures were performed in accordance with the guideline principles for the care and use of experimental animals established by the Physiological Society of Japan and the University of Tokyo.

Electrophysiology

For the electrophysiological experiments, the fish were chilled by immersing them in crushed ice and quickly killed by decapitation. After careful removal of ventral meningeal membranes, the olfactory bulbs and telencephalons were separated from the rest of the brain, and the dorsal telencephalon was manually cut out with razor blades in an artificial cerebrospinal fluid (ACSF) consisting of (in mM) 140 NaCl, 5.0 KCl, 1 $MgCl_2$, 1.5 $CaCl_2$, 10 HEPES, and 10 glucose (pH 7.4 adjusted with NaOH). This 'brain block' containing the olfactory bulb and ventral telencephalon was then placed ventral side up in a hand-made recording chamber and continuously perfused with ACSF. All the experiments were performed at room temperature (20–24°C). Patch pipette solution contained (in mM) 130 KCl, 3 $MgCl_2$, 10 HEPES, 0.4 EGTA, and 2 Na_2-ATP (pH 7.4 adjusted with KOH). Patch electrodes were made of borosilicate glass (G-1.5, Narishige, Tokyo, Japan) using a Flaming-Brown micropipette puller (P-97; Sutter Instruments, Novato, CA). The tip resistance of patch electrodes in ACSF was 4–7 MΩ. Because the liquid

junction potential was so small and negligible (c.a. 1.2 mV), I did not compensate for it. In my preparations, TN-GnRH3 neurons of dwarf gouramis form a morphologically distinct neuronal cluster immediately beneath the ventral meningeal membrane (Oka and Ichikawa 1991), and they can be easily identified under a dissecting microscope or microscopes equipped with differential interference optics (Abe and Oka 2006; Abe and Oka 2009; Oka 2002; Oka and Matsushima 1993). The patch pipette was visually guided to the cluster of TN-GnRH3 neurons, located on the ventral surface of the transitional area between the olfactory bulb and the telencephalon under an upright microscope (E-600FN, Nikon, Tokyo, Japan) equipped with a 40× water-immersion objective lens (0.8 numerical aperture), infrared (IR) differential interference contrast optics, and an IR-CCD camera (C3077-78, Hamamatsu photonics, Hamamatsu, Japan). All recordings were performed with an Axopatch 200B patch-clamp amplifier (Molecular Devices, Sunnyvale, CA). Whole cell voltage- and current-clamp recordings were digitized (2 k and 10 kHz, respectively) and stored on a computer using the Digidata 1322A and pCLAMP 9.2 software (Molecular Devices, Sunnyvale, CA). After gigaohm seal formation and "break in" for whole cell recording, characteristic spontaneous pacemaker activities were confirmed in current-clamp mode. The membrane resistance and capacitance of these neurons measured 83.0 ± 25.3 MΩ and 184.1 ± 53.2 pF, respectively (n = 5). During the whole recording periods of ramp stimulation experiment procedures, the baseline changes of the current responses were also monitored at 1 kHz using

MiniDigi 1A and pCLAMP 9.2 software (Molecular Devices, Sunnyvale, CA). I assessed the quality and stability of all recordings by applying hyperpolarizing step pulses (from -60 mV to -80 mV, 1.5s) before each ramp protocol to confirm that the membrane conductance had not changed.

Drugs

Drugs were dissolved in ACSF and used as follows: RF9 (10 μM, Sigma-Aldrich, St. Louis, MO), tetrodotoxin (TTX; 0.75 μM, Sigma-Aldrich, St. Louis, MO), 4-aminopyridine (4-AP; 5 mM, Wako, Osaka, Japan), Tetraethylammonium (TEA; 20mM, Sigma-Aldrich, St. Louis, MO), LaCl3 (100 μM, Wako, Osaka, Japan), and 2-aminoethoxydiphenyl borate (2-APB; 100μM, Merck KGaA, Darmstadt, Germany). Peptides corresponding to medaka RFRP1 (SLDLESFNIRVTPTSSKLNLPTIIKLYPPTAKPLHMHANMPLRF-NH_2), RFRP2 (VSNSSPNMPQRF-NH_2), and RFRP3 (SVREAPSPVLPQRF-NH_2) were synthesized by GL Biochem. (Shanghai, China) and used at 0.01 to 2.5 μM. Prior to RFRP applications, bovine serum albumin (0.1 %, 1 ~ 2 min; Sigma-Aldrich, St. Louis, MO) was perfused over the cells to prevent nonspecific binding of the peptides.

Statics

Statistical analyses were performed by the Kyplot5 software (Kyence, Tokyo, Japan) and the

Igor Pro 6 software (WaveMetrics Inc., Lake Oswego, OR, USA) with Taro tool (Igor macro set written by Dr. Taro Ishikawa, Jikei University School of Medicine). Different statistical tests were used for different experiments, as described in the Results and Figure legends. All data in the present study are presented as mean ± S.E.M

Results

RFRP2 inhibits the pacemaker activity of TN-GnRH3 neurons

The regular spontaneous pacemaker activity of TN-GnRH3 neurons was inhibited by bath application of RFRP2 peptide. Fig. 1-1A illustrates the inhibition of pacemaker activity by RFRP2 (1 μM). In normal ACSF, TN-GnRH3 neurons showed regular pacemaker activity (6.3 ± 0.4 Hz, n = 5). The firing frequency of this pacemaker activity was gradually decreased by bath application of RFRP2, and firing was completely inhibited about 2 min after the onset of RFRP2 application. This inhibitory effect of RFRP2 on the pacemaker activity was accompanied by hyperpolarization of membrane potentials (-20.7 ± 0.3 mV, n = 5). After the end of RFRP2 perfusion, the pacemaker activity of TN-GnRH3 neuron showed an almost complete recovery to its original level.

Many vertebrates possess three forms of RFRP (RFRP1-3), and the three kinds of RFRP peptides in teleosts are processed from the same precursor molecule (Hinuma et al. 2000). To identify the RFRP peptide that inhibits the pacemaker activity of TN-GnRH3 neurons, I compared the normalized decrease in firing frequency of pacemaker activity by each kind of RFRP peptide at a concentration of 1 μM (Fig. 1-1B). The normalized decrease in firing frequency was defined as

$\text{Frequency}_{(RFRP+)} / \text{Frequency}_{(RFRP-)} \times 100$ (%).

The frequency was calculated from the number of spikes during 0.4 min periods, counted around 1.5 min before and after the onset of RFRP application (RFRP- and RFRP+, respectively). In Fig.1B, lower normalized frequency indicates stronger inhibition of the pacemaker activity. Among the three types of RFRPs, only RFRP2 application significantly decreased the firing frequency of TN-GnRH3 neurons [100.1 ± 2.0 % (vehicle; n = 5) versus 102.8 ± 1.8 % (+RFRP1; n = 6; n.s.), 33.6 ± 12.7 % (+RFRP2; n = 9; $P < 0.001$), and 83.3 ± 8.1 % (+RFRP3; n = 7; n.s.); Dunnet's multiple comparison test]. I therefore, focused on the effects of RFRP2 in the analysis below. Next, the normalized decrease in firing frequency of pacemaker activity was plotted against the concentration of RFRP2 (Fig. 1-1C). This concentration response curve (Fig. 1C solid line) can be well fitted by the equation

$$R = [RFRP2]^n / (EC_{50}^n + [RFRP2]^n)$$

where R is the normalized decrease in the firing frequency. The EC_{50} of RFRP2 was determined to be 839 nM, and n was 2.07. Since the n value for Hill's equation indicates cooperativity, n = 2.07 here demonstrates that the ligand binding reaction is positively cooperative. Once RFRP2 is bound to the receptor, its affinity for the other RFRP2 molecules may increase. For NPFF binding to GPR74 (NPFFR2), on the other hand, Hill's n is c.a. 1, which suggests that NPFF does not show cooperativity (Gouarderes et al. 1997; Zeng et al. 2003). RFRPs are thus considered to be different from NPFF in not only the binding affinity but also the mode of binding, although they

do bind to the same receptor.

RFRP2 directly inhibits the pacemaker activity of TN-GnRH3 neurons via specific receptors

To elucidate possible mechanisms underlying the RFRP2-induced decrease in firing frequency, I next examined whether RFRP2 directly inhibits pacemaker activities of TN-GnRH3 neurons after blockage of action potential-dependent synaptic inputs from other neurons by TTX application. In the presence of TTX (0.75 μM), RFRP2 reversibly induced hyperpolarization of the membrane potential (-21.3 ± 1.9 mV, n = 6; Fig. 1-2). This result suggests that RFRP2 directly modulates the pacemaker activity of TN-GnRH3 neurons.

To further understand the possible mechanisms of RFRP2-induced inhibition of pacemaker activity, I next examined the effect of RF9, a potent antagonist of GPR147/74, which have been identified as candidate NPFF and RFRP receptors (Simonin et al. 2006). Pretreatment with RF9 (10 μM) blocked the inhibitory action of RFRP2 peptide (1 μM) on the pacemaker activity of TN-GnRH3 neurons (Fig. 1-3A and B). In normal ACSF, TN-GnRH3 neurons showed a regular beating discharge pattern (5.5 ± 0.4 Hz; Fig. 1-3Ba). Prior perfusion of RF9 alone did not affect firing activity (Fig. 1-3Bb). In the presence of RF9 (10 μM), the inhibitory effect of RFRP2 (1 μM) was clearly diminished (Fig. 1-3Bc). The decrease in firing frequency was significantly diminished by RF9 [Fig. 1-3C; 71.4 ± 6.0 % (n = 6) by RFRP2 with RF9 vs. 100.1 ± 2.0 % (n =

5) by vehicle; n.s.]. RF9 alone did not decrease the firing frequency of TN-GnRH3 neurons [98.0 ± 2.9 %, n = 6, vs. vehicle; n.s.]. These results suggest that the inhibitory effects of RFRP2 on pacemaker activity of TN-GnRH3 neurons are mediated by GPR 147/74.

RFRP2 modifies multiple ion conductances in TN-GnRH3 neurons

To examine the ionic mechanisms of RFRP2-induced hyperpolarization of TN-GnRH3 neurons, I recorded changes in the membrane current at a holding potential of -60 mV in the presence of TTX using whole-cell patch-clamp recordings (Fig. 1-4A). Perfusion of a supramaximal concentration of RFRP2 (2.5 μM) reversibly induced outward current responses (183.9 ± 21.5 pA; n = 6). Before and during RFRP2 application (Fig. 1-4A dashed vs solid boxes), I recorded currents in response to slow voltage ramps (Fig. 1-4B) to determine which ionic permeability contributes to the current changes induced by RFRP2. In this experiment, I depolarized TN-GnRH3 neurons from -60 to -10 mV for 1.5 s before applying a voltage ramp to inactivate the voltage-gated calcium channels: the falling phase of the voltage ramp, from -10 to -110 mV during 1.5 s period, was used for plotting the current-voltage (I/V) relationship (dashed rectangle in Fig. 1-4B). The I/V relationships before RFRP2 (dotted curves) and during RFRP2 perfusion (solid curves) under various extracellular ionic concentrations are shown in Fig. 1-4C. From the intersection of two I/V curves, I determined the reversal potential for the RFRP2-induced current. In normal ACSF ($[K^+]_o$ = 5 mM), the recorded reversal potential was -38.0 ± 2.0

mV (*n* = 6; Fig. 1-4Cb and D). This value is far from the theoretical equilibrium potentials for K^+ (-82.0 mV) and Na^+ (+89.6 mV) calculated using the Nernst equation, and instead suggests that RFRP2 changes permeability for multiple ionic species. I therefore, identified the ions comprising the RFRP2-induced current by changing the extracellular concentrations for K^+, Na^+ and Ca^{2+}.

At different extracellular K^+ concentrations ($[K^+]_o$; 1 and 20 mM), the reversal potentials for RFRP2-induced currents were -51.0 ± 3.7 (Fig. 1-4Ca, n = 5) and -13.0 ± 0.7 mV (Fig. 1-4Cc, n = 5), respectively. Similarly, a decrease in extracellular Na^+ concentration shifted the reversal potentials of RFRP2-induced currents (-59.7 ± 2.9 and -49.0 ± 1.5 mV in 46 and 70 mM $[Na^+]_o$; n = 5 for both; Fig. 1-4Cd and e, respectively). When these reversal potentials were plotted as a function of $[K^+]_o$ or $[Na^+]_o$, the relations could be well fitted by straight lines predicted from the Nernst equation for K^+ or Na^+ (Fig. 1-4D; 58 mV per log unit changes, r^2 = 0.95 and 0.99 for K^+ (○) and Na^+(■), respectively). However, changing extracellular Ca^{2+} concentrations did not shift the reversal potential (-38.0 ± 2.0 and -40.7 ± 2.7 mV in 1.5 and 6 mM $[Ca^{2+}]_o$, n = 6 and 5, n.s. by Student's t-test; Fig. 1-4Ca and f, and ◊ in Fig. 1-4D), suggesting that RFRP2 changes permeability for both K^+ and Na^+, but not for Ca^{2+}.

RFRP2 modulates both TRPC and voltage-independent K^+ currents

Because RFRP2 changed the permeability of both Na^+ and K^+, I searched for ionic current(s) that are sensitive to RFRP2 application. Subtraction of the ramp current responses recorded during

RFRP2 application from those obtained before the application (Fig. 1-5Aa, dotted and solid curves, respectively) yielded an I/V relationship for the net RFRP2-sensitive current (Fig. 1-5Ab). The obtained I/V relationship exhibited a region of negative slope conductance from -110 to -70 mV, outward rectification, and a reversal potential at ~ -40 mV. This I/V relationship suggests that RFRP2 blocks an inward current at the physiological membrane potential (-40 ~ -60 mV) of TN-GnRH3 neurons.

To elucidate the identity of this RFRP2-sensitive current, I next recorded current responses before and during RFRP2 application in the presence of La^{3+} (an antagonist of TRPC1, 3, 6 and 7 and agonist of TRPC4 and 5; 100 μM) or 2-APB (an antagonist of TRPC3, 4, 5 and 6; 200 μM). Figures 1-5C and D show subtraction of the current responses recorded before RFRP2 application from those obtained during the application in the presence of La^{3+} and 2-APB, respectively. The addition of La^{3+} shifted the reversal potential of the RFRP2-sensitive current from -38.0 ± 2.0 to -83.4 ± 3.4 mV (n = 8; Fig. 1-5C and F), and the addition of 2-APB resulted in a shift of -90.6 ± 7.2 mV (n = 5; Fig. 1-5D and F). These plots showed nearly linear I/V relationships with polarities that reversed around the theoretical equilibrium potential for K^+ (-82.0 mV). In addition, I compared the RFRP2-induced current changes at a holding potential of -60 mV (Fig. 1-5G). La^{3+} and 2-APB significantly decreased the amplitude of RFRP2-induced changes in the holding current (183.9 ± 21.5 pA in normal ACSF vs. 76.0 ± 16.2 pA in La^{3+} or 71.2 ± 13.3 pA in 2-APB;

n = 6, 8 and 5; $p < 0.001$ and $p < 0.01$, respectively). These results suggest that RFRP2 in the presence of La^{3+} or 2-APB increased the magnitude of a K^+ current that has no voltage dependence, because RFRP2 still induced changes in the holding current and its reversal potential was near the theoretical equilibrium potential for K^+. To confirm the presence of a voltage-independent K^+ current, I next recorded current responses in response to the same voltage ramp in the presence of 0.1 mM Ba^{2+}, which serves as a less-selective blocker of the voltage-independent K^+ currents (= leak K^+ currents). In this experiment, the reversal potential for the RFRP2-induced current was changed from -38.0 ± 2.0 mV to -12.9 ± 5.5 mV (Fig. 1-5E and F), and the subtraction of the current responses recorded during RFRP2 application from those obtained before the application exhibited a constant inward current region from -110 to -60 mV (Fig. 1-5E). The shape of the I/V relationship resembles that of the TRPC current (Qiu et al. 2010). Ba^{2+} also reduced the RFRP2-induced increase in the holding current (Fig. 1-5G). However, prior application of 4-AP (5 mM), a classical blocker of voltage dependent K^+ channels, did not change the reversal potential of RFRP2 induced current (-43.3 ± 2.5 mV; Fig. 1-5B and F, n = 7), although 4-AP did decrease the RFRP2-induced current changes at a holding potential of -60 mV (Fig. 1-5G). Furthermore, when TEA (20 mM), another blocker of voltage dependent K^+ channels, was added in either the extracellular or the intracellular solution, the reversal potential for the RFRP2-induced current did not shift (-41.8 ± 7.8 mV with TEA and 5mM 4AP in the extracellular solution,

n = 4; -27.1 ± 6.4 mV with TEA in the intracellular solution, n = 6; both n.s. by Dunnet's test). These results suggest that RFRP2 opens voltage-independent K^+ current(s). Taken together, I conclude that RFRP2 induces both the closure of TRPC current and the opening of voltage-independent K^+ currents.

Discussion

In the present study, I found that RFRP (particularly RFRP2) reversibly inhibits the pacemaker activities of TN-GnRH3 neurons by simultaneously blocking TRPC channels and opening voltage-independent K^+ channels via GPR147/74.

RFRP was discovered during the search for a human RFamide using the rat genome database (Hinuma et al. 2000). Previous studies suggested that RFRP3 inhibits the electrical activities of hypothalamic GnRH1 neurons in mice (Ducret et al. 2009). Recent anatomical observation that RFRP immunoreactive fibers densely project near the TN-GnRH3 neurons in medaka (Matsumoto et al. 2006) led me to my present electrophysiological investigation to determine whether RFRP affects the pacemaker activity of teleost non-hypophysiotropic TN-GnRH3 neurons. To the best of my knowledge, this is the first report that hypothalamic reproduction-related peptide, RFRP, affects the firing activity of non-hypophysiotropic TN-GnRH3 neurons.

The present results suggest that RFRP2 inhibits the TRPC channels and activates voltage-independent K^+ channels. First, La^{3+} and 2-APB, antagonists of TRPC, diminished the change in the permeability of multiple ions in response to RFRP2. Both La^{3+} and 2-APB reduced the increase in the holding current by RFRP2. Because RFRP2 increased the outward current, I deduce that RFRP2 also inhibits TRPC-mediated inward currents. Zhang et al. (2008) reported that kisspeptin, another member of RFamide family of peptides, opens TRPC channels in rat GnRH1 neurons. Together, this study and the present results suggest that kisspeptin and RFRP

reciprocally open / close TRPC current, because both kisspeptin and RFRP change the permeability of Na^+ and K^+ but not Ca^{2+}, and their effect was blocked by TRPC antagonists.

In the presence of La^{3+} or 2-APB, RFRP2 still induced an outward current with a reversal potential close to the equilibrium potential for K^+. This residual RFRP-induced outward current was probably comprised of voltage-independent (= leak) K^+ current(s), because Ba^{2+}, a blocker of voltage-independent K^+ currents (Lesage 2003), shifted the reversal potential of RFRP-induced currents and diminished the increase in the holding current by RFRP2. In addition, 4-AP, a classical voltage-dependent K^+ current blocker, did not inhibit the effect of RFRP2. Therefore, I suggest that RFRP2 decreased TRPC current and increased voltage-independent K^+ currents. This is supported from the fact that: i) the sum of the increase in RFRP2-induced holding current in the presence of La^{3+} and Ba^{2+} was approximately the same as that in normal ACSF, and ii) the shape of the I/V relationship of RFRP2-induced current in normal ACSF was similar to the sum of those in La^{3+} and Ba^{2+}.

How does RFRP modulate voltage-independent K^+ and TRPC currents? It has been suggested that RFRP receptors (GPR147/74) are coupled to Gi proteins (Fukusumi et al. 2006; Mollereau et al. 2002), and some voltage-independent K^+ (KCNK) channels are opened through the activation of Gi by noradrenalin (Xiao et al. 2009). As to the signaling mechanisms for the K^+ conductance modulation, it is interesting to note that serotonin also enhances the opening of leak K^+ channels

called TREK through Gi-coupled receptor signaling (Honore 2007). Here, the physiological level of cAMP is inhibitory to the opening of TREK and the activation of the Gi-coupled receptor diminishes the level of cAMP, which results in the opening of TREK channels, leading to hyperpolarization. Similar mechanisms may apply to the upregulation of voltage-independent K^+ currents by RFRP. In addition, activation of Gi inhibits phospholipase C (PLC; Watkins et al. 1994). Because TRPC channels are known to be activated by PLC (Rasolonjanahary et al. 2002), RFRP2 may inhibit TRPC current via the Gi signaling pathway.

A question arises: what is the physiological significance of the effect of RFRP? As the name implies, TN-GnRH3 neurons release the peptide GnRH3, and the released GnRH3 is suggested to modulate activities of target neurons (Abe and Oka 2011). Thus, TN-GnRH3 neurons are probably responsible for controlling the motivational or arousal state of the animal, including sexual behavior (Yamamoto et al. 1997). In addition, it has been suggested that the firing frequency of TN-GnRH3 neurons plays an important role in controlling the release of GnRH3 peptide (Ishizaki et al. 2004). On the other hand, it has been reported in the rat that the somata of RFRP neurons are located in the dorsomedial nucleus of the hypothalamus and their fibers project widely in the brain (Kriegsfeld et al. 2006). Because RFRP was originally discovered as an inhibitor of gonadotropin release (Tsutsui et al. 2000), many researchers have focused on the mechanisms of RFRP actions on pituitary gonadotropes and the effects of RFRP in its projection

areas in the CNS and neural inputs to the RFRP neurons have not yet been investigated. In previous study, Saito et al. (2010) reported that NPFF, which is also a ligand of GPR147/74, inhibits the pacemaker activity of TN-GnRH3 neurons in an auto- and paracrine manner. Interestingly, the functional role of NPFF peptide in teleosts has not been examined, although NPFF has been reported as one of the mediators of nociceptive stimulus in mammals (Roumy and Zajac 1998). Fujita et al. (1991) performed an in vivo extracellular recording of TN neuronal activity in goldfish and reported that tail pinching (= nociceptive stimulus) induced a decrease in firing frequency of TN-GnRH3 neurons. Previous and the present studies demonstrate that the pacemaker activity of TN-GnRH3 neuron is inhibited by both NPFF and RFRP. In medaka, RFRP immunoreactive cell bodies are located in the hypothalamus, and they densely project their axons near the TN-GnRH3 neurons (Matsumoto et al. 2006). Taken together, it may be possible that RFRP neurons in the hypothalamus function as an integrator of nociception and reproductive status. Here, the changes in the activity of ionic current, whose gating is controlled at subthreshold membrane potentials by TRPC currents or leak K^+ currents, probably contributes to the regulation of the activity of TN-GnRH3 neurons continuously. The present results may at least partially explain the physiological significance of RFRP at the single cell level, which is believed to serve as an interface between the sensory inputs and the motivation for reproductive behaviors. Furthermore, the results of the previous studies suggest that immobilization stress increases RFRP

mRNA expressions in rats (Johnson et al. 2007; Kirby et al. 2009) and in bird brains (Calisi et al. 2008). Further, RFRP neurons express glucocorticoid receptors and receive stress information via glucocorticoids released from the adrenal cortex (Kirby et al. 2009). Moreover, intracerebroventricular (icv) injection of RFRP decreases sexual behavior in mammals (Johnson et al. 2007). Taken together with these studies, I hypothesize that RFRP-induced inhibition of firing in TN-GnRH3 neurons may function as one of the negative motivational signals for sexual behavior by stress.

Figure legends

Figure 1-1 RFRP2 inhibits the pacemaker activity of TN-GnRH3 neurons

A: Bath application of RFRP reversibly inhibited the pacemaker activity of TN-GnRH3 neurons. B: Among the three RFRP peptides, RFRP1-3, only RFRP2 showed a significant decrease in the normalized firing frequency (Dunnet's multiple comparison test; ***: $p < 0.001$). C: Dose-response relationship between RFRP2 concentration and normalized frequency during RFRP2 application. Numbers in parentheses near the filled circles represent the numbers of neurons tested for each RFRP2 concentration. The concentration-response curve was fitted with the Hill equation, and the EC50 was 839 nM.

Figure 1-2 RFRP2 directly inhibits the pacemaker activity of TN-GnRH3 neurons

RFRP2 hyperpolarized the membrane potential of TN-GnRH3 neuron in the presence of 0.75μM TTX. After washout, the membrane potential of TN-GnRH3 neuron recovered to the pre-treatment level (dotted line).

Figure 1-3 RF9 (a potent antagonist of GPR147/74, candidate NPFF and RFRP receptors) diminishes the inhibitory effect of RFRP2

A: In whole cell current clamp recording, prior application of RF9 (10 μM) diminished the inhibitory effect of RFRP2 (1 μM) on pacemaker activity. B: In ACSF, TN-GnRH3 neurons show

a beating discharge pattern (a). Prior application of RF9 alone did not change the firing activity (b). In the presence of RF9, RFRP2 did not show any inhibitory effect on the firing frequency of pacemaker activity (c). C: RFRP2-induced decrease in the normalized frequency was significantly diminished by RF9 (Dunnett's multiple comparison test; ***: $p < 0.001$).

Figure 1-4 RFRP2 changes the membrane permeability for Na^+ and K^+ ions

A: In voltage clamp recording (holding potential = -60 mV), the holding current was increased by RFRP2 perfusion in the presence of 0.75 μM TTX. B: A voltage ramp protocol was applied before (dotted rectangle in A) and during (solid rectangle in A) the application of RFRP2. C: I/V relationships are plotted using the falling phase of the voltage ramp protocol (dotted rectangle in B), while the extracellular concentration of each ion is changed. The I/V relationships before RFRP2 (dotted curves) and during RFRP2 perfusions (solid curves) under various extracellular ionic concentrations are shown. The ionic composition of normal ACSF is $[K^+]$ = 5 mM, $[Na^+]$ = 140 mM and $[Ca^{2+}]$ = 1.5 mM. D: The reversal potentials of RFRP2-induced currents are plotted as logarithmic functions of the extracellular ion concentrations (○ for K^+, ■ for Na^+ and ◊ for Ca^{2+}). The lines indicate the slopes for K^+ (solid line) or Na^+ (dashed line) that were calculated from the Nernst equation.

Figure 1-5 RFRP2 modulates TRPC and voltage-independent K^+ currents

A: I/V relationship of the RFRP2-induced current in normal ACSF. (a) Current responses of a TN-GnRH3 neuron before (dotted line) and during (solid line) RFRP2 application. (b) Subtracted current response during and before RFRP2 applications is used to generate the I/V relationship of net RFRP2-sensitive current. B: The I/V relationship of RFRP2-sensitive current in the presence of 4-AP (5 mM), a blocker of voltage-dependent K^+ channels. It is not changed by 4-AP. C, D: The I/V relationships of RFRP2-sensitive currents in the presence of La^{3+} (100 μM; C) or 2-APB (200 μM; D), antagonists of TRPC1, 3, 6 and7 (La^{3+}) or TRPC 3, 4, 5 and 6 (2-APB). Note that the shape of the I/V relationships indicates no clear rectification in the presence of La^{3+} or 2-APB. E: I/V relationship of RFRP2-sensitive current in the presence of Ba^{2+} (100 μM), a less selective blocker of voltage-independent K^+ channels. Note that the reversal potential becomes more depolarized to ~ -20 mV and the shape of the I/V relationship exhibits a constant inward current region from -110 to -60 mV, resembling the TRPC current. F: The reversal potentials for RFRP2-sensitive current are more depolarized, in comparison with normal, in the presence of Ba^{2+} or are more hyperpolarized in the presence of La^{3+} or 2-APB (Dunnett's multiple comparison test; ** : $p < 0.01$, *** : $p < 0.001$). G: RFRP2-induced outward shift in holding currents is sensitive to 4-AP, Ba^{2+}, La^{3+}, and 2-APB. Each current difference is calculated by subtracting the holding

current before application of RFRP2 from that measured during RFRP2 application (Dunnet's multiple comparison test; * : $p < 0.05$, ** : $p < 0.01$).

Figure 1-1

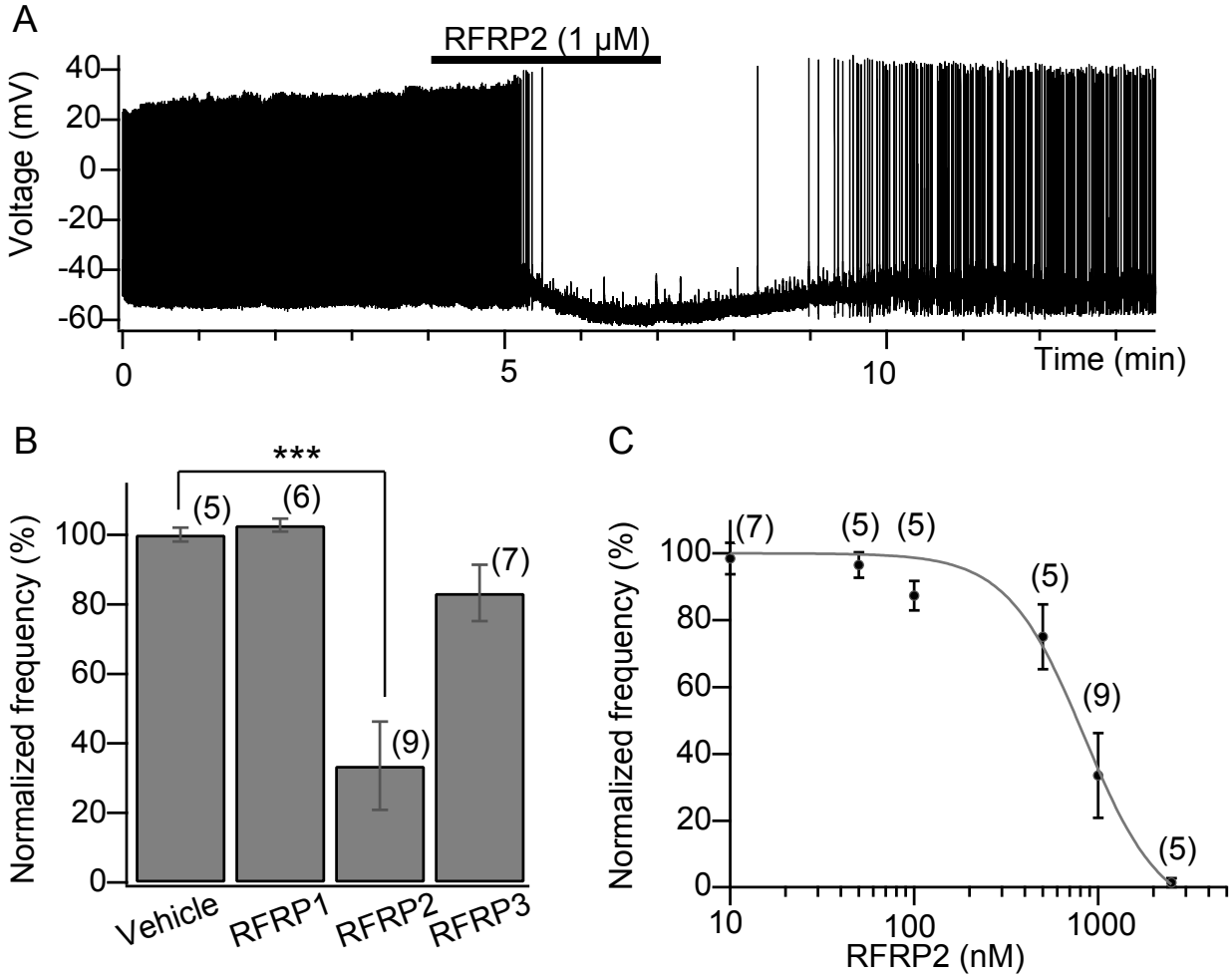
A
RFRP2 (1 μM)
Voltage (mV)
40
20
0
-20
-40
-60
0
5
10
Time (min)
B
***
(5)
(6)
(9)
(7)
Normalized frequency (%)
100
80
60
40
20
0
Vehicle
RFRP1
RFRP2
RFRP3
C
(7)
(5)
(5)
(5)
(9)
(5)
Normalized frequency (%)
100
80
60
40
20
0
10
100
1000
RFRP2 (nM)

Figure 1-2

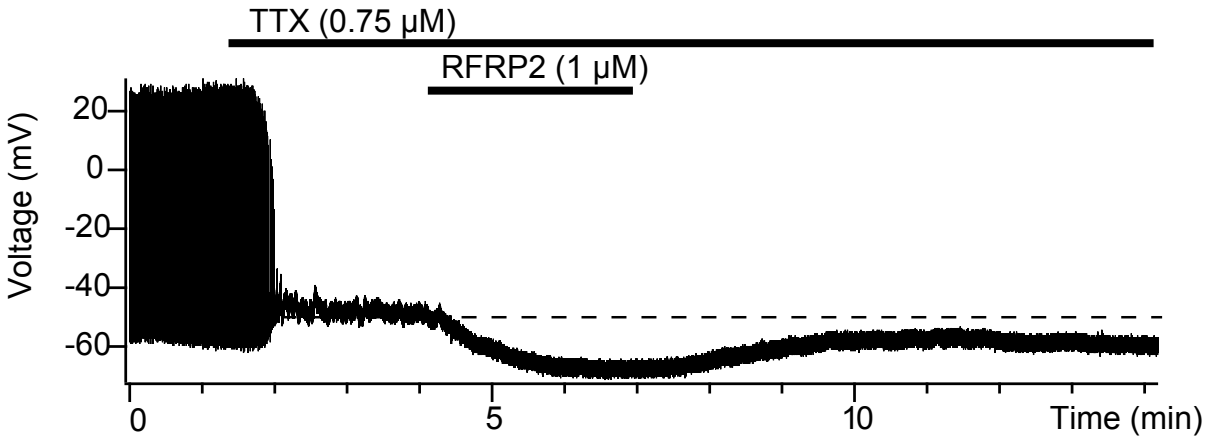

Figure 1-3

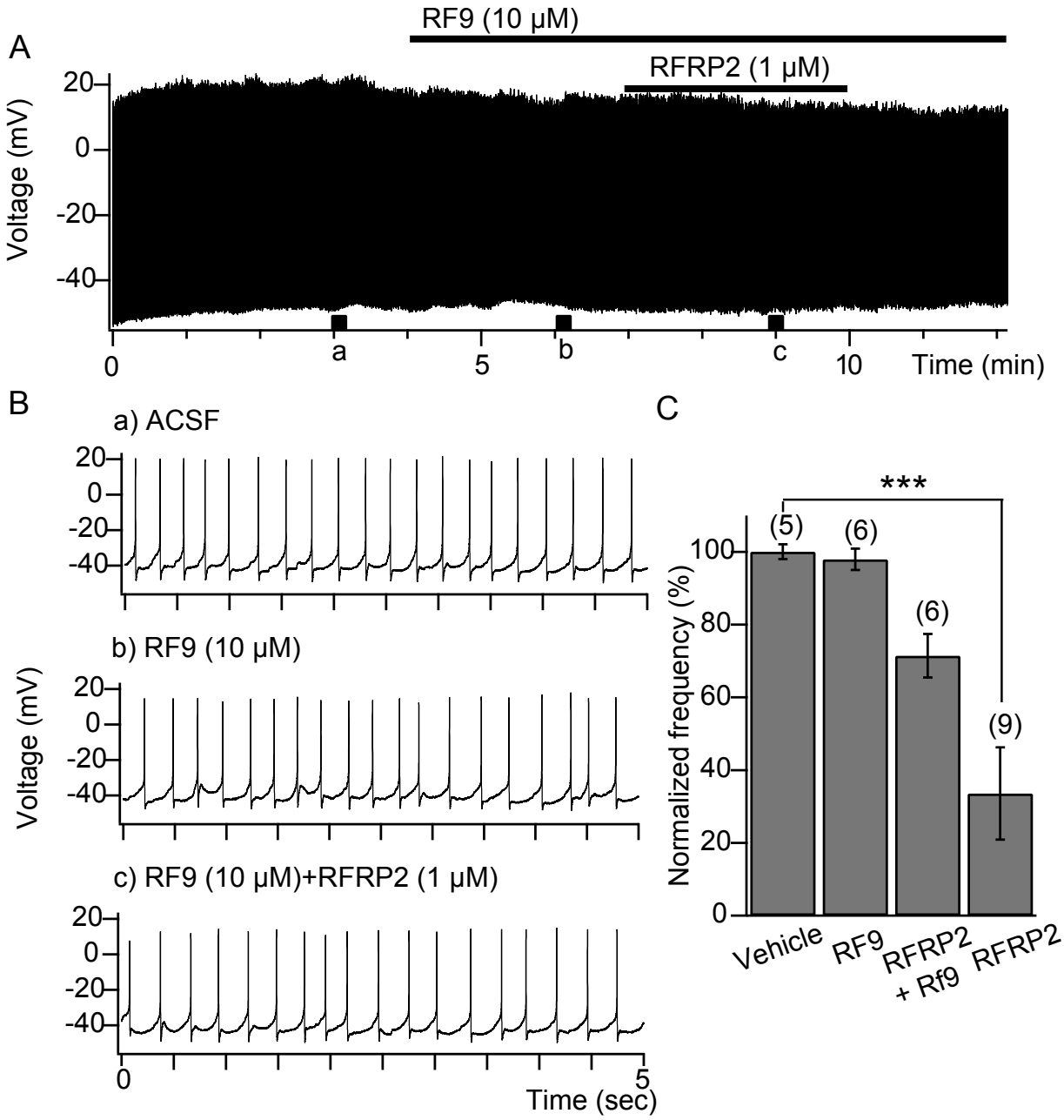
A
RF9 (10 μM)
RFRP2 (1 μM)
Voltage (mV)
20
0
-20
-40
0
a
5
b
c
10
Time (min)
B
a) ACSF
b) RF9 (10 μM)
c) RF9 (10 μM)+RFRP2 (1 μM)
Voltage (mV)
Time (sec)
C
***
(5)
(6)
(6)
(9)
Normalized frequency (%)
100
80
60
40
20
0
Vehicle
RF9
RFRP2 + Rf9
RFRP2

Figure 1-4

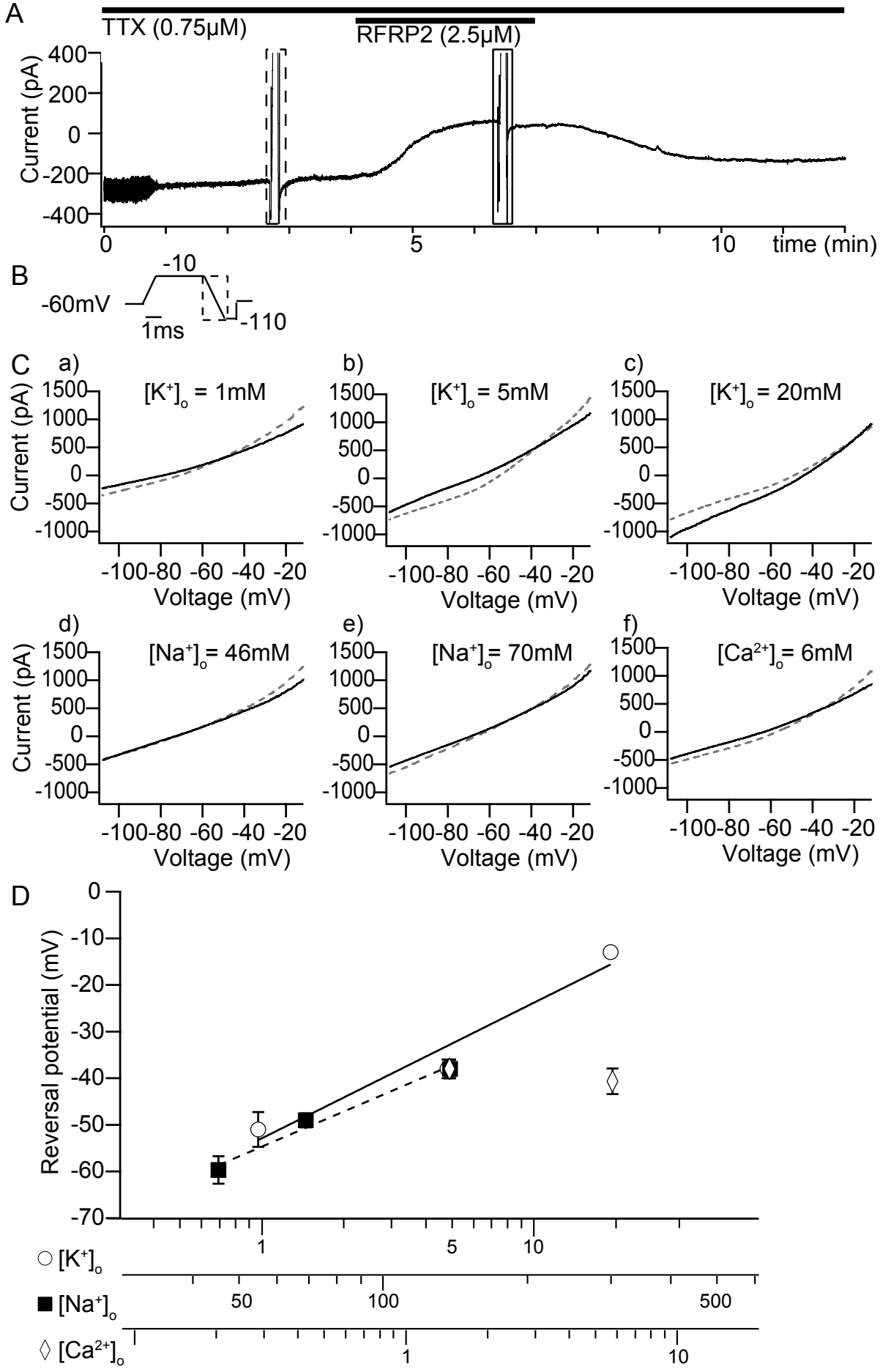
A
TTX (0.75μM)
RFRP2 (2.5μM)
Current (pA)
400
200
0
-200
-400
0
5
10
time (min)
B
-10
-60mV
-110
1ms
C
a)
[K+]o = 1mM
b)
[K+]o = 5mM
c)
[K+]o = 20mM
Current (pA)
1500
1000
500
0
-500
-1000
-100 -80 -60 -40 -20
Voltage (mV)
d)
[Na+]o = 46mM
e)
[Na+]o = 70mM
f)
[Ca2+]o = 6mM
D
Reversal potential (mV)
0
-10
-20
-30
-40
-50
-60
-70
1
5
10
○ [K+]o
■ [Na+]o
◊ [Ca2+]o
50
100
500
1
10

Figure 1-5

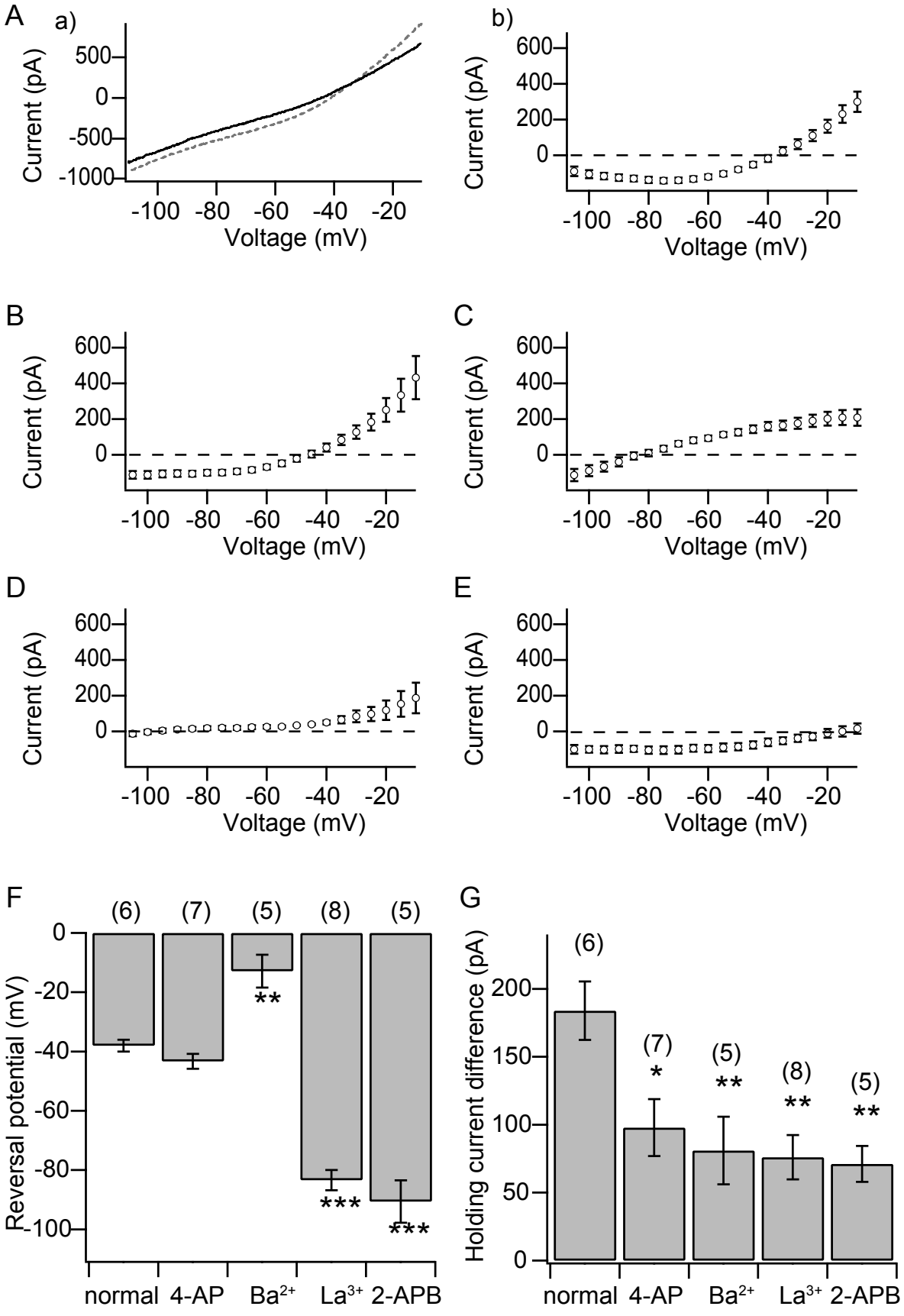
A
a)
Current (pA)
500
0
-500
-1000
-100 -80 -60 -40 -20
Voltage (mV)
b)
Current (pA)
600
400
200
0
-100 -80 -60 -40 -20
Voltage (mV)
B
Current (pA)
600
400
200
0
-100 -80 -60 -40 -20
Voltage (mV)
C
Current (pA)
600
400
200
0
-100 -80 -60 -40 -20
Voltage (mV)
D
Current (pA)
600
400
200
0
-100 -80 -60 -40 -20
Voltage (mV)
E
Current (pA)
600
400
200
0
-100 -80 -60 -40 -20
Voltage (mV)
F
(6) (7) (5) (8) (5)
Reversal potential (mV)
0
-20
-40
-60
-80
-100
**
***
***
normal 4-AP Ba2+ La3+ 2-APB
G
Holding current difference (pA)
200
150
100
50
0
(6)
(7)
*
(5)
**
(8)
**
(5)
**
normal 4-AP Ba2+ La3+ 2-APB

Chapter 2

Synaptically induced high frequency firing and neuropeptide release of TN-GnRH3 neurons

Abstract

In this chapter, I analyzed the nature of high frequency firing and the neuropeptide release of TN-GnRH3 neurons by electrophysiology and Ca^{2+} imaging, respectively. In preliminary recordings of firing activities of TN-GnRH3 neurons using medaka of various ages, I found that juvenile medaka (before 10 weeks post fertilization) were more likely to show burst firing than adults. Because neuropeptide release has been suggested to require high frequency firing, e.g., burst firing, I analyzed the nature of firing and neuropeptide release of TN-GnRH3 neurons using not only adult but also juvenile medaka.

I found in electrophysiological recording of spontaneous activity from adult TN-GnRH3 neurons that local puffer application of glutamate, which should mimic excitatory synaptic inputs to these neurons, quickly increased firing activities. Glutamate puffer application also evoked a quick and large increase in intracellular Ca^{2+} concentration. On the other hand, similar local puffer application of $GABA_A$ receptor agonist also increased firing activities (excitatory, because of higher intracellular Cl^- concentration of TN-GnRH3 neurons), but it increased intracellular Ca^{2+} concentration rather mildly. Interestingly, in juvenile medaka, global blockage of $GABA_A$ receptors by perfusion of bicuculline, a $GABA_A$ receptor antagonist, induced burst firing of TN-GnRH3 neurons indirectly through excitation of other glutamatergic neurons. The burst firing thus evoked was also suggested to be capable of inducing neuropeptide release by Ca^{2+} imaging analysis. From the results of the present chapter, the TN-GnRH3 neurons in both adult and

juvenile medaka are suggested to be capable of firing at high frequency and thus of releasing neuropeptide in response to various synaptic inputs.

Introduction

In Chapter 1, I found that RFRP inhibit firing of TN-GnRH3 neurons as a new synaptic modulator by which I could add new information as to the mechanisms of modulation of firing activity of TN-GnRH3 neurons. There is a small number of studies to show that peptidergic neurons, including GnRH neurons, generally have to fire at high frequency to release neuropeptides (Dutton and Dyball 1979; Liu et al. 2011). GnRH3 peptide that is released from TN-GnRH3 neurons is suggested to modulate neuronal activities in the olfactory bulb, retina and so on (Kawai et al. 2010; Umino and Dowling 1991). However, these studies were performed by application of GnRH3 peptide experimentally, and it has not been clarified under which conditions the TN-GnRH3 neurons fire at frequencies high enough to trigger release of GnRH3 peptides. In a preliminary experiments on the spontaneous electrical activity of TN-GnRH3 neurons using medaka of various ages, I found that TN-GnRH3 neurons of juvenile medaka (before 10 weeks post- fertilization) were more likely to show burst firing than adult (Fig. 2-1). Inspired by this finding, I suspected that juvenile medaka may be useful for the analysis of neuropeptide release from TN-GnRH3 neurons, which is contrary to what people may expect from the fact that GnRH peptide was originally identified as a hypophysiotropic peptide hormone that stimulates the release of gonadotropins and is essential for reproduction.

In this chapter, to study the regulatory mechanisms of neuropeptide release from TN-GnRH3 neurons, I analyzed the spontaneous firing activities of TN-GnRH3 neurons by electrophysiology

and neuropeptide release by Ca^{2+} imaging using not only adult but also juvenile medaka. Then, I concluded that the TN-GnRH3 neurons in both adult and juvenile are capable of firing at high frequency and thus of releasing neuropeptide in response to various synaptic inputs, such as glutamate and GABA.

Material and Methods

Gnrh3: egfp medaka (*Oryzias latipes*) (Takahashi et al. 2015) was maintained at 27 ℃ at a 14:10 light:dark cycle. The fish were daily fed with live brine shrimp and flake food. I used juvenile medaka (6 ~ 9 weeks after fertilization) and adult medaka (> 9 weeks after fertilization). All procedures were performed in accordance with the guideline principles for the care and use of experimental animals established by the Physiological Society of Japan and the University of Tokyo.

Electrophysiology

The fish were anesthetized by 0.02 % 3-aminobenzoic acid ethyl ester (MS-222; Sigma Aldrich, St Louis, MO, USA). They were quickly killed by decapitation, and the whole brain was isolated. The isolated brain was put in an artificial cerebrospinal fluid (ACSF) consisting of (in mM) 134 NaCl, 2.9 KCl, 1.2 $MgCl_2$, 2.1 $CaCl_2$, 10 HEPES, and 10 glucose (pH 7.4 adjusted with NaOH and ~300 mOsm adjusted with Sucrose). Then, the ventral meningeal membrane was carefully removed. For the whole cell recording, internal solution was the following (mM): K-gluconate 112.5, KCl 17.5, NaCl 4, EGTA 1, $MgCl_2$ 1, $CaCl_2$ 0.5, HEPES 10, and K_2ATP 4 (pH 7.2 adjusted with KOH and ~290 mOsm adjusted with Sucrose). The junction potential was -13.8 mV, and the membrane potentials were adjusted by using this value. The tip resistance of patch electrodes (Narishige, GD-1.5) in ACSF was 10-15 MΩ. For the on-cell patch clamp recording, the pipette solution was the same as ACSF. The both recordings were performed using an

Axopatch 200B patch-clamp amplifier (Molecular Devices, Sunnyvale, CA, USA). The whole cell voltage-clamp recordings were digitized (10 kHz) and stored on a computer using the Digidata 1322A and pCLAMP 9.2 software (Molecular Devices, Sunnyvale, CA, USA). Bath application of drugs was performed by mixing drugs in the ACSF, and puff application (100 ms, ~60 kPa) was performed by using electric microinjector IM-31 (Narishige, Tokyo, Japan). The tip diameter of glass pipette (Narishige, GD-1) for puff application was 1 ~ 5 μm, and the pipette was placed 10 ~ 30 μm from the cell bodies of TN-GnRH3 neurons.

Ca^{2+} imaging

The whole brain was isolated as described above. The tissue covering the TN-GnRH3 neurons was removed with the aid of a glass pipette under a microscope, in order to expose the surface of the TN-GnRH3 neurons. Then, the brain was incubated in ACSF at room temperature for 30 mins. I prepared Fura2 solution (ACSF with 10 μM Fura2-AM (Dojindo, Kumamoto, Japan) and 0.04 % Cremophor-EL (Sigma Aldrich, St Louis, MO, USA)) and vortexed it for 10 s. After the incubation, I put the brain into the 1.5 ml tube containing a Fura2 solution. The tube was shaken mildly at 30 °C for 1 hour. The brain was washed by incubation with normal ACSF at room temperature for 15 min and perfusion of normal ACSF at room temperature for 15 min. After that, I placed the brain in a recording chamber with ACSF in the ventral side-up direction. The preparation was perfused with ACSF at a continuous flow rate (2 mL/min). Bath application of

drugs and puff application were performed as described in the previous section. Fura2 and EGFP fluorescence were detected by the Chroma 74000 filter set (D480×, D340×, D380× exciter; 505DCLP dichroic mirror; HQ535/50m emitter) housed in the Lambda DG-4 Xenon light source, excitation filter exchanger (Sutter Instruments, Novato, CA, USA), and the BX-51WI upright epifluorescence microscope (Olympus, Tokyo, Japan). The fluorescence was recorded (exposure: 80 ms [340 nm, 380 nm], 50 ms [480 nm]; 5 MHz EM Gain; interval: 2 s) using QuantEM 512SC EMCCD camera (Photometrics, Tucson, AZ, USA) and the Metafluor imaging software (Molecular Devices, Sunnyvale, CA, USA). For EGFP, the intensity ratio of emission (at 510 nm) from the alternating 480-nm excitation was monitored. For Fura2, the intensity ratio of emission (at 510 nm) from the alternating 340 and 380-nm excitation was monitored. The imaging data was analyzed by the following method. The fluorescence intensity F_0 was calculated as the average of five frames from the first one. The fluorescence intensity change ($\Delta F/F_0$) was calculated as $(F - F_0)/F_0$. I set up the Region of Interest (ROI) on one of the TN-GnRH3 neurons by referring to the EGFP images and averaged those fluorescence intensity changes of the neurons in one hemisphere of telencephalon (2 ~ 8 neurons were identified in one hemisphere).

Drugs

Glutamate and γ-aminobutyric acid (GABA) was purchased from Wako (Osaka, Japan). Muscimol and Bicuculline were purchased from Sigma Aldrich (St Louis, MO, USA). D-(-)-2-

amino-5-phosphonopentanoic acid (D-AP5) and 6-cyano-7-nitroquinoxaline-2,3-dione (CNQX) were purchased from Tocris (Bristol, UK).

Statics

Statistical analyses were performed by using the Kyplot5 software (Kyence, Tokyo, Japan) and the Igor Pro 6 software (WaveMetrics Inc., Lake Oswego, OR, USA) with Taro tool (Igor macro set written by Dr. Taro Ishikawa, Jikei University School of Medicine). Different statistical tests were used for different experiments, as described in Results and Figure legends. All the data in the present study are presented as mean ± S.E.M

Results

Local glutamate application induces high frequency firing and increase in intracellular Ca^{2+} concentration of TN-GnRH3 neurons

To induce high frequency firing in TN-GnRH3 neurons, glutamate was applied locally and transiently by using a local puffer application method, mimicking a glutamatergic excitatory synaptic input to TN-GnRH3 neurons (see Kiya and Oka 2003). The local glutamate application quickly induced transient high frequency firing of TN-GnRH3 neurons in both juvenile (Fig. 2-2Aa) and adult medaka (Fig. 2-2Ba). The maximum frequency reached 10 times as much as that before the application, and the increase continued for a few seconds (Fig. 2-2Ab, Bb).

Previous literature reported that neuropeptide release requires an increase in intracellular Ca^{2+} concentration (Peng and Zucker 1993; van den Pol 2012). To examine whether intracellular Ca^{2+} concentration increases during high frequency firing of TN-GnRH3 neurons evoked by puffer application of glutamate, I performed Ca^{2+} imaging of TN-GnRH3 neurons using a Ca^{2+} indicator, Fura2. Puffer application of glutamate transiently increased intracellular Ca^{2+} concentration of TN-GnRH3 neurons in both juvenile (Fig. 2-3Aa) and adult medaka (Fig. 2-3Ba). The increase in the intracellular Ca^{2+} concentration was dependent on the concentration of glutamate (Fig. 2-3Ab, Bb). Thus, the results of the electrophysiological experiments and Ca^{2+} imaging strongly suggest that glutamatergic synaptic inputs can induce neuropeptide release in TN-GnRH3 neurons.

Local puffer application of $GABA_A$ receptor agonist also increases firing frequency of TN-GnRH3 neurons

To examine whether GABA, which is another excitatory input to TN-GnRH3 neurons (Nakane and Oka 2010), also induces high frequency firing, I performed local puffer applications of a potent and selective $GABA_A$ receptor agonist, muscimol (Fig. 2-4Aa, Ba). Puffer application of 20 μM muscimol transiently increased firing frequency to about 1.5 times higher than before the application in both juvenile and adult medaka (Fig. 2-4Ab, Bb). In Fig. 2-4Ab, Bb, a transient decrease of firing was observed following the spike just after muscimol application. Because similar muscimol application induced large depolarization in the whole cell recording mode, the decrease in firing is suggested to be because of the Na^+ channel inactivation due to strong depolarization in response to muscimol (Fig. 2-S1, and see Nakane and Oka 2010). These results show that TN-GnRH3 neurons in juvenile medaka are also activated, but not inhibited, by GABA as in adults, unlike the other non-GnRH neurons (see Nakane and Oka 2010).

Similar to the experiments of glutamate puffer applications, I examined whether local puffer application of $GABA_A$ receptor agonist also induces an increase in intracellular Ca^{2+} concentration. Fig. 2-5A, B show representative data of Fura2 imaging. A puffer application of 10mM GABA increased intracellular Ca^{2+} concentration in both juvenile (Fig. 2-5C) and adult (Fig. 2-5D) medaka. However, 1 mM muscimol (Fig. 2-5E, F) and lower concentration of GABA and muscimol (data not shown) did not induce an increase in intracellular Ca^{2+} concentration

significantly, although experiments using higher concentration of muscimol as in GABA application is necessary in future. Therefore, GABA receptor activation may not be sufficient in itself to induce peptide release.

Global blockage of $GABA_A$ receptor by perfusion of its antagonist, bicuculline, induces burst firing of TN-GnRH3 neurons in juvenile medaka through activation of glutamatergic synapses

Next, to examine whether tonic synaptic inputs to TN-GnRH3 neurons contribute to the generation of their spontaneous firing activities, I recorded spontaneous firing activities of TN-GnRH3 neurons during perfusion of ACSF containing antagonist of glutamate or GABA receptor. Drug application by perfusion is generally considered to act globally on almost every neuron in the brain preparation, and the drug effect should persist at least during perfusion (tonic effect). First, antagonist of AMPA type glutamate receptor (AMPA-R), CNQX, was perfused for four minutes (Fig. 2-6Aa), which silenced during perfusion all the glutamatergic synapses to TN-GnRH3 neurons, while leaving other synaptic inputs intact. The CNQX perfusion decreased firing frequency of juvenile TN-GnRH3 neurons (Fig. 2-6Aa-d) but did not change that of adult ones (Fig. 2-6Ba-d). Thus, tonic glutamatergic synaptic inputs via AMPA-R may contribute to the "spontaneous firing" pattern of TN-GnRH3 neurons in juvenile, but not in adult medaka.

On the other hand, perfusion of an antagonist of $GABA_A$ receptor, bicuculline, induced burst firing of juvenile TN-GnRH3 neurons similar to those sometimes observed spontaneously (Fig.

2-6C; see Fig. 1A). In adults, however, bicuculline did not induce such change in firing pattern (Fig. 2-6D). Thus, it is suggested that tonic $GABA_A$ receptor-mediated synaptic inhibition keep TN-GnRH3 neurons from bursting in juvenile medaka. To examine whether this burst firing is dependent on the developmental stage of medaka, I performed the bicuculline perfusion experiments in medaka at various developmental stages and found that bicuculline induces burst firing until 9 weeks post fertilization (Fig. 2-6E), but it ceased to do so later than 10 weeks post fertilization. As already described above, GABA excites TN-GnRH3 neurons in both juvenile and adult medaka, and therefore, this bicuculline-induced burst firing may be generated by synaptic inputs from glutamatergic neurons during bicuculline perfusion. To prove this possibility, I recorded spontaneous firing activities of TN-GnRH3 neurons in the ACSF containing CNQX, an AMPA type of glutamate receptors, and then applied bicuculline. As shown in Fig. 2-7A, bicuculline failed to induce burst firing during CNQX perfusion (see Fig. 2-6C). Furthermore, bicuculline also failed to induce burst firing during perfusion of D-AP5, an antagonist of NMDA type of glutamate receptor (Fig. 2-7B). Thus, it is suggested that both AMPA and NMDA types of glutamatergic synaptic inputs contribute to the bicuculline-induced bursting of juvenile medaka (Fig. 2-6C).

Bicuculline-induced burst firing increases intracellular Ca^{2+} concentration of TN-GnRH3 neurons

Finally, to examine whether intracellular Ca^{2+} concentration is also increased when TN-GnRH3 neurons show bicuculline-induced burst firing (Fig. 2-6C), I performed Ca^{2+} imaging during perfusion of bicuculline, similar to the electrophysiological experiment. Bath application of ACSF containing bicuculline induced multiple peaks of intracellular Ca^{2+} concentration increase during its perfusion (Fig. 2-8A, B, C). The duration of one peak lasted for about 5 ~ 10 s, which is quite similar to the duration of one cluster of burst firing in juvenile TN-GnRH3 neurons (Fig. 2-6C). The percentage change in Fura2 fluorescence intensity during bicuculline perfusion was higher than that of the vehicle control (Fig. 2-8D). Therefore, bicuculline-induced burst firing in juvenile medaka is also suggested to induce neuropeptide release.

Discussion

Synaptically induced high frequency firing is capable of triggering neuropeptide release from TN-GnRH3 neurons

In the present Chapter, I clearly showed that local puffer application of glutamate, which is considered to mimic glutamatergic synaptic inputs, induces high frequency firing and increase in intracellular Ca^{2+} concentration of TN-GnRH3 neurons in both juvenile and adult medaka. Furthermore, I found that not only glutamate but also GABA increase the frequency of firing and intracellular Ca^{2+} concentration of TN-GnRH3 neurons to a certain degree. The excitatory GABAergic action agrees well with the previous experimental evidence in mammalian (Herbison and Moenter 2011) as well as in teleost GnRH neurons (Nakane and Oka 2010) that $GABA_A$ receptor activation depolarizes the GnRH neurons. In addition to these, I newly found in juvenile medaka that global blockage of $GABA_A$ receptors by bicuculline perfusion induces high frequency burst firing of TN-GnRH3 neurons, which is considered to be effective for facilitating peptide release (see also below).

The most important finding in the present chapter, in terms of functional significance, is that, by combining electrophysiology and Ca^{2+} imaging, I could clearly demonstrate that glutamate puffer application mimicking glutamatergic synaptic input induces high frequency firing of about 10 Hz and rather large increase in intracellular Ca^{2+} concentration (Fig. 2-2, 2-3). It has been recently reported in hypophysiotropic GnRH (GnRH1) neuron and kisspeptin neuron that high

frequency firing (more than 10Hz) effectively induces neuropeptide release *in vivo* (Campos and Herbison 2014; Han et al. 2015). The release of these neuropeptides is triggered by increase in intracellular Ca^{2+} concentration (Moenter et al. 2003). Therefore, it is strongly suggested that glutamate-induced high frequency firing of TN-GnRH3 neurons in juvenile and adult medaka triggers release of GnRH3 peptide *in vivo* as well.

In fact, previous electrophysiological studies in our laboratory have suggested occurrence of various types of excitatory synaptic inputs to TN-GnRH3 neurons via a variety of ionotropic as well as metabotropic glutamate receptors (Kiya and Oka 2003) and $GABA_A$ receptors (Nakane and Oka 2010) in fish brain. On the other hand, neuroanatomical tract tracing analysis has revealed a variety of afferent synaptic sources projecting to the TN-GnRH3 neurons from various sensory brain areas (Yamamoto and Ito 2000). Therefore, it is presumable that excitatory synaptic inputs of various sensory modalities cause high frequency firing and associated intracellular Ca^{2+} increase, which triggers release of GnRH3 peptide from TN-GnRH3 neurons.

As noted above, the increase in intracellular Ca^{2+} concentration by GABA was much less than that by glutamate. In my preliminary RNA-seq data in medaka (not shown), TN-GnRH3 neurons express NKCC1, which is a Na^+-K^+-Cl^- co-transporter and increases intracellular Cl^- concentration (Watanabe et al. 2014). This is considered to give a molecular basis for the excitatory action of GABA to TN-GnRH3 neurons as reported electrophysiologically (Nakane

and Oka 2010). The equilibrium potential for Cl^- in TN-GnRH3 neurons is calculated to be about -45 mV under the present experimental conditions (calculated from the intracellular and extracellular solutions), and nearer to the resting potential of TN-GnRH3 neurons (c.a. -50~60 mV) than the reversal potential of AMPA type glutamate receptor (c.a. 0 mV). Therefore, depolarization by GABA is considered to be milder compared to that by glutamate, which explains the present results that GABA contributed less to the high frequency firing of TN-GnRH3 neurons compared with glutamate.

Functional significance of synaptically induced GnRH3 peptide release from TN-GnRH3 neurons

As to the functional significance of the synaptically driven high-frequency and burst firing activities of the TN-GnRH3 neurons, it should be noted that TN-GnRH3 neurons of both juvenile and adult medaka responded to local puffer application of glutamate with high frequency firing and intracellular Ca^{2+} rise (Fig. 2-9A, B, and D). Therefore, it is suggested that TN-GnRH3 neurons receive both GABAergic and glutamatergic synaptic inputs (Fig. 2-9A, B). On the other hand, recording of TN-GnRH3 neurons at various developmental stages of medaka showed some differences between juvenile and adult in firing activities and possible neural circuitry regulating the firing patterns and frequencies. TN-GnRH3 neurons in juvenile showed spontaneous burst firing more frequently than that in adult (Fig. 2-1) and a characteristic bicuculline-induced burst

firing (Fig. 2-6C), which was not observed in adults. Considering the fact that bicuculline did not induce burst firing under tonic and global blockage of AMPA or NMDA types of glutamate receptors, it is suggested that AMPA and NMDA types of glutamatergic synaptic inputs act in ensemble to generate the bicuculline-induced bursting of juvenile medaka. Interestingly, a similar mechanism for burst generation has also been proposed for the central locomotor pattern generator circuitry in the spinal cord (Grillner et al. 1995; Wallen and Grillner 1987). The intracellular Ca^{2+} increase induced by global bicuculline-application may be caused by voltage gated Ca^{2+} channels, NMDA type receptors, or both, which needs to be further clarified in future. In TN-GnRH3 neurons, global bicuculline application in juvenile is considered to block the tonic GABAergic inhibition to the glutamatergic neurons, and this disinhibitory action of bicuculline may have facilitated the ensemble glutamate receptor-mediated burst firing in juvenile medaka (Fig. 2-9C). It should be noted that spontaneous intracellular Ca^{2+} increase was sometimes observed in Ca^{2+} imaging experiments using juvenile medaka (data not shown). These results suggest that TN-GnRH3 neurons in juvenile fish may release neuropeptide(s) more actively than those in adult. In addition, the bicuculline-induced firing was no longer observed about 10 weeks post fertilization onward. The timing of this transition roughly corresponded to that of the sexual maturation in medaka (Iwamatsu 2006; Kinoshita et al. 2009), and the changes in bicuculline responsiveness and the spontaneous firing pattern may therefore be related to the sexual maturation. Thus, the

juvenile-specific burst firing (Fig 2-9C) may be caused by a mechanism that is lost in adulthood and possibly has novel physiological functions. Although previous studies on TN-GnRH3 neurons and GnRH3 have mainly been performed by using adult animals (Eisthen et al. 2000; Ramakrishnan and Wayne 2009), and the function(s) of this juvenile-specific burst firing in TN-GnRH3 neurons remain to be enigmatic, it should be an exciting future topic to search for the physiological functions of GnRH3 peptide release and the generation mechanisms of burst firing in juvenile medaka.

Anyway, the present chapter has shown that glutamatergic synaptic inputs may effectively trigger GnRH3 peptide release, and GnRH3 peptide are considered to act as neuromodulators in the brain areas that receive dense axonal projections from TN-GnRH3 neurons (Abe and Oka 2011; Karigo and Oka 2013). Therefore, in Chapter 3, I analyzed the mechanisms of GnRH3-induced neuromodulation in the optic tectum, which receives dense axonal projections from TN-GnRH3 neurons.

Figure legends

Figure 2-1 Recording of spontaneous firing activity of TN-GnRH3 neurons.

A: High frequency burst-like firing in juvenile medaka. B: pacemaker activity in adult medaka.

Figure 2-2 Local puffer application of glutamate quickly induces transient high frequency firing of TN-GnRH3 neurons.

Glutamate (500 μM, dissolved in ACSF) was applied to the TN-GnRH3 neurons for 100ms by using a puffer pipette at the point indicated by an arrow. Representative recordings (a) and frequency histograms (b) (n=12) from juvenile (A) and adult (B) medaka. bin: 0.5 s.

Figure 2-3 Puffer application of glutamate quickly increases intracellular Ca^{2+} concentrations in a dose-dependent manner.

Glutamate (500 μM, dissolved in ACSF) was applied to the TN-GnRH3 neurons for 100ms by using a puffer pipette at the point indicated by an arrow. The ratio of Fura2-fluorescence intensity was transiently increased after puff application of glutamate (each trace represents the average of 3 traces) (a) in both juvenile (A) and adult (B) medaka. The maximum change in ratio is plotted against the glutamate concentrations in (b). The values were calculated by Taro tool of Igor software (Karigo et al. 2014). The numbers in parentheses indicate the number of trials.

Figure 2-4 $GABA_A$ receptor activation by local puffer application of a $GABA_A$ receptor agonist increases firing frequency.

$GABA_A$ receptor agonist muscimol (20 μM, dissolved in ACSF) was applied at the arrow for 100ms. Representative recordings (a) and frequency histograms (b) (n=7) from juvenile (A) and adult (B) medaka. bin: 0.5s.

Figure 2-5 Local activation of $GABA_A$ receptor by puffer application of GABA increases intracellular Ca^{2+} concentration.

A, B: $GABA_A$ receptor agonist GABA (10 μM, dissolved in ACSF) was applied at the arrow for 100ms. The ratio of Fura2-fluorescence intensity (each trace represents the average of 3 traces) (a) from juvenile (A) and adult (B) medaka. C, D: Maximum amount of ratio change with or without GABA in juvenile (C) and adult (D) medaka. Student's t-test, ***: $p < 0.001$, *: $p < 0.05$. E, F: Maximum amount of ratio change with or without 1mM muscimol in juvenile (E) and adult (F) medaka. Student's t-test, n.s. In C~F, maximum amount of ratio change was calculated by subtraction from peak ratio during 30 s after drug application to average ratio of 10s before application.

Figure 2-6 Analysis of spontaneous firing during global blockage of glutamate or $GABA_A$

receptors by perfusion of antagonists for each receptor

A, C: juvenile medaka. B, D: adult medaka. a: Spontaneous firing activity before (b), during (c), and after (d) perfusion of CNQX, an AMPA type glutamate receptor antagonist. ACSF containing CNQX was applied for 4 min (indicated by the bar on top of the trace). b, c, d: Expanded traces in Fig. 2-6Aa. e: Firing frequency before (1~2 min before application), during (3~4 min after application), and after (2~3 min after start of washout) perfusion of CNQX normalized by frequency before the application. ANOVA and Turkey-Kramer's test, *: $p < 0.05$. C and D: Firing activity of juvenile (C) and adult (D) medaka during perfusion of bicuculline, a $GABA_A$ receptor antagonist. Bicuculline was applied during the period indicated by the bars (Bic 20μM). E: Number of burst firing during bicuculline perfusion recorded from TN-GnRH3 neurons of medaka at various developmental stages. One bout of burst firing was defined as the time period containing more than three spikes at high frequency (more than twice the frequency in normal ACSF), followed by interburst hyperpolarization with a longer interspike interval than that in normal ACSF.

Figure 2-7 Bicuculline-induced burst firing in juvenile medaka is inhibited by CNQX and D-AP5.

Bicuculline-induced burst firing activity of juvenile medaka (Fig. 2-6C) was inhibited during perfusion of CNQX (an AMPA type glutamate receptor antagonist) (A) or D-AP5 (B) (NMDA

type glutamate receptor antagonist).

Figure 2-8 Bicuculline-induced burst firing increases intracellular Ca^{2+} concentration

A: EGFP image of TN-GnRH3 neurons. B, C: Fluorescence intensity change ($\Delta F/F_0$) of Fura2 during application of ACSF with (B) or without (C) bicuculline. Each colored trace represents data for the cell circled with the same color in Fig. 2-8A. D: Percentage change in fluorescence intensity during bicuculline perfusion. The values represent percentage of $\Delta F/F_0$ during vehicle (control) or bicuculline (Bic) application (4 min). ANOVA and paired Welch's test, **: $p < 0.01$.

Figure 2-9 Summary diagram indicating neural circuitries involved in neuropeptide release from the TN-GnRH3 neurons in juvenile and adult medaka brains.

A, B: neural circuitries involved in neuropeptide release from the TN-GnRH3 neurons in juvenile (A) and adult (B). GABA, GABAergic neuron; Glu, glutamatergic neuron; GnRH, TN-GnRH3 neurons. Note that GABAergic synapses are inhibitory (⊣) to glutamatergic neurons but are excitatory (→) to GnRH3 neurons. C: Global perfusion of bicuculline induced burst firing and intracellular Ca^{2+} increase of TN-GnRH3 neurons in juvenile. D: Local glutamate application induced high frequency firing and intracellular Ca^{2+} increase of TN-GnRH3 neurons in both juvenile and adult. Both firing patterns (Fig. 2-9C, D) are suggested to induce neuropeptide

release.

Figure 2-S1 local application of muscimol induced depolarization of TN-GnRH3 neuron

A representative recording of a TN- GnRH3 neuron in response to a local application of muscimol (juvenile medaka). 10 μM muscimol was applied locally (1 s) around the cell bodies of TN-GnRH3 neurons.

Figure 2-1

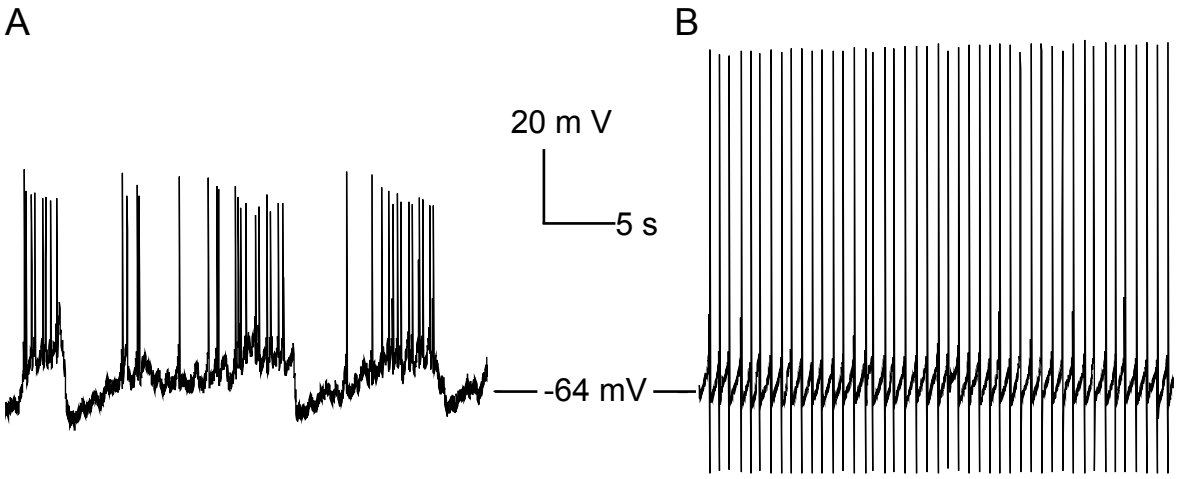

Figure 2-2

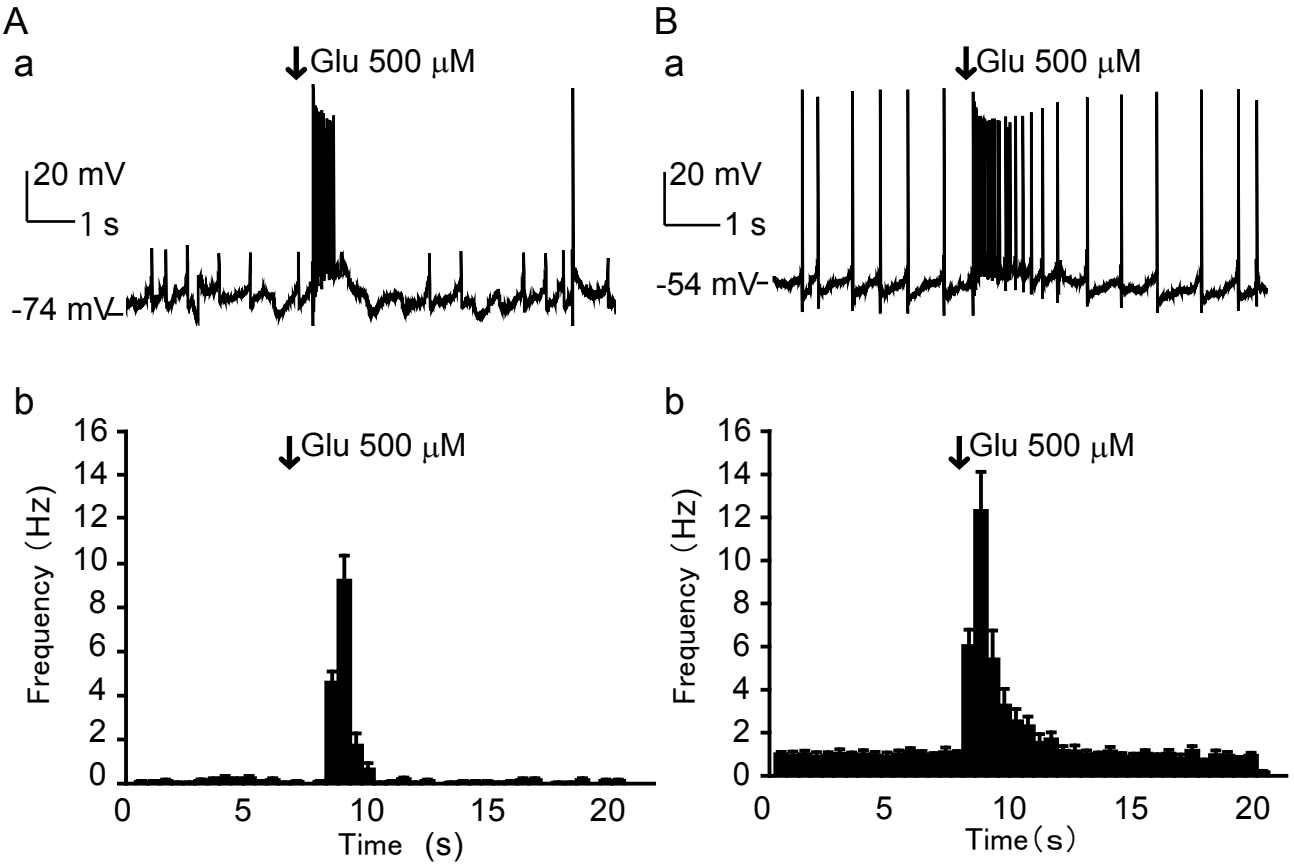
A
a
Glu 500 μM
20 mV
1 s
-74 mV
b
Glu 500 μM
Frequency (Hz)
Time (s)
B
a
Glu 500 μM
20 mV
1 s
-54 mV
b
Glu 500 μM
Frequency (Hz)
Time (s)

Figure 2-3

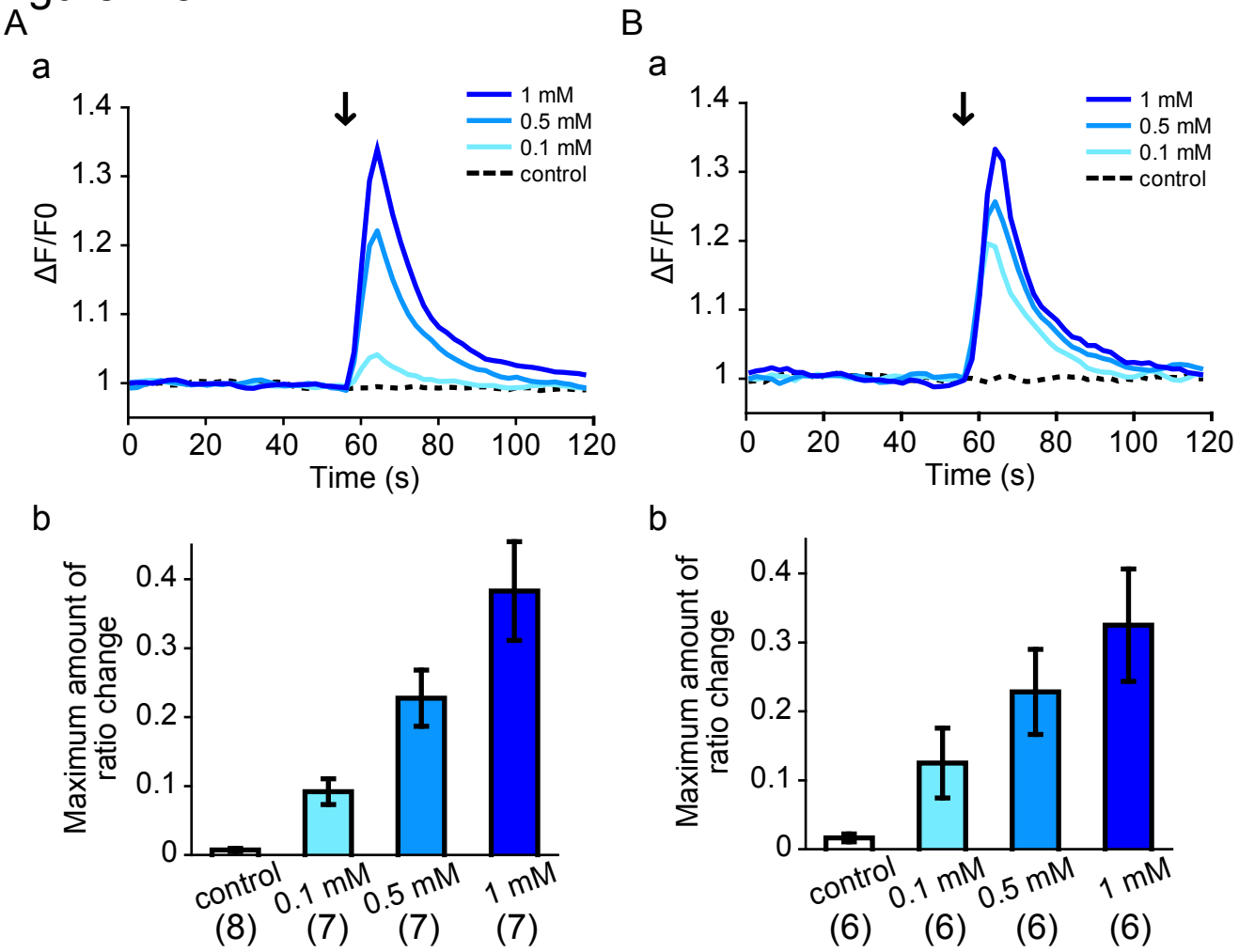
A
a
1 mM
0.5 mM
0.1 mM
control
ΔF/F0
Time (s)
b
Maximum amount of ratio change
control
0.1 mM
0.5 mM
1 mM
(8)
(7)
(7)
(7)
B
a
1 mM
0.5 mM
0.1 mM
control
ΔF/F0
Time (s)
b
Maximum amount of ratio change
control
0.1 mM
0.5 mM
1 mM
(6)
(6)
(6)
(6)

Figure 2-4

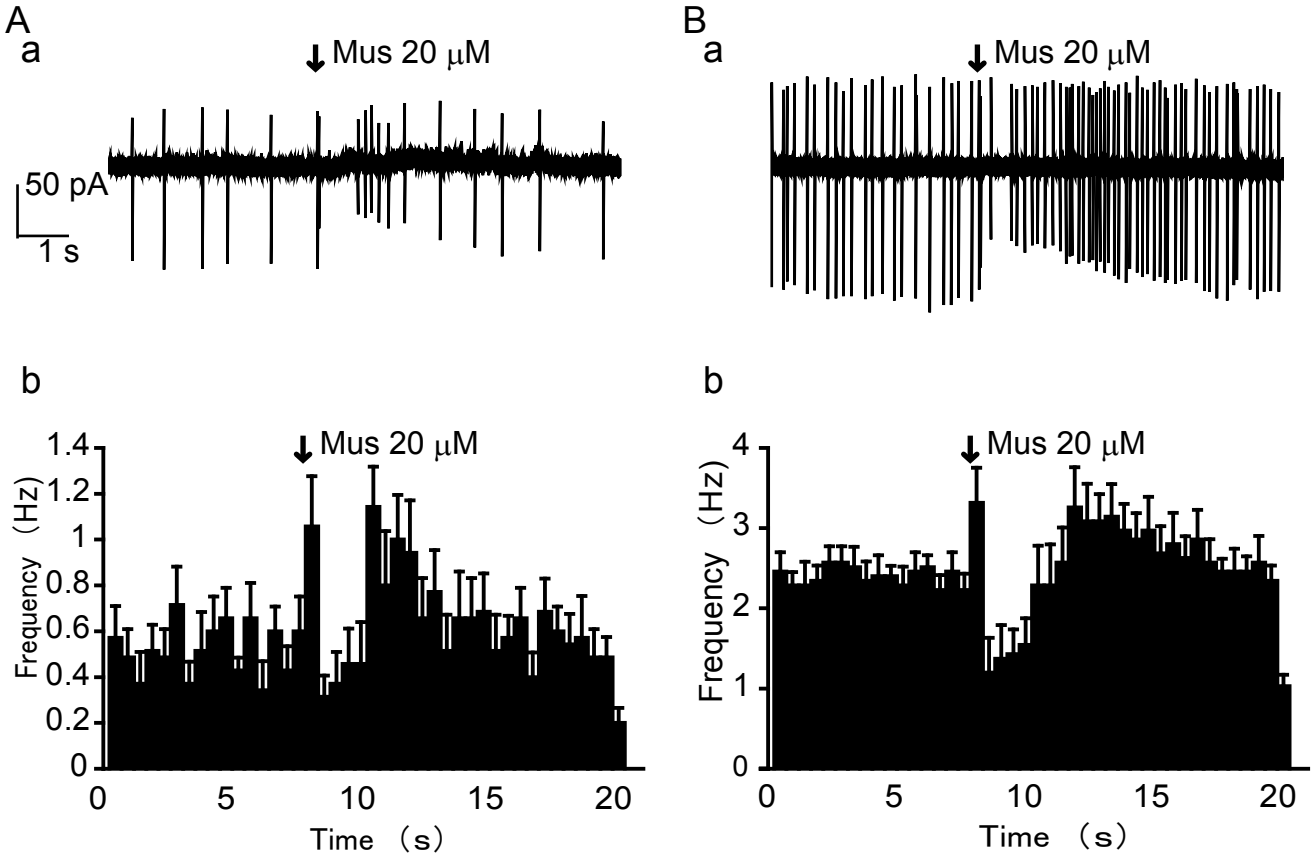
A
a
Mus 20 μM
50 pA
1 s
B
a
Mus 20 μM
b
Mus 20 μM
Frequency (Hz)
1.4
1.2
1
0.8
0.6
0.4
0.2
0
0
5
10
15
20
Time (s)
b
Mus 20 μM
Frequency (Hz)
4
3
2
1
0
0
5
10
15
20
Time (s)

Figure 2-5

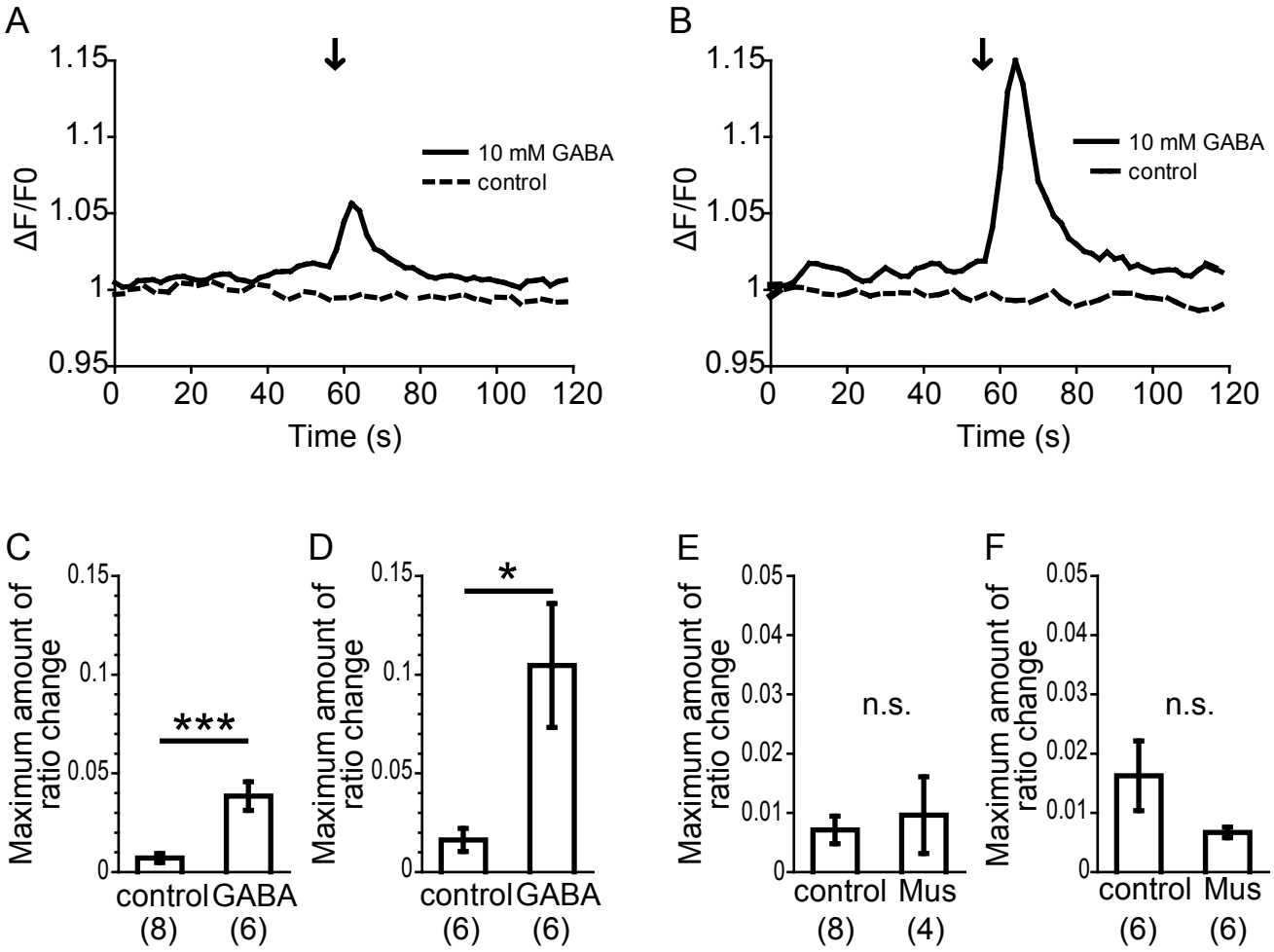
A
B
1.15
1.1
1.05
1
0.95
ΔF/F0
10 mM GABA
control
0
20
40
60
80
100
120
Time (s)
C
D
E
F
Maximum amount of ratio change
0.15
0.1
0.05
0
***
*
n.s.
0.05
0.04
0.03
0.02
0.01
control
GABA
Mus
(8)
(6)
(4)

Figure 2-6

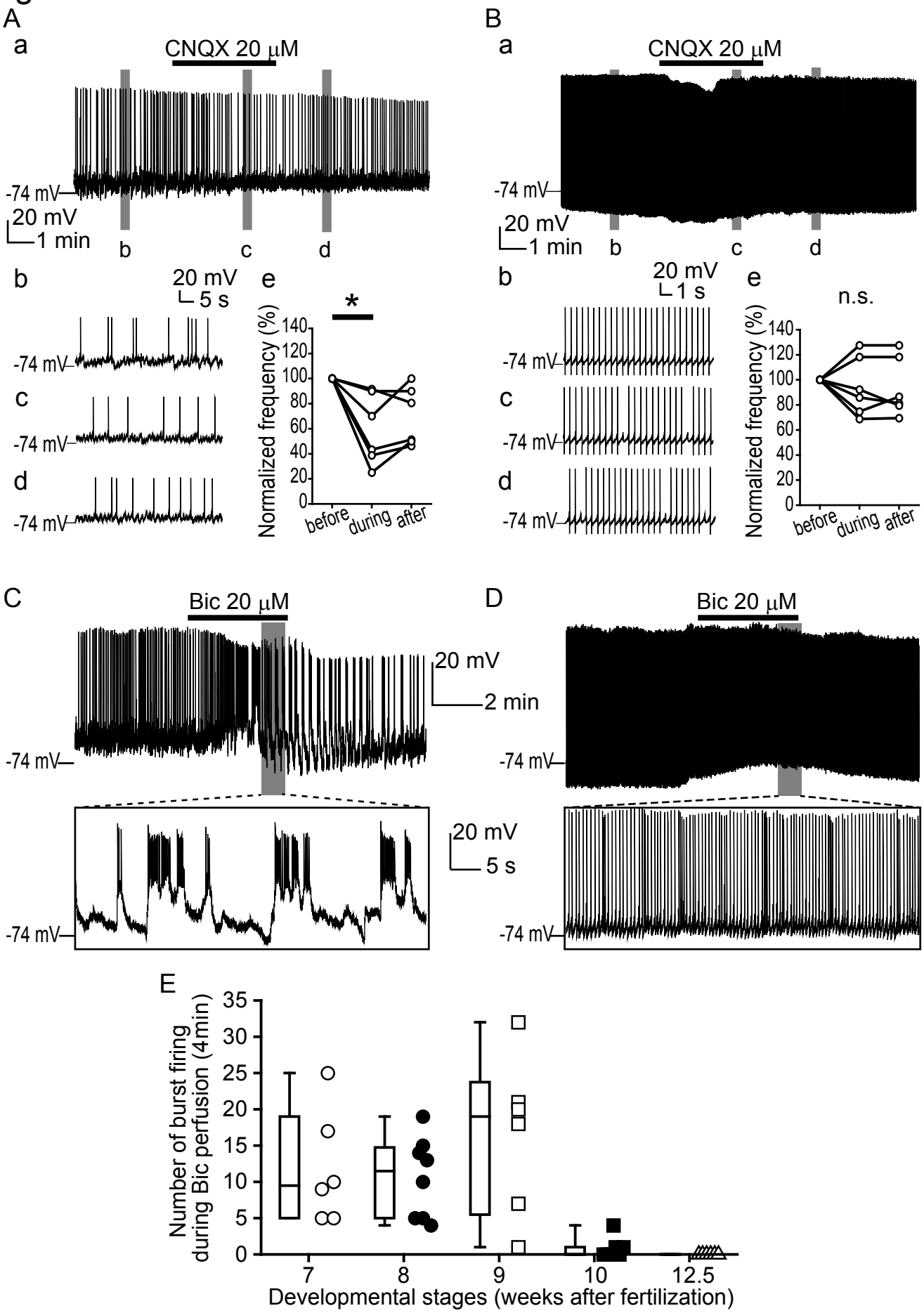
A
a
CNQX 20 μM
-74 mV
20 mV
1 min
b
c
d
b
20 mV
5 s
-74 mV
c
-74 mV
d
-74 mV
e
*
Normalized frequency (%)
140
120
100
80
60
40
20
0
before
during
after
B
a
CNQX 20 μM
-74 mV
20 mV
1 min
b
c
d
b
20 mV
1 s
-74 mV
c
-74 mV
d
-74 mV
e
n.s.
Normalized frequency (%)
140
120
100
80
60
40
20
0
before
during
after
C
Bic 20 μM
20 mV
2 min
-74 mV
20 mV
5 s
-74 mV
D
Bic 20 μM
-74 mV
-74 mV
E
Number of burst firing during Bic perfusion (4min)
35
30
25
20
15
10
5
0
7
8
9
10
12.5
Developmental stages (weeks after fertilization)

Figure 2-7

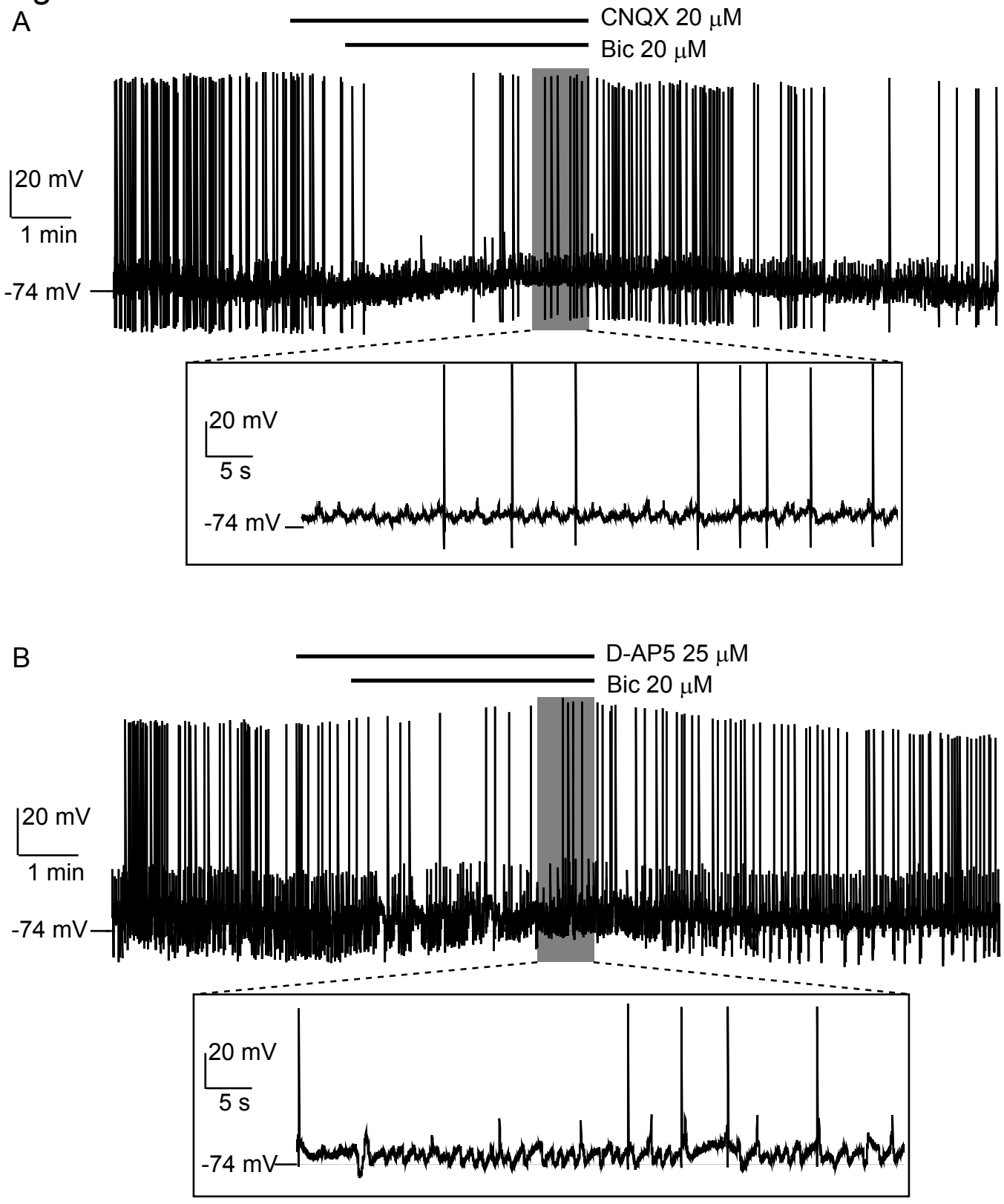
A
CNQX 20 μM
Bic 20 μM
20 mV
1 min
-74 mV
20 mV
5 s
-74 mV
B
D-AP5 25 μM
Bic 20 μM
20 mV
1 min
-74 mV
20 mV
5 s
-74 mV

Figure 2-8

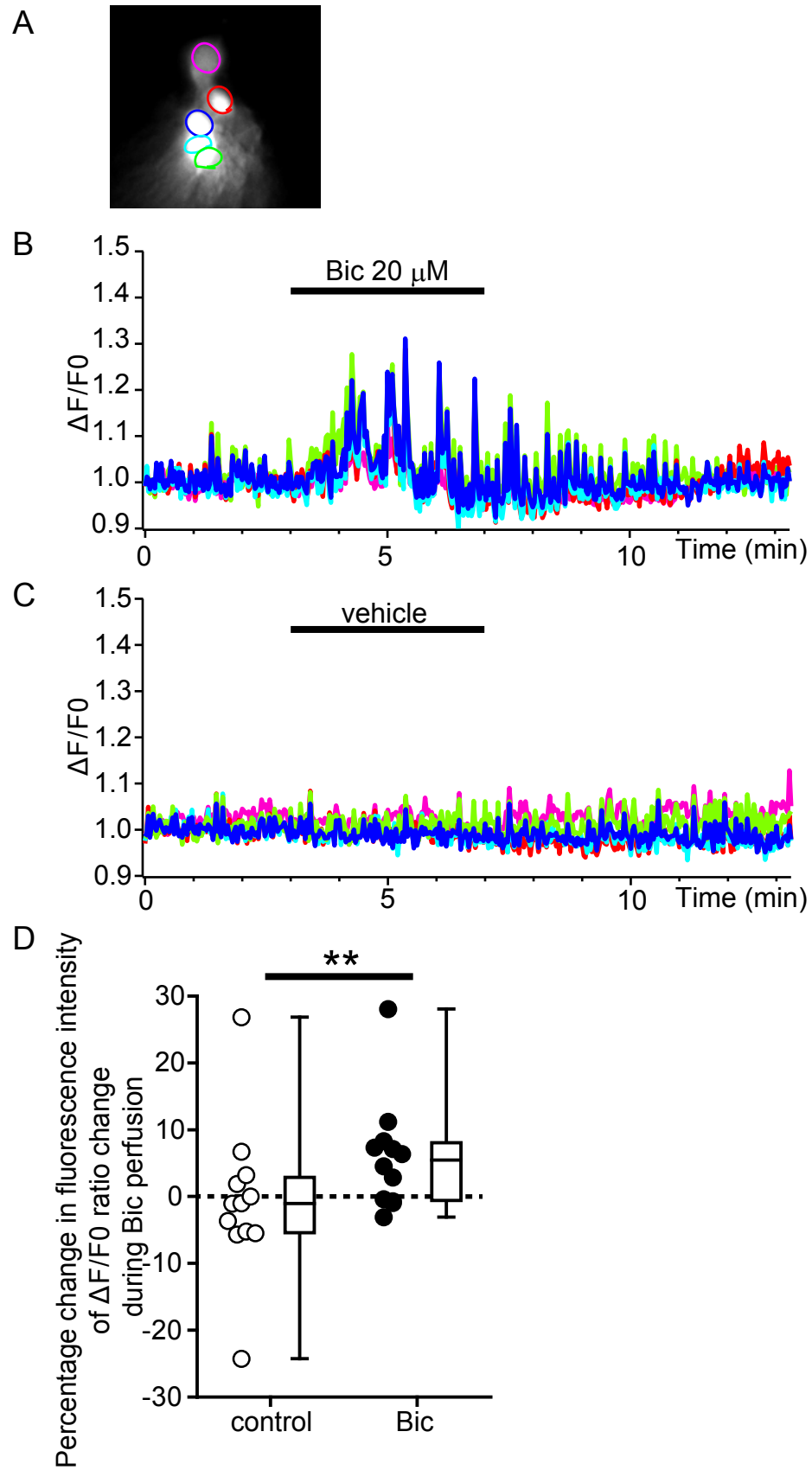
A
B
Bic 20 μM
ΔF/F0
1.5
1.4
1.3
1.2
1.1
1.0
0.9
0
5
10
Time (min)
C
vehicle
ΔF/F0
1.5
1.4
1.3
1.2
1.1
1.0
0.9
0
5
10
Time (min)
D
**
Percentage change in fluorescence intensity of ΔF/F0 ratio change during Bic perfusion
30
20
10
0
-10
-20
-30
control
Bic

Figure 2-9

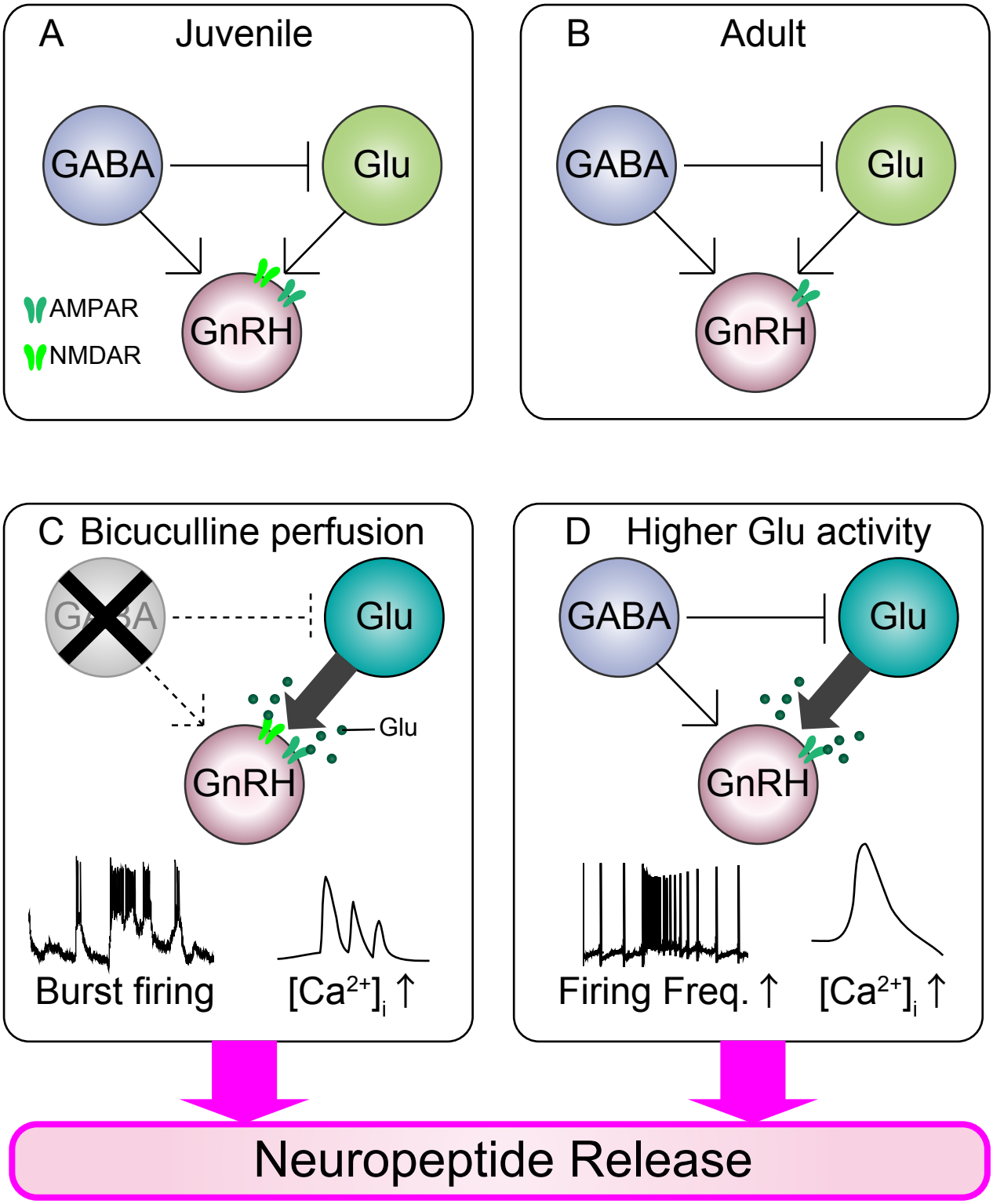
A Juvenile
GABA
Glu
AMPAR
NMDAR
GnRH
B Adult
GABA
Glu
GnRH
C Bicuculline perfusion
GABA
Glu
Glu
GnRH
Burst firing
[Ca2+]i ↑
D Higher Glu activity
GABA
Glu
GnRH
Firing Freq. ↑
[Ca2+]i ↑
Neuropeptide Release

Figure 2-S1

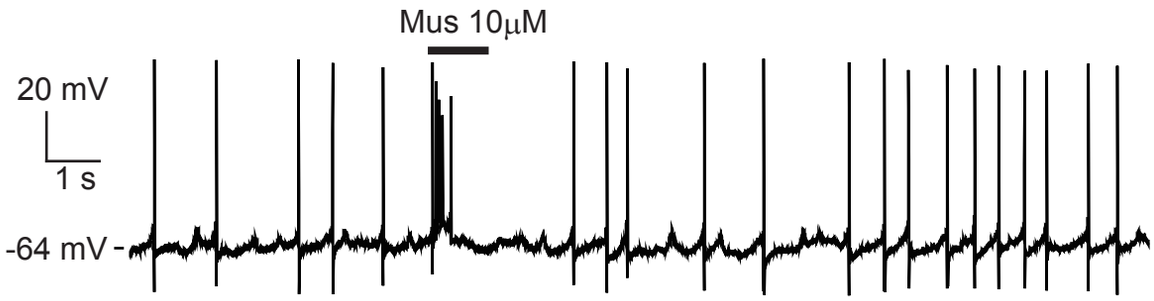

Chapter 3

GnRH3-induced neuromodulation in the optic tectum, one of the major axonal projection areas of the TN-GnRH3 neurons

Abstract

In the previous chapters, I elucidated neural inputs, firing pattern, and neuropeptide release of TN-GnRH3 neurons. Therefore, in Chapter 3, I examined the output of TN-GnRH3 neurons, i.e., the mechanism of GnRH3-mediated neuromodulation in visual information processing.

TN-GnRH3 neurons have massive projections to the optic tectum in teleosts. It has been proposed that synaptic transmission from the optic tract fibers to the deep tectal (SPV) neurons (retino-tectal neurotransmission) is essential for visual processing in the optic tectum. Here, I hypothesized that TN-GnRH3 neurons play an important role in modulating visual information processing according to the sensory information and physiological status of the animal, and examined whether GnRH3, which is a neuropeptide expressed in TN-GnRH3 neurons, modulates the retino-tectal neurotransmission. The results of the present electrophysiological and morphological analyses suggest that GnRH3 modulates the retino-tectal neurotransmission by suppressing the excitability of SPV neurons in the optic tectum through activation of Ca^{2+}-activated K^+ (BK) channels in SPV neurons. This GnRH3-induced modulation of synaptic transmission from the optic tract fibers to SPV neurons should play an important role in the neuromodulation of behaviorally relevant visual information processing according to sensory information and physiological status.

Introduction

TN-GnRH3 neurons are suggested to receive information concerning sensory information and physiological status of the animal (Umatani et al. 2013; Yamamoto and Ito 2000; Zempo et al. 2013) and modulate reproductive behaviors (Yamamoto et al. 1997). These neurons also have massive projections to the optic tectum, which plays an important role in visual processing in teleosts (Amano et al. 2002; Oka and Matsushima 1993; von Bartheld and Meyer 1986). Therefore, I hypothesized that TN-GnRH3 neurons play an important role in modulating visual information processing according to the sensory information and physiological status.

In nonmammalian vertebrates, the retino-tectal neurotransmission in the optic tectum is important for visual processing (Karten and Shimizu 1989; Kinoshita and Ito 2006). It has been proposed that synaptic transmission from the optic tract fibers to the deep tectal (stratum periventricular, SPV) neurons (retino-tectal neurotransmission) is essential for visual processing in the optic tectum (Kinoshita and Ito 2006; Vanegas 1974; Vanegas et al. 1974b). Here, I examined whether GnRH3 modulates the retino-tectal synaptic transmission by analyzing field potentials and the membrane excitability of visual information processing neuron in the dwarf gourami, a teleost fish that has frequently been used for the study of neuromodulatory GnRH neurons (Abe and Oka 2002; Ishizaki et al. 2004; Wirsig-Wiechmann and Oka 2002).

The present field potential analysis revealed that GnRH3 modulates the retino-tectal neurotransmission postsynaptically. Furthermore, I showed that GnRH3 suppresses excitability

of SPV neurons, which have been reported as postsynaptic neurons for the retino-tectal neurotransmission (Kinoshita et al. 2005; Vanegas et al. 1974a; Vanegas et al. 1971), by activating large conductance Ca^{2+}-activated K^+ (BK) channels. Finally, I examined the localization of GnRH receptors in the optic tectum morphologically using an improved method that employs GnRH peptides labeled with fluorescence (GnRH-fluoroprobe). In brain slices treated with GnRH-fluoroprobe, the fluorescent signals were observed mainly near the cell bodies of the SPV neurons. The results of the present electrophysiological and morphological analyses suggest that GnRH3 modulates the retino-tectal neurotransmission by suppressing the excitability of postsynaptic neurons in the optic tectum.

Material and Methods

Animals

Adult male dwarf gouramis (*Trichogaster lalius*), ~5 cm in standard length, were purchased from a local dealer. Each aquarium containing ~20 fish was maintained at 27°C on a 14:10-h light-dark cycle. All fish were fed worms daily. All procedures were reviewed and approved by the appropriate University of Tokyo animal experimentation committee.

Slice preparation

Fish were anesthetized by chilling in ice. I quickly killed them by decapitation and isolated the whole brain. The brain was put in artificial cerebrospinal fluid (ACSF) consisting of (in mM) 134 NaCl, 2.9 KCl, 1.2 $MgCl_2$, 2.1 $CaCl_2$, 10 HEPES, and 10 glucose (pH 7.4 adjusted with NaOH). I embedded the brain in a 3.6% low-melting-temperature agar (agarose type IX-A; Sigma-Aldrich, St. Louis, MO) solution prepared with ACSF. Four hundred micrometer sagittal sections were cut in ACSF containing choline chloride instead of NaCl with a Vibratome 3000 (Leica Biosystems). The brain slices were incubated in ACSF on ice for 1 h and brought back to room temperature before the experiments.

Electrophysiology

For field potential recordings, a slice was placed in a chamber filled with ACSF containing 0.1% BSA to prevent nonspecific binding of peptides to the plastic and glassware. This ACSF was perfused gravitationally at 1–2 ml/min. Recording electrodes were made of borosilicate glass

(GD-1.5; Narishige, Tokyo, Japan) with a Flaming-Brown micropipette puller (P-97; Sutter Instrument, Novato, CA). The borosilicate electrode filled with 0.1% agar in 2 M NaCl was placed 100 m under the surface of the brain slice for recording in the superficial tectal layers [stratum opticum (SO) and stratum fibrosum et griseum superficiale (SFGS)], where the retino-tectal synapses are formed on the distal dendrites of SPV neurons and the largest synaptic responses were recorded (Vanegas 1983; Vanegas et al. 1971), ~200 μm away from the stimulating electrode. The field potential was amplified by AVH-11 (2,000; Nihon Kohden, Tokyo, Japan) and recorded with a Digidata 1322A and pCLAMP 8.2 software (Molecular Devices, Sunnyvale, CA). Electrical stimuli were applied with an electronic stimulator (SEN-3301; Nihon Kohden) through an isolation unit (SS-201J; Nihon Kohden). The bipolar stainless steel electrode consisted of a pair of electrolytically polished stainless steel insect pins, ~10 μm apart and 1 μm in tip diameter, that were lacquer coated, leaving 20- to 30-μm uncoated bare tips. For stimulation of the optic tract fibers, I placed the bipolar stainless steel stimulating electrode in the superficial tectal layers, the main layers of optic tract fiber projections (SO and SFGS). Electrical pulse stimuli of 0.1-ms duration at 0.5–1 mA were applied every 30 s. Synthetic GnRH3 peptides were purchased from GL Biochem (Shanghai, China). Five minutes after the start of recording, GnRH3 was applied for 4 min. I used the following drugs depending on experiments: 6-cyano-7-nitroquinoxaline-2,3-dione (CNQX;

Abcam, Cambridge, UK), Antide (Sigma-Aldrich), and iberiotoxin (IBX; Abcam).

For whole cell recording, the internal solution consisted of (in mM) 100 K-gluconate, 30 KCl, 0.05 EGTA, 4 $MgCl_2$, 10 HEPES, 4 K_2ATP, and 0.5 Na_2GTP. The junction potential was 12 mV, and membrane potentials were adjusted using this value. The tip resistance of patch electrodes in ACSF was 10–15 MΩ. Recordings were performed with an Axopatch 200B patch-clamp amplifier (Molecular Devices). Whole cell current- and voltage-clamp recordings were digitized at 10 kHz and stored on a computer with a Digidata 1322A and pCLAMP 9.2 software (Molecular Devices). For analysis of membrane excitability, I used the minimum response that elicited at least one action potential during current injections of three different intensities (0.01, 0.015, or 0.02 nA).

Luciferase assay

HEK293T cells (70–80% confluent) were cultured in 100-mm dishes. The culture medium contained 5% FBS (Life Technologies, Carlsbad, CA), 4 mM L-glutamine (Wako), and 4.5 g of Dulbecco's modified Eagle's medium (Nissui Pharmaceutical) in 500 ml of water. Thirty microliters of polyethylenimine (PEI, Polyethylenimine "Max"; Polysciences, Warrington, PA) and 1.5 ml Opti-MEM (Life Technologies) were mixed and incubated for 5 min. I then added the following constructs into another 1.5 ml of Opti-MEM: 5.5 μg of each GnRH receptor (gift from Dr. K. Okubo; Okubo et al. 2001, 2003), 9 μg of firefly luciferase vector

(pGL4.33[luc2P/SRE/Hygro] vector; Promega, Madison, WI), and 0.5 μg of Renilla luciferase vector (pGL4.74[hRluc/TK] vector; Promega). After incubation in PEI solution, both Opti-MEM solutions were mixed and incubated for 20 min at room temperature. I then replaced the culture medium with mixed transfection solution and incubated the dish at 37°C overnight. The transfected HEK cells were then subcultured into 24-well plates in a culture medium containing 1% FBS. Eighteen hours later, 1μM GnRH2 or 1 μM fluorescence probe in the culture medium containing 1% FBS (vehicle) or the vehicle only was applied for 6 h. GnRH-fluoroprobes [pGlu-His-Trp-Ser-His-D-Lys(N^{ε}-FAM)-Trp-Tyr-Pro-Gly-NH_2 (GnRH-FL) and pGlu-His-Trp-Ser-His-D-Lys(N^{ε}-TAMRA)-Trp-Tyr-Pro-Gly-NH_2 (GnRH-TAMRA)] were designed based on a previous report (Hazum et al. 1980). Probes were synthesized with standard Fmoc-based solid-phase peptide synthesis by Dr. Misu and Dr. Oishi (Oishi et al. 2008). Cells were collected and the luminescence measured by LUMAT LB9507 (Berthold Technologies) according to the manual for the Dual-Luciferase Reporter Assay System (Promega).

Analysis of localization of GnRH receptors in HEK cells

For morphological observation, HEK cells were cultured on poly-L-lysinecoated glass (Matsunami Glass Industries) in 60-mm dishes. HEK293T cells were transfected with GnRH receptor (1 μg/60-mm dish) and EGFP-N1 (0.4 μg/dish; Takara) with PEI (2.88 μl/dish) as described above. After two overnight incubations, each glass covered with cells was put in a 24-

well plate filled with serum-free medium. Thirty minutes later, HEK cells were incubated with 1 μM GnRH-fluoroprobe or plain serum-free medium for 30 min at 37°C. I then washed cells with PBS twice and examined them under a LSM-710 confocal laser-scanning microscope (Carl Zeiss) at 1-μm optical section.

Analysis of localization of GnRH receptors with fluoroprobes

Two hundred-micrometer-thick frontal slices were used for the analysis. Brain sections were cut as described above and incubated at room temperature for 1 h after slicing. To block nonspecific binding, the slices were treated with 0.1% BSA-ACSF for 30 min and then the fluorescence probe solution or vehicle control was applied for 1 h. The GnRH-fluoroprobe (GnRH-FL) was designed based on a previous report (Hazum et al. 1980). I chose GnRH2 as the backbone of GnRH-fluoroprobe because GnRH2 shows the highest affinity for each GnRH receptor in fish for GnRH1-3 (Illing et al. 1999; Okubo et al. 2003; Okubo et al. 2001). The probe was synthesized with standard Fmoc-based solid-phase peptide synthesis (Oishi et al. 2008). After application of the GnRH-fluoroprobe, the brain slices were fixed with 4% PFA-PBS at 4°C overnight. The slices were then incubated for 6–8 h with a mouse antiserum against fluorescein, diluted 1:1,000 in the blocking solution. For analysis of localization of GnRH receptors with fluoroprobes, the signals were intensified by sequentially incubating the slices in biotinylated anti-mouse IgG (Vector Laboratories, Burlingame, CA) for 6–8 h, the ABC kit (Vector

Laboratories) in PBST for 30–45 min, and streptavidin-Alexa 555 for 4 h. Nuclei were counterstained with Hoechst 33342 (Life Technologies). The slices were then mounted on slides and coverslipped with CC/Mount (Diagnostic BioSystems, Pleasanton, CA). The slides were examined and photographed with a LSM-710 confocal laser-scanning microscope (Carl Zeiss), and the resulting images were analyzed with ImageJ software with the MBF ImageJ plug-ins (Tony Collins, McMaster University). All images were captured in the same exposure condition, and I used the same brightness and contrast values for ImageJ in all three groups.

Statics

Statistical analyses were performed with Kyplot5 software (Kyence, Tokyo, Japan) and IGOR Pro 6 software (WaveMetrics, Lake Oswego, OR) with the Taro tool (an IGOR macro set written by Dr. Taro Ishikawa, Jikei University School of Medicine). Different statistical tests were used for different experiments, as described in RESULTS. All data in the present study are presented as means ± S.E.M

Results

GnRH3 modulates retino-tectal neurotransmission

I examined whether GnRH3 modulates retino-tectal neurotransmission by stimulating optic tract fibers and recording the evoked local field potential (LFP) from the synaptic region of SPV neurons (Vanegas et al. 1974b). Because the tectal neurons form distinctive layers and show characteristic LFPs in each layer, field potential recordings have often been used in analyses of retinotectal neurotransmission (Vanegas et al. 1971; Vanegus 1983). The field potential evoked by electrical stimulation is shown in Fig. 3-1, A and B. The first large positive peak indicates an artifact produced by stimulation and almost masks the presynaptic responses. The subsequent large negative wave most probably represents the postsynaptic response of the SPV neurons in the optic tectum (Kinoshita and Ito 2006; Vanegas et al. 1974a). This synaptic transmission is likely monosynaptic (Kinoshita and Ito 2006; Vanegas et al. 1974b). Because the negative waves were almost completely blocked by 20 μM CNQX (Fig. 3-1A), they probably reflect glutamatergic neurotransmission. Thus, the negative waves are at least suggested to contain monosynaptic glutamatergic current components of SPV neurons in response to optic tract fiber stimulation. It should be noted, however, that the negative waves have also been suggested to contain regenerative population spike components (see Vanegas 1983 as well as DISCUSSION). The evoked LFPs were then recorded and compared with those in the presence of GnRH3. Figure 3-1B shows representative traces before, during, and after GnRH3 application. GnRH3

application increased the rise time from 10% to 90% of peak amplitude (Fig. 3-1C) and the negative wave duration measured at half-maximum amplitude (Fig. 3-1D). These effects were diminished by Antide, which is a GnRH receptor antagonist (Fig. 3-1C: vehicle: 91.8 ± 3.9%, GnRH3: 134.0 ± 15.9%, GnRH3 + Antide: 93.9 ± 4.2%; Steel's test, $P < 0.05$, Fig. 3-1D: vehicle: 95.9 ± 1.4%, GnRH3: 115.8 ± 4.1%, GnRH3 + Antide: 98.1 ± 3.1%; Steel's test, $P < 0.01$). On the other hand, the peak amplitudes of the field potentials were not significantly affected by GnRH3 application [Fig. 3-1E; vehicle: 98.8 ± 1.0%, GnRH3: 92.6 ± 6.0%, GnRH3 + Antide: 102.2 ± 7.4%; Steel's test, nonsignificant (n.s.)]. Overall, the present results indicated that GnRH3 modulated the shape of LFPs evoked by stimulation of optic fibers, which is suggested to be mediated by the GnRH receptors (see below).

GnRH3 modulates LFP postsynaptically

I used the paired-pulse ratio (PPR) to determine whether GnRH3-induced modulation is a presynaptic or postsynaptic effect. Comparing the PPR (ratio of amplitude of the responses to the first and second stimulations) before and after treatment allows one to determine whether the effect is pre- or postsynaptic (Manabe et al. 1993); if the PPR changes after treatment the modulation is suggested to be presynaptic, and vice versa. Figure 3-2A shows the LFP in response to paired stimulation of retino-tectal fibers at an interval of 150 ms (Kawai et al. 2010). Figure 3-2B shows the time course of the PPR. Given that the PPRs appear not to change before and after

GnRH application, the results suggest that GnRH3-induced modulation is mainly postsynaptic.

GnRH3 suppresses excitability of visual processing neurons in optic tectum.

In the optic tectum, SPV neurons receive direct synaptic inputs from optic tract fibers and project to the other brain regions. SPV neurons are thought to play a principal role in visual information processing in the teleost optic tectum (Kinoshita et al. 2005; Kinoshita and Ito 2006; Vanegas 1974; Vanegas et al. 1974b). The data presented in Figs. 3-1 and 3-2 suggest that GnRH3 modulates these postsynaptic SPV neurons. For further analysis of the postsynaptic mechanism induced by GnRH3, I examined effects of GnRH3 on the excitability of SPV neurons with whole cell patch-clamp recording. I generated action potentials in SPV neurons by applying a series of current steps (50 ms, 0.01– 0.02 nA) through a recording whole cell pipette. Figure 3-3A–C, show representative action potentials of a SPV neuron before (Fig. 3-3A), during (Fig. 3-3B), and after (Fig. 3-3C) application of GnRH3. As illustrated in Fig. 3-3B, the number of action potentials decreased during application of GnRH3. The normalized response for each condition is plotted in Fig. 3-3D; the y-axis indicates the response normalized by the spike number evoked by the minimum current step before GnRH3 application. GnRH3 markedly suppressed the ability of spike generation in the SPV neurons (before: 100%, GnRH3: 45.3 ± 17.3%, washout: 107.1 ± 7.1%; ANOVA and Tukey-Kramer test, n =7 in each group, $P < 0.01$). The result clearly demonstrates that GnRH3 suppressed the excitability of SPV neurons in the optic tectum.

GnRH3 activates large-conductance Ca^{2+}-activated K^+ channel

To analyze the ionic mechanisms underlying GnRH3-induced modulation, I compared the current-voltage relationships of SPV neurons with or without GnRH3 application. I applied ramp stimulation (Fig. 3-4A, inset) and analyzed the current-voltage relationship before, during, and after GnRH3 application under voltage clamp (Fig. 3-4A). The results indicate that the current increased during GnRH3 application and recovered after washout to the level before application. The reversal potential (calculated by the point of intersection of during and before lines) was -85.6 ± 2.4 mV (n = 7), which was near the calculated reversal potential for potassium, -97mV. Therefore, this result suggests that GnRH3 modulates one or more K^+ conductance. Because GnRH receptors are coupled to $G_{q/11}$ protein (Naor et al. 1995; Stojilkovic et al. 1994a), GnRH3 is expected to modulate the current-voltage relationships via modulation of K^+ conductance(s) activated by intracellular Ca^{2+} increase. To examine whether Ca^{2+}-activated K^+ channels are modulated by GnRH3, I analyzed the GnRH3-induced current recorded in plain ACSF or in ACSF containing IBX, a blocker of BK channel (Waring and Turgeon 2009). Figure 3-4B shows the GnRH3-induced current [(current during GnRH3 application) - (current before GnRH3 application)]. The GnRH3-induced current was almost completely blocked by IBX application. This result suggests that GnRH3 suppresses the excitability of SPV neurons by activating BK channels.

Next I examined whether blockage of BK channel diminishes the GnRH3-induced modulation of the field potential. I performed the field potential recording as shown in Fig. 3-1B while blocking BK channels by perfusing IBX during the entire recording (Fig. 3-5). When GnRH3 was applied in the presence of IBX, the GnRH3-induced modulation of the field potential was nullified (Fig. 3-5A); as shown in Fig. 5, B and C, the differences in rise time and the duration measured at half-maximum amplitude were not significant (Fig. 3-5B: vehicle: 100.6 ± 0.2% vs. GnRH3: 98.3 ± 1.9%; Student's t-test, n.s.; Fig. 3-5C: vehicle: 99.0 ±2.0% vs. GnRH3: 103.0 ± 3.6%; Student's t-test, n.s.). This result strongly suggests that GnRH3 modulates retino-tectal neurotransmission by activating BK channels of the SPV neurons postsynaptically.

Localization of GnRH receptors in optic tectum

Finally, I examined the localization of GnRH receptors in SPV neurons in brain slices with a slight modification of a method involving fluorescently labeled GnRH peptides (GnRH-fluoroprobe) developed for dissociated cells (Hazum et al. 1980; Hazum and Nimrod 1982; Lloyd and Childs 1988). Because technical difficulties so far have prevented analysis of the localization of GnRH receptors by immunohistochemistry or *in situ* hybridization in the brain, I here examined the localization of GnRH receptors in the optic tectum by an improved method using GnRH-fluoroprobe. I first demonstrated that synthesized fluoroprobe selectively binds to GnRH

receptors with a luciferase assay and a morphological binding assay (Fig. 3-6A, B). In luciferase assay, GnRH-fluoroprobes, GnRH-TAMRA and GnRH-fluorescein, showed almost the same activity as GnRH2 in each experiment using cells expressing each subtype of GnRH receptor (Fig. 3-6A). Moreover, after incubation with GnRH-TAMRA, the signals of GnRH-fluoroprobe were localized near the membrane of cells expressing each GnRH receptor (Fig. 3-6B). Some dotted signals were also observed in the cytoplasm, which may represent internalization of GnRH receptors (Hazum et al. 1980; Hazum and Nimrod 1982). Therefore, the GnRH-fluoroprobes are considered to work physiologically like the native GnRH. I used fluorescein-labeled GnRH for brain slices because the fluorescein signals can be amplified by immunohistochemical methods. GnRH-fluoroprobe was applied for 1 h and was amplified with the methods described in MATERIALS AND METHODS. Figure 3-7 shows GnRH-fluoroprobe signal (Fig. 3-7A), Hoechst nuclear counterstain (Fig. 3-7B), and overlay (Fig. 3-7C and D) in the optic tectum. As shown in Fig. 3-7C and D, the GnRH-fluoroprobe signals were observed to surround the cell bodies of the SPV neurons (Fig. 3-7Aa, Ca, and Da). Vehicle application did not result in specific binding (Fig. 3-7Ab, Cb, and Db). The binding of the fluoroprobe was competitively inhibited by a high dose (10 μM) of nonlabeled GnRH3 peptide (Fig. 3-7Ac, Cc, and Dc). The binding of fluoroprobes on synaptic terminals was hard to detect, indicating that the concentration of GnRH receptors in the terminals is very low (Maruska and Tricas 2007). The results of the GnRH-

fluoroprobe experiment provide morphological supports for the hypothesis that GnRH3 modulates postsynaptic neurons, the SPV neurons, indicated by the present electrophysiological results.

Discussion

In the present study, I showed that GnRH3 modulates retino-tectal neurotransmission postsynaptically. GnRH3 increased the rise time and the duration measured at half maximum amplitude of the field potentials evoked by optic tract fiber stimulations. GnRH3 also suppressed the excitability of SPV neurons by activating BK channels. The present morphological analysis using a GnRH-fluoroprobe indicated that SPV neurons express GnRH receptors.

GnRH3 suppresses excitability of SPV neurons and modulates LFPs by activating BK channels via GnRH receptors

I first analyzed field potentials, which represent monosynaptic neurotransmission from optic tract fibers to SPV neurons in the optic tectum (Vanegas et al. 1974a; Vanegas et al. 1974b). The results of analysis showed that GnRH3 modulates the field potential, and the present PPR analysis indicates that the modulatory effects are postsynaptic. I then showed that GnRH3 suppresses the excitability of SPV neurons by activating BK channels. It has been generally accepted that currents that are induced by BK channels decrease the number of action potentials and thereby suppress the excitability of neurons (Arias-Garcia et al. 2013; Sun and Dale 1998).

I next analyzed the distribution of GnRH-fluoroprobe binding sites as a way to examine the localization of GnRH receptors. Previous immunohistochemical studies in teleost brains indicated that TN-GnRH3 neurons have massive projection to the deep layers [stratum album centrale (SAC) and stratum griseum centrale (SGC)] and sparse projection to the surface layers in the optic

tectum (Maruska and Tricas 2007; Oka and Ichikawa 1990). On the other hand, the optic tract fibers mainly project to the superficial layers (SO and SFGS, where I recorded LFPs) and also sparsely to SAC and SGC (Maruska and Tricas 2007; von Bartheld and Meyer 1987). The present analysis of the localization of GnRH receptors in the optic tectum with GnRH-fluoroprobe showed that GnRH receptors are expressed in SPV neurons. Taken together, these results suggest that TN-GnRH3 neurons mainly act on the cell bodies of the SPV neurons in the deep layer of the optic tectum.

Figure 3-8 schematically shows the hypothetical model (Fig. 3-8A), the GnRH3-induced modulation of the field potential (Fig. 3-8B), and SPV neuron action potentials (Fig. 3-8C). I illustrated the schematic diagram in Fig. 3-8B by referring to Vanegas (1983), who suggested that the long dendrite of the SPV neuron possesses an ability to generate regenerative action potentials, and Rall and Shepherd (1968), who also suggested the presence of active dendrites of the mitral cell. I further assumed that the LFP evoked by optic nerve stimulation represents superimposition of excitatory postsynaptic potentials (EPSPs) and back-propagated dendritic spikes. The dashed and solid lines in Fig. 3-8B indicate the LFP before and during GnRH3 application, respectively. Although the difference in the anatomical localization of GnRH receptors (somatic region of SPV neurons in deep layer) and recording site of the LFPs (synaptic region in superficial layer) may appear puzzling at first sight, the above-mentioned interpretation of the LFP can reasonably

explain the present experimental results. Actually, Vanegas (see Fig. 1,Vanegas et al. 1974a; p. 59 and 60,Vanegus 1983) suggested that the negative component of the LFP evoked by the stimulation of optic nerve in fish optic tectum was the superimposition of extracellularly recorded EPSPs and regenerative population spikes. He also suggested that the rise time and duration of the LFP evoked by optic tract fiber stimulation change as shown in Fig. 3-8B (present study), when the number of action potentials of SPV neurons was experimentally decreased.

In summary, considering the present electrophysiological and morphological results, I propose a model of GnRH3-induced modulation of retino-tectal neurotransmission (Fig. 3-8A). First, GnRH3 activates BK channels in SPV neurons, suppressing the excitability of those neurons (Fig. 3-8C). Then the number of synaptically driven action potentials in SPV neurons evoked by optic tract fiber stimulation is decreased because GnRH3 suppresses excitability. As a result, the rise time and the duration of the LFP increase (Fig. 3-8B).

Possible intracellular mechanisms of GnRH3-induced modulation.

Here I discuss possible intracellular mechanisms of GnRH3-induced modulation. Although one previous study in rainbow trout examined GnRH-induced modulation of retino-tectal neurotransmission (Kinoshita et al. 2007), the study did not analyze the mechanisms in detail. The results of the present study suggest the following mechanisms. It has been reported that GnRH receptors are $G_{q/11}$ protein-coupled receptors (Naor et al. 1995; Stojilkovic et al. 1994a).

The $G_{q/11}$-type G proteins are coupled to the phospholipase C-mediated signaling pathway (Naor et al. 1995; Stojilkovic et al. 1994a; Stojilkovic et al. 1994b). By activating this pathway, GnRH3 induces intracellular Ca^{2+} increase due to release from IP3-sensitive Ca^{2+} stores (Abe and Oka 2002; Karigo et al. 2014). This intracellular Ca^{2+} increase is considered to activate BK channels. On the other hand, phospholipase C-mediated signaling pathways also induce diacylglycerol production (Naor et al. 1995). Diacylglycerol can be converted to arachidonic acid, and arachidonic acid in turn activates BK channels in mouse vomeronasal neurons (Zhang et al. 2008). One or both of these pathways, intracellular Ca^{2+} increase and/or arachidonic acid modulation, may operate in SPV neurons and suppress the excitability of SPV neurons via activation of BK channels. In the presence of an intracellular solution with high EGTA (1 mM) and no GTP, GnRH3 did not induce a K^+ current (data not shown), which strongly supports my hypothesis that GnRH3 activates BK channels by causing an increase in intracellular Ca^{2+}. Similar modulation of BK channels by GnRH has also been reported in previous studies of gonadotrophs (Sikdar et al. 1989; Waring and Turgeon 2009). Previous studies of modulation of neuronal excitability by GnRH have focused on facilitation caused by inhibition of the K^+ M current (Brown 1988). Thus, to my knowledge, the present study is the first to show the inhibition of neuronal excitability by GnRH3.

Expected physiological functions of GnRH3-induced modulation.

Retino-tectal neurotransmission plays a central role in visual processing in nonmammalian

vertebrates (Karten and Shimizu 1989; Kinoshita and Ito 2006). Tectal neurons in vertebrates receive visual inputs in the surface layer and somatosensory inputs in the deep layer, integrate them, and use this input to select appropriate behaviors (Butler and Hodos 1996; Finlay et al. 1978; Llinas and Precht 2012). The present study contributes to my understanding of GnRH3-induced modulation of visual processing in the optic tectum. I demonstrated that GnRH3 suppresses the excitability of postsynaptic neurons via BK channels, thereby modulating retino-tectal neurotransmission. This modulation of visual information processing could have several effects. For example, it is possible that habituation of visual information processing (Northmore and Gallagher 2003) is prevented by suppressing the excitability of projection neurons. GnRH3-induced modulation may expand the dynamic range of optic tectum response to visual input, as is the case in modulation of auditory system via BK channels (Kurt et al. 2012). Some animals showed odor-induced neuromodulation of visual processing and odor-induced change of visual dependent behavior (Maaswinkel and Li 2003; Seo et al. 2010; Stephenson et al. 2012), or stress-related change of visual evoked response (Champney et al. 1976). Therefore, GnRH3-induced modulation of synaptic transmission from optic tract fibers to SPV neurons should play an important role in the neuromodulation of behaviorally relevant visual information processing according to sensory information and physiological status.

Figure legends

Figure 3-1 GnRH3 modulates the field potential of retino-tectal neurotransmission

A: Field potentials evoked by electrical stimulation of optic tract fibers (average of three traces) before (solid black line) and during 20 μM CNQX (dotted gray line) application. The first large positive peak represents an artifact, and the subsequent large negative peak indicates the postsynaptic response of the SPV neurons. B: Field potentials evoked by electrical stimulation of optic tract (average of three traces) before (dotted black line), during (solid black line), and after GnRH3 application (solid gray line). C~E: Rise time (C), duration measured at half maximum amplitude (D), and peak amplitude (E) in vehicle, GnRH3 (100 nM) or GnRH3 (100 nM) plus antide (1 μM). All values were normalized by dividing the average of three trials during GnRH3 application (two minutes after application) to the average of three trials measured 2.5 minutes after the start of recording. In the box plot, bottom and top bars are minimum and maximum of each group respectively, the box is the quartile area, and the middle horizontal bar shows the median. Data were analyzed using Steel's multiple comparison test (*: $p < 0.05$, **: $p < 0.01$).

Figure 3-2 GnRH3 modulates field potentials postsynaptically

A: Field potentials in response to paired stimulation of retino-tectal fibers (average of three traces) before (dotted line) and during GnRH3 (solid line). B: Time course of the paired pulse ratio ($n = 6$). In the box plot, bottom and top bars are minimum and maximum of each group

respectively, box is quartile area, and the horizontal bar in the middle shows the median.

Figure 3-3 GnRH3 suppress the excitability of SPV neurons

A-C: The action potential responses of SPV neurons evoked by current injection (bottom inset) before (A), during (B), and after application of 1 μM GnRH3 (C). D: The normalized response before, during, and after application of 1 μM GnRH3. The vertical axis indicates the response normalized by the minimum spike number before GnRH3 application. n = 7 for each group. Data were analyzed using ANOVA and Tukey Kramer's test (**: $p < 0.01$). Error bars indicate S.E.M. before: 1min before GnRH3 application, during: 2 min after GnRH3 application, after: 5 min after finishing GnRH3 application.

Figure 3-4 GnRH3 modulates the large conductance Ca^{2+}-activated K^+ channel

A: Current-voltage relationship before (dotted line), during (black line), or after application of 1 μM GnRH3 (gray line) during the falling phase of the ramp stimulation (dotted rectangle in inset). Inset shows the entire ramp protocol. Inset scale: 50 mV, 1.5 ms. before: 1min before GnRH3 application, during: 2 min after GnRH3 application, after: 5 min after finishing GnRH3 application. B: GnRH3-induced current calculated by subtracting the current before GnRH3 application from the current during GnRH3 application. n = 7 for 1 μM GnRH3: black dot, n = 4

for 1 μM GnRH3 with 100 nM Iberiotoxin (IBX): dark gray dot. The vertical bar through each symbol indicates the S.E.M.

Figure 3-5 GnRH3 modulates retino-tectal neurotransmission via large conductance Ca^{2+}-activated K^+ channel

A: Field potentials evoked by electrical stimulation of the optic tract (average of three traces) in the presence of 100 nM Iberiotoxin (IBX) before (gray dotted line) and during 100 nM GnRH3. B, C: Normalized rise time (B) and duration measured at half maximum amplitude (C) during application of vehicle or GnRH3 (100 nM) in the presence of IBX. There was no significant statistical difference between vehicle and GnRH3 in B, C (n = 5, Student's t-test). before: 1 min before GnRH3 application, during: 2 min after GnRH3 application. In the box plot, bottom and top bars are minimum and maximum of each group respectively, 688 box is quartile area, and the horizontal bar in the middle indicates the median.

Figure 3-6 GnRH-fluoroprobes increase luciferase activity and bind to GnRH receptors expressed in HEK293T

A: Luciferase activity after 6 hours' incubation with either GnRH-fluoroprobe or GnRH2 is shown. GnRH-FL: GnRH labeled with fluorescein, GnRH-TAMRA: GnRH labeled with

TAMRA. Data were analyzed using Dunnett's multiple comparison test (GnRHR1: n = 4 in each group, GnRHR2: n = 5 in each group, GnRHR3: n = 4 in each group; *: $p < 0.05$, **: $p < 0.01$, ***: $p < 0.001$). B: Signals of GnRH-fluoroprobe (upper row), EGFP (the middle row), and overlay images (lower row). In the overlay images, the GnRH-fluoroprobe signal is magenta and EGFP is green. GnRH-fluoroprobe was applied at 1 μM. Scale bar: 50 μm. Some dotted signals were also observed in the cytoplasm, which may represent internalization of GnRH receptors (Hazum et al. 1980; Hazum and Nimrod 1982). Therefore, the GnRH-fluoroprobes are considered to work physiologically like the native GnRH.

Figure 3-7 GnRH receptors are mainly localized in SPV neurons

A: Fluorescent signals of GnRH-fluoroprobe (GnRH-FL), B: signals of Hoechst nuclear stain, C: overlay images, and D: the magnified overlay images of the area indicated in white squares in C, in the presence of 1 μM GnRH-fluoroprobe (a), vehicle (b), and 1 μM GnRH-fluoroprobe plus 10 μM GnRH3 (c). Each photograph is representative from three trials. In the overlay images, magenta is GnRH-fluoroprobe, and green is Hoechst. Scale bar: 20 μm (C), 10 μm (D)

Figure 3-8 Hypothetical model of GnRH3-induced modulation of retino-tectal neurotransmission

A: Experimental arrangement and schematic image of GnRH3-induced modulation of retino-

tectal neurotransmission. B: Schematic diagram of LFP illustrated following Venegas (Vanegus 1983) and Rall & Shepherd (Rall and Shepherd 1968). Dotted line: field potential before GnRH3 application. Solid line: field potential during GnRH3 application. The negative component of the LFP evoked by the stimulation of optic nerve in the optic tectum is based on the assumption that the LFP is the superimposition of extracellularly recorded EPSPs and regenerative population spikes. C: Illustration of the result of whole-cell recording of SPV neurons evoked by current injection showing that the excitability of SPV neurons is suppressed by GnRH3.

Figure 3-1

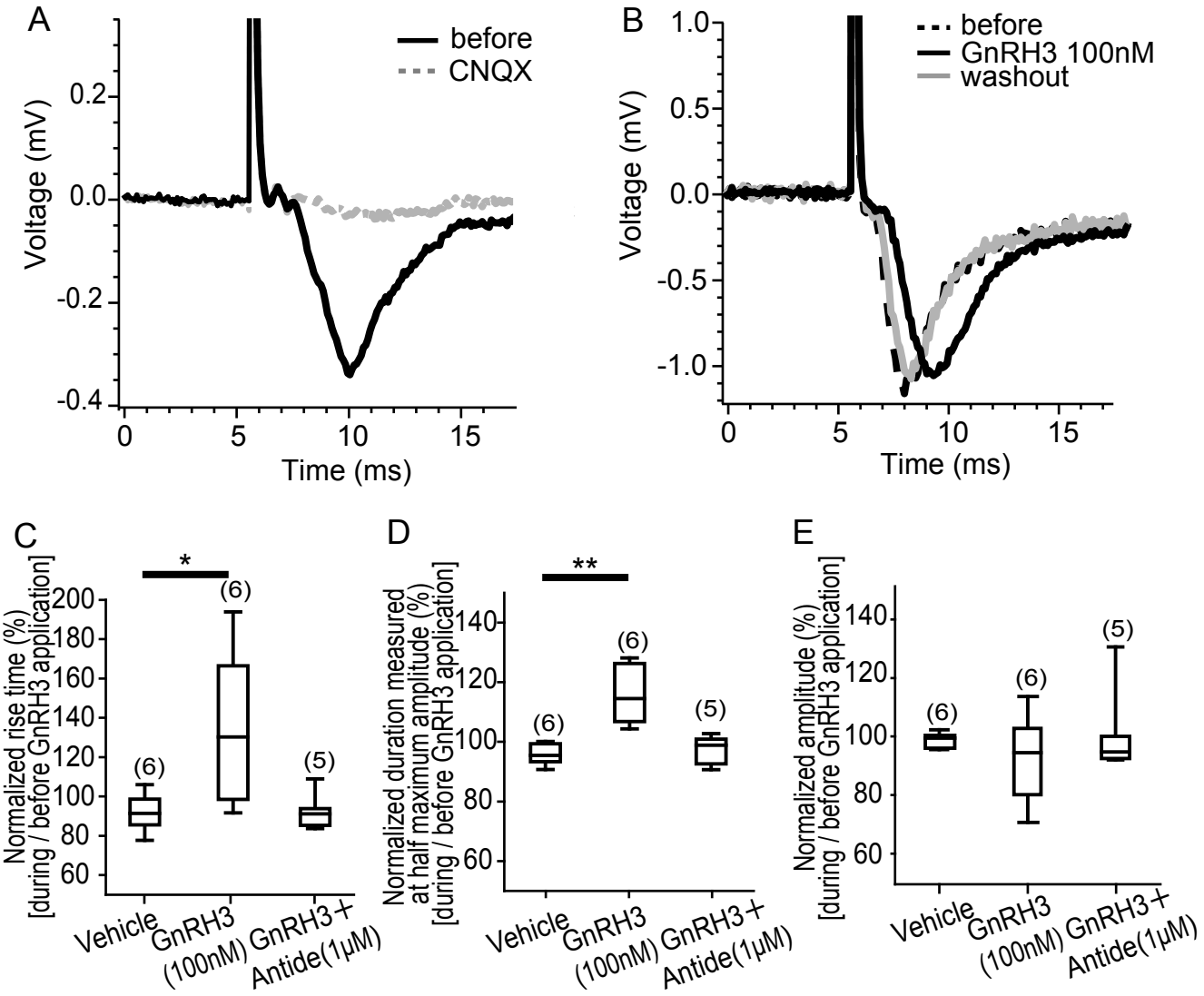
A
before
CNQX
Voltage (mV)
Time (ms)
B
before
GnRH3 100nM
washout
Voltage (mV)
Time (ms)
C
Normalized rise time (%)
[during / before GnRH3 application]
*
(6)
(6)
(5)
Vehicle
GnRH3 (100nM)
GnRH3+ Antide(1μM)
D
Normalized duration measured at half maximum amplitude (%)
[during / before GnRH3 application]
**
(6)
(6)
(5)
Vehicle
GnRH3 (100nM)
GnRH3+ Antide(1μM)
E
Normalized amplitude (%)
[during / before GnRH3 application]
(6)
(6)
(5)
Vehicle
GnRH3 (100nM)
GnRH3+ Antide(1μM)

Figure 3-2

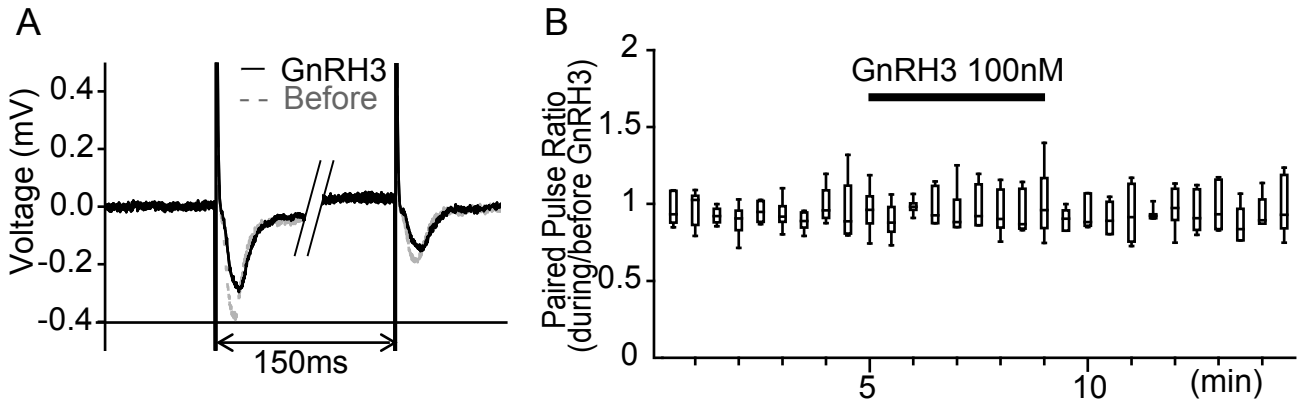
A
GnRH3
Before
Voltage (mV)
0.4
0.2
0.0
-0.2
-0.4
150ms
B
GnRH3 100nM
Paired Pulse Ratio
(during/before GnRH3)
2
1.5
1
0.5
0
5
10
(min)

Figure 3-3

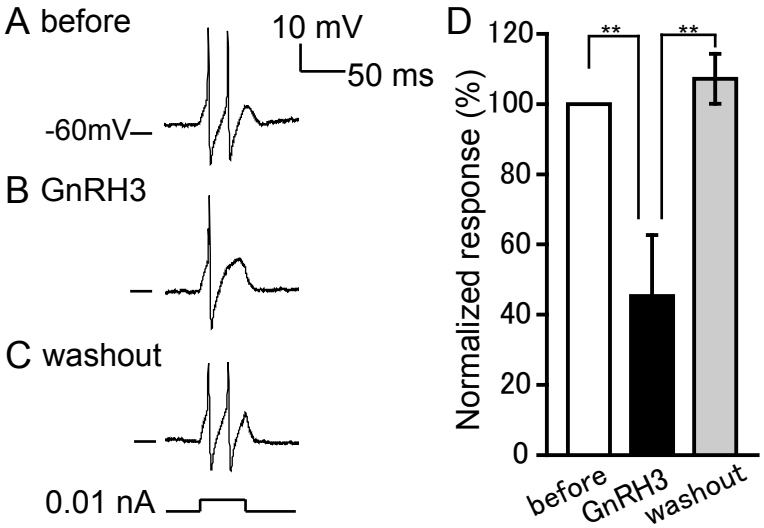
A before
10 mV
50 ms
-60mV
B GnRH3
C washout
0.01 nA
D
Normalized response (%)
120
100
80
60
40
20
0
**
**
before
GnRH3
washout

Figure 3-4

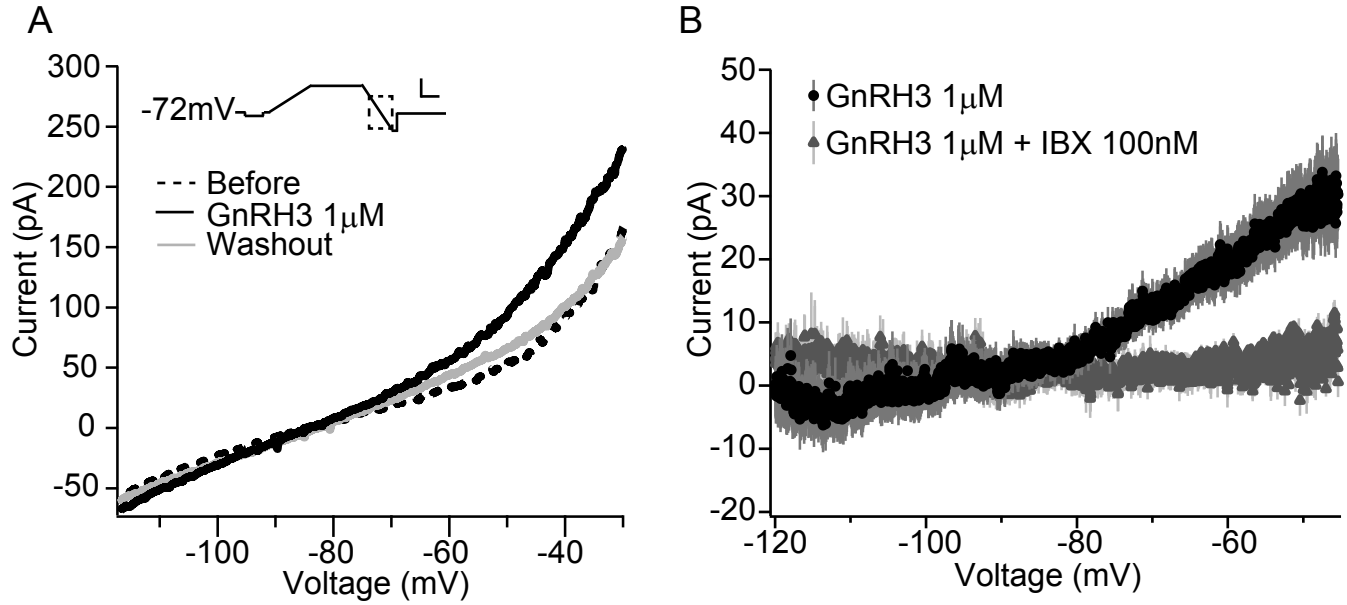
A
300
250
200
150
100
50
0
-50
-72mV
Before
GnRH3 1μM
Washout
Current (pA)
-100
-80
-60
-40
Voltage (mV)
B
50
40
30
20
10
0
-10
-20
GnRH3 1μM
GnRH3 1μM + IBX 100nM
Current (pA)
-120
-100
-80
-60
Voltage (mV)

Figure 3-5

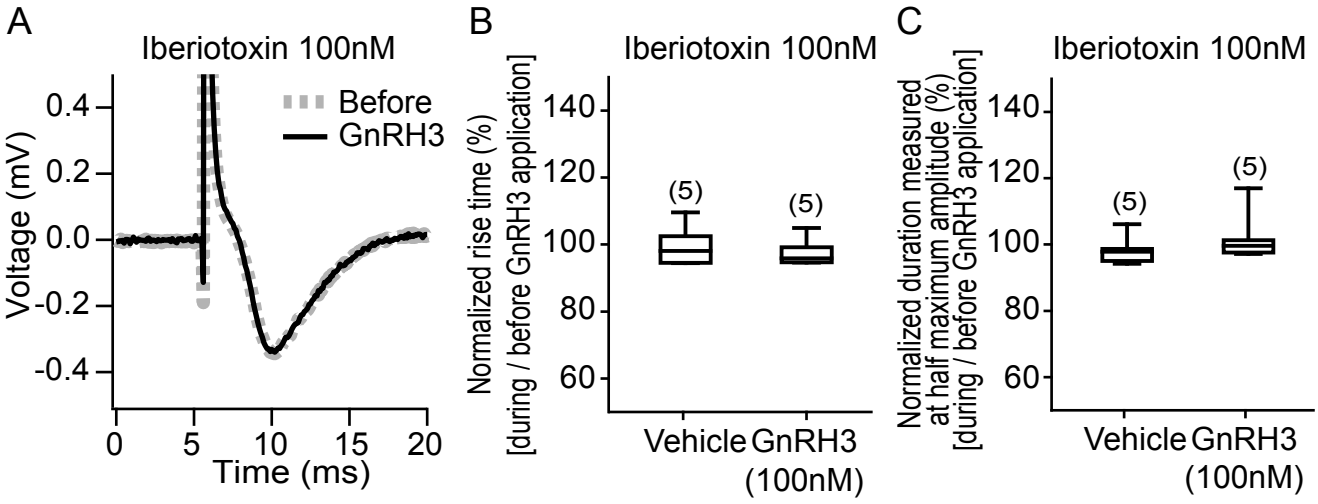
A
Iberiotoxin 100nM
Before
GnRH3
Voltage (mV)
0.4
0.2
0.0
-0.2
-0.4
0
5
10
15
20
Time (ms)
B
Iberiotoxin 100nM
Normalized rise time (%)
[during / before GnRH3 application]
140
120
100
80
60
(5)
(5)
Vehicle
GnRH3
(100nM)
C
Iberiotoxin 100nM
Normalized duration measured
at half maximum amplitude (%)
[during / before GnRH3 application]
140
120
100
80
60
(5)
(5)
Vehicle
GnRH3
(100nM)

Figure 3-6

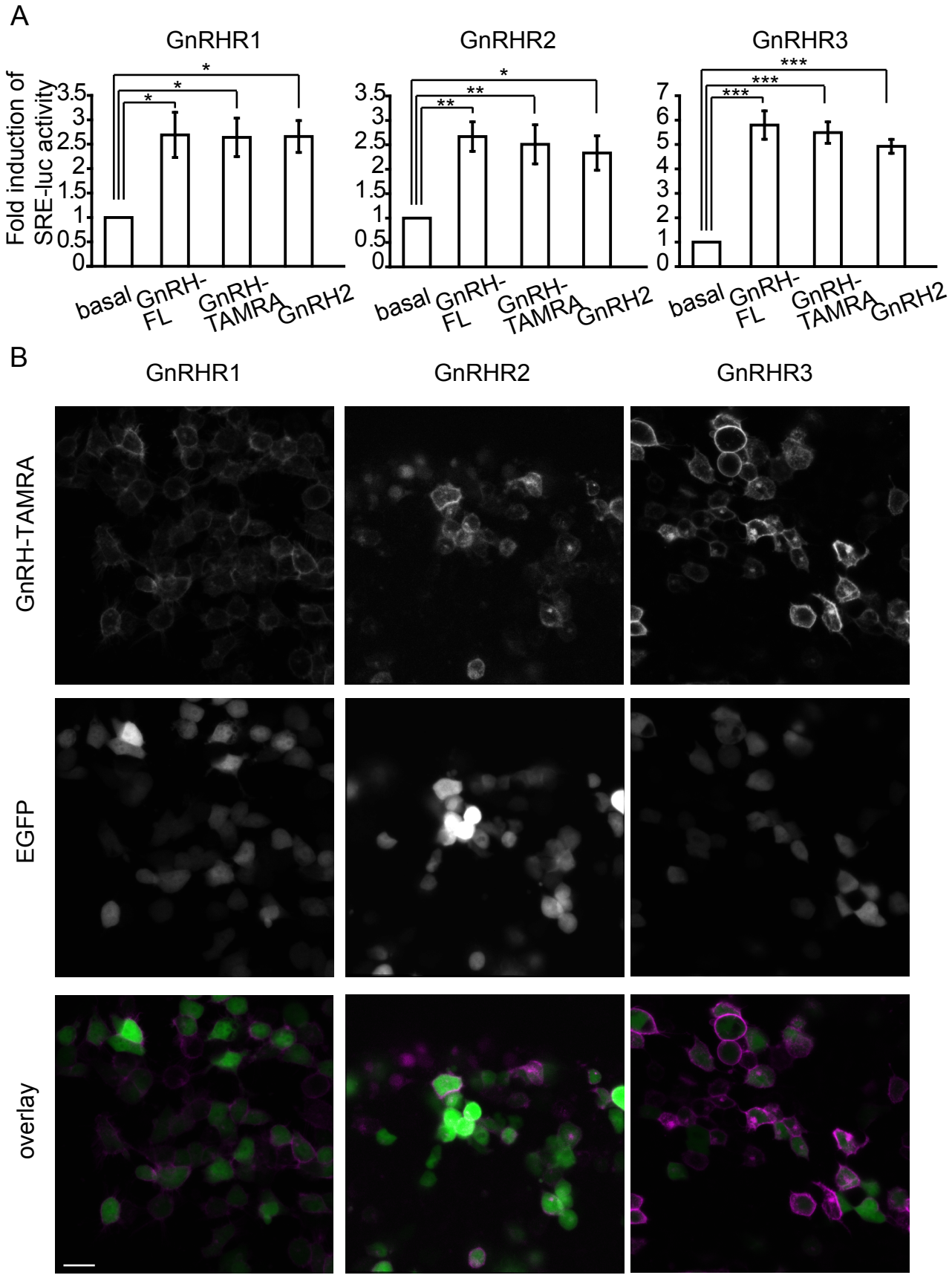
A
GnRHR1
GnRHR2
GnRHR3
Fold induction of SRE-luc activity
basal
GnRH-FL
GnRH-TAMRA
GnRH2
B
GnRHR1
GnRHR2
GnRHR3
GnRH-TAMRA
EGFP
overlay

Figure 3-7

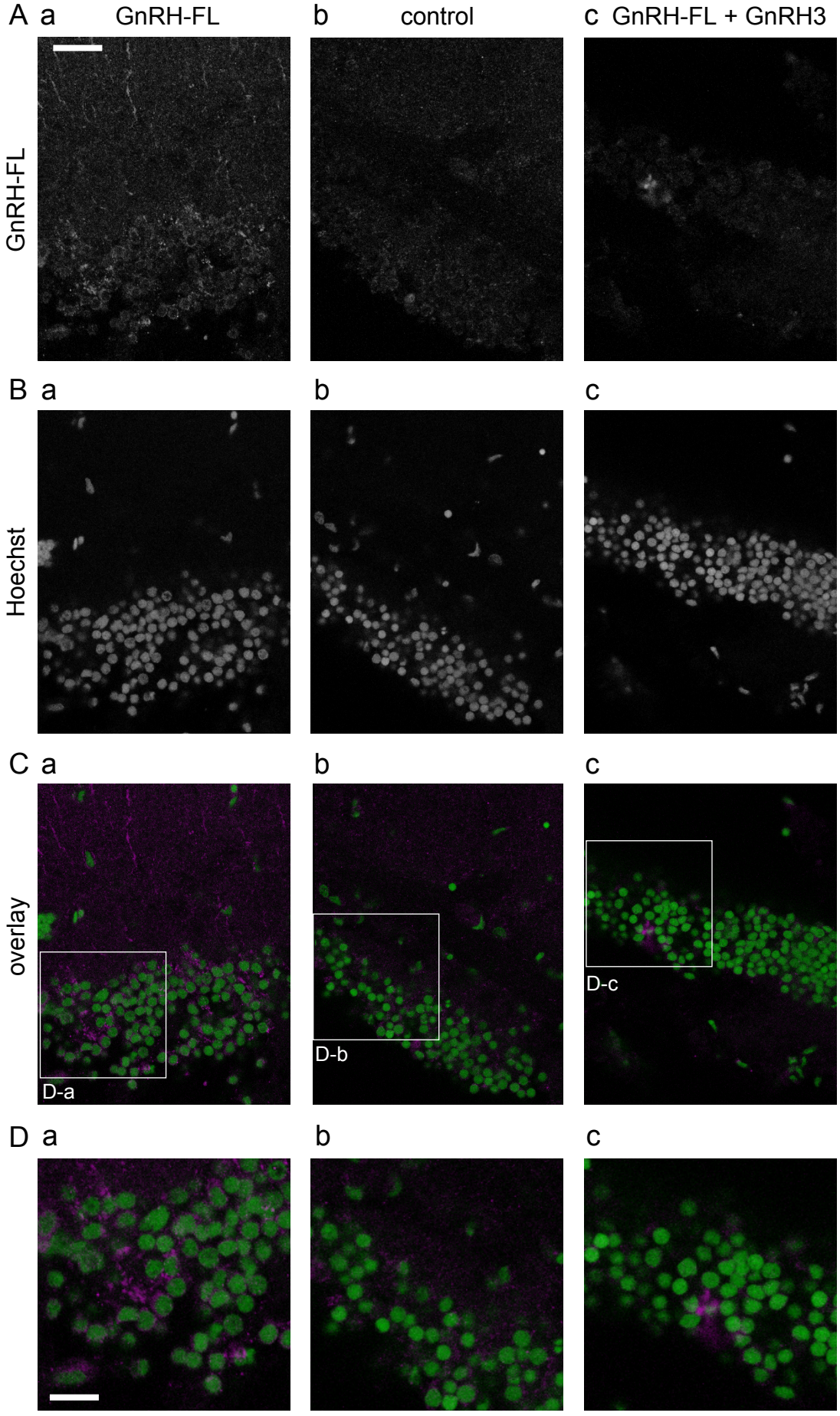
A a GnRH-FL
b control
c GnRH-FL + GnRH3
GnRH-FL
B a
b
c
Hoechst
C a
b
c
overlay
D-a
D-b
D-c
D a
b
c

Figure 3-8

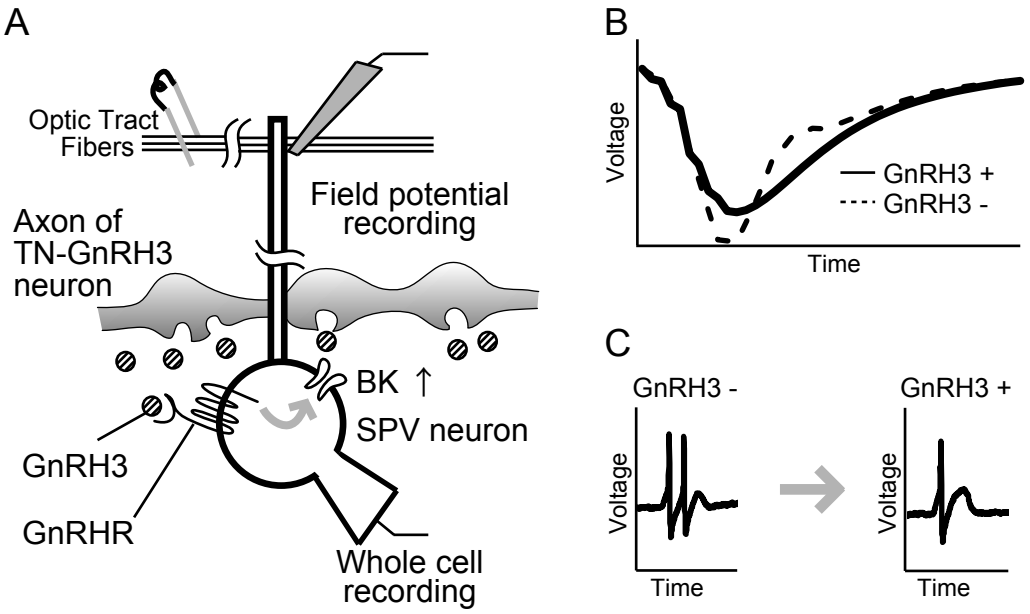
A
Optic Tract
Fibers
Field potential
recording
Axon of
TN-GnRH3
neuron
BK ↑
SPV neuron
GnRH3
GnRHR
Whole cell
recording
B
Voltage
GnRH3 +
GnRH3 -
Time
C
GnRH3 -
GnRH3 +
Voltage
Time
Voltage
Time

General discussion

In the present thesis, I aimed at comprehensive understanding of the mechanisms of neuromodulation by TN-GnRH3 neuron in the brain, which is considered to be one of the peptidergic neurons that can induce modulation of behaviors depending on the surrounding environment and the intrinsic physiological status. Here, I elucidated in Chapter 1 a novel modulator of TN-GnRH3 neurons and in Chapter 2 the relationship between firing activities and neuropeptide release of TN-GnRH3 neurons, which should give new insights into the general functions of modulatory peptidergic neurons. Finally, in Chapter 3 I showed mechanisms of neuromodulation in the optic tectum induced by GnRH3, which is considered to be released by the mechanism shown in Chapter 2.

Chapter 1: TN-GnRH3 neurons receive various neural inputs and change their spontaneous firing activities accordingly

In Chapter 1, I demonstrated by using electrophysiology that RFRP functions as a novel inhibitory synaptic modulator for the spontaneous pacemaker activity of TN-GnRH3 neurons, which is important for their neuromodulatory functions. Previous studies have shown that axons of RFRP neurons densely project to the TN-GnRH3 neurons (Matsumoto et al. 2006) and that TN-GnRH3 neurons express RFRP receptors (Yamamoto et al., unpublished). On the other hand, RFRP has been suggested to be released in response to stress (Kirby et al. 2009; Ubuka et al. 2015) and decrease sexual motivation (Johnson et al. 2007; Piekarski et al. 2013). Thus, RFRP-

induced modulation of the neuromodulatory TN-GnRH3 neurons may be important for the physiological responses such as stress-induced suppression of behavioral motivation. Moreover, the finding of a novel inhibitory synaptic modulator for TN-GnRH3 neurons is significant for understanding of functions of the peptidergic modulatory neurons because of the following reasons: cell bodies of TN-GnRH3 neurons form cluster, and these neural activities are electrically coupled to each other via gap junctions (Abe and Oka 2011; Karigo and Oka 2013), which may enable TN-GnRH3 neurons to modulate neurons in multiple target regions (neuromodulation) simultaneously by releasing GnRH3 in various brain regions at the same time. Because the firing frequency of peptidergic neurons is closely related to the neuropeptide release, the finding of RFRP-induced modulation of spontaneous activity of modulatory TN-GnRH3 neurons may give new insights into the understanding of the first step (inputs to the modulatory TN-GnRH3 neurons in Fig.4-2) during the process of adaptive regulation of behavior in response to the environment and the intrinsic physiological state of the animal.

Chapter 2: TN-GnRH3 neurons show high frequency firing in response to synaptic inputs, leading to neuropeptide release

In Chapter 2, I found that local puffer application of glutamate/$GABA_A$ receptor agonists, which mimics synaptic activation of TN-GnRH3 neurons, increases the frequency of their spontaneous firing activities. It is generally accepted that peptidergic neurons, including GnRH

neurons, have to fire at high frequency to release neuropeptides (Dutton and Dyball 1979; Liu et al. 2011). The present study showed that the firing frequency of the TN-GnRH3 neurons in response to the glutamate puffer application was almost the same as that reported to be necessary for the peptide release from the GnRH1 (hypophysiotropic GnRH) or Kisspeptin neurons *in vivo* (Campos and Herbison 2014; Han et al. 2015). In the present Ca^{2+} imaging analysis, local application of glutamate induced an increase in intracellular Ca^{2+}, which is suggested to trigger GnRH3 release. Taken together with previous literature (Abe and Oka 2000; Kawai et al. 2013; Kiya and Oka 2003; Nakane and Oka 2010; Umatani et al. 2013), the present Ca^{2+} imaging analysis strongly suggests that synaptic inputs via glutamate, among other various neurotransmitters and neuromodulators (shown in Fig. 4-1), is the most likely candidate to induce GnRH3 release *in vivo*. The other neurotransmitters and neuromodulators may play important roles in the regulation of low frequency regular pacemaker firing of TN-GnRH3 neurons, which may play a different role from the GnRH3 release (Karigo and Oka 2013). Because I analyzed GnRH-induced modulation in Chapter3, I would like to discuss functions of GnRH3 in the next section (see below).

In addition, I newly found that TN-GnRH3 neurons of juvenile medaka (before 10 weeks post-fertilization) were more likely to show burst firing than those of adult fish in a preliminary experiments of recording spontaneous activities. In the Ca^{2+} imaging analysis, I also found

occasional spontaneous intracellular Ca^{2+} increase like that observed during the local puffer application of glutamate. Previous studies on the TN-GnRH3 neurons have mainly focused on their neuromodulatory functions using adult animals, and there has been a very few studies using animals just after hatching (Ramakrishnan et al. 2010; Zhao et al. 2013). Ramakrishnan et al. suggested that some TN-GnRH3 neurons just after hatching showed burst firing and may release GnRH3 and affect projections of TN-GnRH3 neurons in an autocrine manner (Ramakrishnan et al. 2010). However, in juvenile, it has recently been reported that the projection of TN-GnRH3 neurons is almost completed in medaka (Takahashi et al. 2015). Thus, TN-GnRH3 neurons in juvenile fish may have different neuromodulatory functions from those in adult or may have other functions. This may be an interesting future topic for further study.

Chapter 3: GnRH3-induced neuromodulation of the retinotectal synaptic transmission is suggested to be important for the regulation of behaviorally-relevant sensory information processing

Effects of GnRH3 to brain regions where TN-GnRH3 neurons project remain to be studied in detail. In Chapter 3 I showed electrophysiologically and histologically that the TN-GnRH3 neurons modulate the retino-tectal neurotransmission, which is important for visual processing, by suppressing the excitability of projection neurons in the optic tectum. It is suggested that this neuromodulation is induced by GnRH3 that is considered to be released from TN-GnRH3 neurons when these neurons show high frequency firing as shown in Chapter 2. GnRH3 has also been

suggested to modulate other brain regions. In the olfactory bulb of the goldfish, GnRH3 modulates mitral cells and increases the release probability of their neurotransmitter (Kawai et al. 2010). In the olfactory receptor neurons of the axolotl, GnRH increases the magnitude of tetrodotoxin-sensitive inward current (Eisthen et al. 2000). Exogenous application of salmon type GnRH (GnRH3) decreases auditory-evoked spikes of neuron in the torus semicircularis and decreases response latency and increases auditory thresholds in a frequency and stimulus type-dependent manner (damselfish, Maruska and Tricas 2011). In the retinal circuit, GnRH agonist depolarizes horizontal cells and increases retinal responses to small light spots, whereas it decreases responses to full-field light (white perch, Umino and Dowling 1991). To my knowledge, the present results showed for the first time detailed GnRH3-induced neuromodulation in the optic tectum, which is an important brain region for visual information processing.

Behavioral significance

Previous anatomical and electrophysiological studies on neural inputs to the TN-GnRH3 neurons have suggested glutamatergic (Kiya and Oka 2003), GABAergic (Nakane and Oka 2010), and AChergic synaptic inputs (Kawai et al. 2013), which should serve as inputs for sensory information, arousal state, and so on to the TN-GnRH3 neurons (Fig. 4-1) (Oka and Matsushima 1993; Yamamoto and Ito 2000). Then, the TN-GnRH3 neurons are considered to integrate these neural inputs and change their firing activities depending on the sensory inputs of various

modalities from various brain regions. It should be noted that the TN-GnRH3 neurons also express estrogen receptors (Zempo et al. 2013) and may receive physiological information depending on the sex steroid hormones, although further studies are necessary to know the effect(s) of estrogen on these neurons. Because the firing activities of TN-GnRH3 neurons are suggested to be functionally related to GnRH3 release (Chapter 2), the neural inputs concerning various sensory information (olfactory, visual, somatosensory, etc.) and physiological status that are integrated in the TN-GnRH3 neurons are suggested to be translated to the release of GnRH3 peptides.

From the results of the present thesis focused on the peptidergic neuromodulatory system, the TN-GnRH3 neurons, I propose a working hypothesis as to their functional role in the integration of sensory information from the environment and the intrinsic physiological status of the animal, which leads to the adaptive changes in behaviors (Fig. 4-2).

Module 1) Environmental information and intrinsic physiological status of the animal are conveyed to the TN-GnRH3 neurons through neurotransmitters (Glu/GABA) and neuropeptides (RFRP).

Module 2) TN-GnRH3 neurons change their firing activities depending on such various neural inputs. Especially, glutamatergic synaptic inputs effectively induce high-frequency firing, sometimes bursting, of the TN-GnRH3 neurons, which effectively cause intracellular increase in

Ca^{2+} in the TN-GnRH3 neurons, leading to GnRH3 peptide release in the wide projection areas in the brain.

Module 3) Neuropeptides, which are released from TN-GnRH3 neurons in response to effective synaptic inputs such as glutamatergic ones, cause modulation of neurons in the target brain regions, such as the brain regions related to sensory processing (olfactory, visual, auditory, etc).

Module 4) These kinds of neuromodulations finally cause adaptive changes in animal behaviors via changing the behavioral pattern generator circuit.

Because the TN-GnRH3 neurons are reported to be conserved during evolution among wide variety of vertebrate species, I propose that the scheme illustrated in Fig. 4-2 may apply to various vertebrates in general.

Figure legends

Figure 4-1 Neurotransmitters and neuromodulators that affect spontaneous firing activities of TN-GnRH3 neurons.

Figure 4-2 Working hypothesis on the mechanism of modulation of behaviors by TN-GnRH3 neurons, depending on the sensory inputs from the environment and the intrinsic physiological status of the animal, suggested by the present thesis.

Figure 4-1

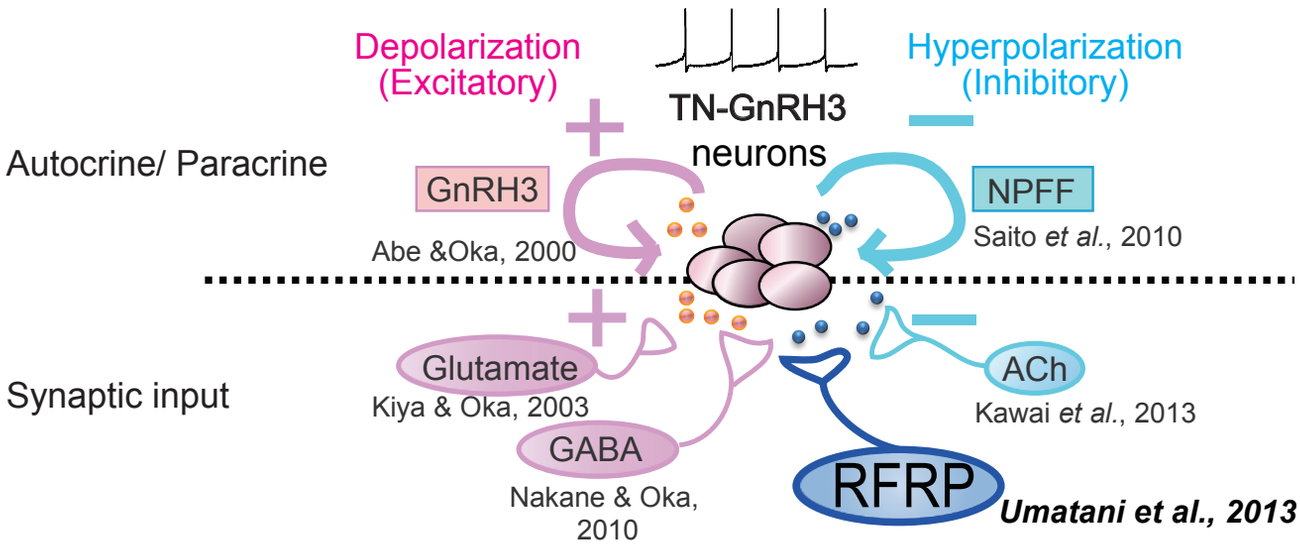
Depolarization
(Excitatory)
TN-GnRH3
neurons
Hyperpolarization
(Inhibitory)
Autocrine/ Paracrine
GnRH3
Abe &Oka, 2000
NPFF
Saito et al., 2010
Synaptic input
Glutamate
Kiya & Oka, 2003
GABA
Nakane & Oka,
2010
ACh
Kawai et al., 2013
RFRP
Umatani et al., 2013

Figure 4-2

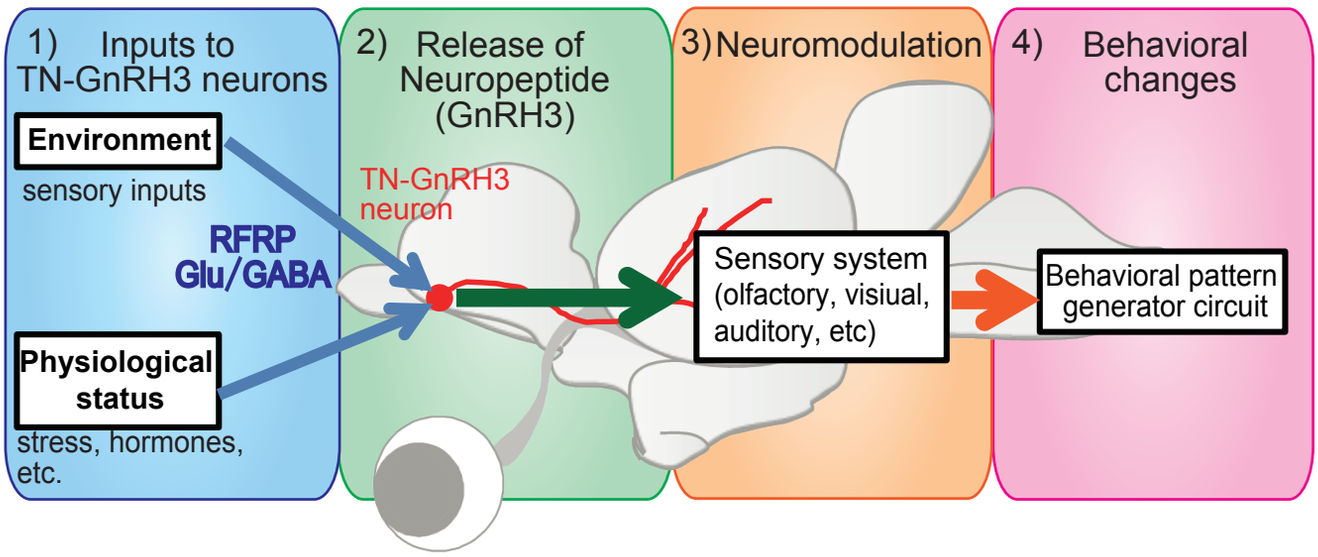
1) Inputs to TN-GnRH3 neurons
Environment
sensory inputs
RFRP
Glu/GABA
Physiological status
stress, hormones, etc.
2) Release of Neuropeptide (GnRH3)
TN-GnRH3 neuron
3) Neuromodulation
Sensory system (olfactory, visiual, auditory, etc)
4) Behavioral changes
Behavioral pattern generator circuit

Acknowledgements

I express deep appreciation for Professor Yoshitaka Oka, Laboratory of Biological Signaling, Department of Biological Sciences, Graduate School of Science, the University of Tokyo, for his constant guidance, encouragement, and valuable discussion. I also thank Dr. Hideki Abe, Min Kyun Park, Yasuhisa Akazome, Shinji Kanda (Graduate School of Science, the University of Tokyo), Kataaki Okubo (Graduate School of Agricultural and Life Sciences, the University of Tokyo) and Kazuhiko Yamaguchi (RIKEN BSI), for their instruction, discussion, and encouragement. I am thankful for Dr. Shinya Oishi and Ryosuke Misu, who gave me GnRH-fluoroprobes. I sincerely wish to thank Ms. Miho Kyokuwa for their technical assistance and animal care. I also thank the members of the Laboratory of Biological Signaling for their helpful support.

I sincerely thank Prof. Takeo Kubo and Kazuo Emoto (Graduate School of Science, the University of Tokyo), Assoc. Prof. Kataaki Okubo, Dr. Kazuhiko Yamaguchi, for critical reading of the present thesis and valuable discussion.

Finally, I am grateful to my family for mental and physical support.

This work was supported by Grants-in-Aid from the JSPS (25-8601).

References

Abe H, and Oka Y. Mechanisms of Neuromodulation by a Nonhypophysiotropic GnRH System Controlling Motivation of Reproductive Behavior in the Teleost Brain. *J Reprod Develop* 57: 665-674, 2011.

Abe H, and Oka Y. Mechanisms of the modulation of pacemaker activity by GnRH peptides in the terminal nerve-GnRH neurons. *Zoolog Sci* 19: 111-128, 2002.

Abe H, and Oka Y. Modulation of pacemaker activity by salmon gonadotropin-releasing hormone (sGnRH) in terminal nerve (TN)-GnRH neurons. *Journal of neurophysiology* 83: 3196-3200, 2000.

Abe H, and Oka Y. Neuromodulatory Functions of Terminal Nerve - GnRH Neurons. In: *Fish Physiology*Academic Press, 2006, p. 455-503.

Abe H, and Oka Y. Primary Culture of the Isolated Terminal Nerve-Gonadotrophin-Releasing Hormone Neurones Derived From Adult Teleost (Dwarf Gourami, Colisa lalia) Brain For the Study of Peptide Release Mechanisms. *J Neuroendocrinol* 21: 489-505, 2009.

Adams PR, and Brown DA. Luteinizing hormone-releasing factor and muscarinic agonists act on the same voltage-sensitive K+-current in bullfrog sympathetic neurones. *Br J Pharmacol* 68: 353-355, 1980.

Amano M, Oka Y, Yamanome T, Okuzawa K, and Yamamori K. Three GnRH systems in the brain and pituitary of a pleuronectiform fish, the barfin flounder Verasper moseri. *Cell Tissue Res* 309: 323-329, 2002.

Argiolas A, and Melis MR. Neuropeptides and central control of sexual behaviour from the past to the present: a review. *Prog Neurobiol* 108: 80-107, 2013.

Arias-Garcia MA, Tapia D, Flores-Barrera E, Perez-Ortega JE, Bargas J, and Galarraga E. Duration differences of corticostriatal responses in striatal projection neurons depend on calcium activated potassium currents. *Front Syst Neurosci* 7: 63, 2013.

Brown D. M-currents: an update. *Trends Neurosci* 11: 294-299, 1988.

Butler AB, and Hodos W. *Comparative Vertebrate Neuroanatomy: Evolution and Adaptation*. Wiley, 1996.

Calisi RM, Rizzo NO, and Bentley GE. Seasonal differences in hypothalamic EGR-1 and GnIH expression following capture-handling stress in house sparrows (Passer domesticus). *General and comparative endocrinology* 157: 283-287, 2008.

Campos P, and Herbison AE. Optogenetic activation of GnRH neurons reveals minimal requirements for pulsatile luteinizing hormone secretion. *Proc Natl Acad Sci U S A* 111: 18387-18392, 2014.

Champney TF, Sahley TL, and Sandman CA. Effects of neonatal cerebral ventricular injection of ACTH 4-9 and subsequent adult injections on learning in male and female albino rats. *Pharmacol Biochem Behav* 5: 3-9, 1976.

de Kloet ER, Joels M, and Holsboer F. Stress and the brain: from adaptation to disease. *Nature reviews Neuroscience* 6: 463-475, 2005.

Dornan WA, and Malsbury CW. Neuropeptides and male sexual behavior. *Neurosci Biobehav Rev* 13: 1-15, 1989.

Ducret E, Anderson GM, and Herbison AE. RFamide-Related Peptide-3, a Mammalian Gonadotropin-Inhibitory Hormone Ortholog, Regulates Gonadotropin-Releasing Hormone Neuron Firing in the Mouse. *Endocrinology* 150: 2799-2804, 2009.

Dutton A, and Dyball RE. Phasic firing enhances vasopressin release from the rat neurohypophysis. *J Physiol* 290: 433-440, 1979.

Eisthen HL, Delay RJ, Wirsig-Wiechmann CR, and Dionne VE. Neuromodulatory effects of gonadotropin releasing hormone on olfactory receptor neurons. *J Neurosci* 20: 3947-3955, 2000.

Finlay BL, Schneps SE, Wilson KG, and Schneider GE. Topography of visual and somatosensory projections to the superior colliculus of the golden hamster. *Brain Res* 142: 223-235, 1978.

Fukusumi S, Fujii R, and Hinuma S. Recent advances in mammalian RFamide peptides: the discovery and functional analyses of PrRP, RFRPs and QRFP. *Peptides* 27: 1073-1086, 2006.

Gouarderes C, Tafani JA, Mazarguil H, and Zajac JM. Autoradiographic characterization of rat spinal neuropeptide FF receptors by using [125I][D.Tyr1, (NMe)Phe3]NPFF. *Brain research bulletin* 42: 231-238, 1997.

Grillner S, Deliagina T, Ekeberg O, el Manira A, Hill RH, Lansner A, Orlovsky GN, and Wallen P. Neural networks that co-ordinate locomotion and body orientation in lamprey. *Trends Neurosci* 18: 270-279, 1995.

Han SY, McLennan T, Czieselsky K, and Herbison AE. Selective optogenetic activation of arcuate kisspeptin neurons generates pulsatile luteinizing hormone secretion. *Proc Natl Acad Sci U S A* 112: 13109-13114, 2015.

Hazum E, Cuatrecasas P, Marian J, and Conn PM. Receptor-mediated internalization of fluorescent gonadotropin-releasing hormone by pituitary gonadotropes. *Proc Natl Acad Sci U S A* 77: 6692-6695, 1980.

Hazum E, and Nimrod A. Photoaffinity-labeling and fluorescence-distribution studies of gonadotropin-releasing hormone receptors in ovarian granulosa cells. *Proc Natl Acad Sci U S A* 79: 1747-1750, 1982.

Herbison AE, and Moenter SM. Depolarising and hyperpolarising actions of GABA(A) receptor activation on gonadotrophin-releasing hormone neurones: towards an emerging consensus. *J Neuroendocrinol* 23: 557-569, 2011.

Hinuma S, Shintani Y, Fukusumi S, Iijima N, Matsumoto Y, Hosoya M, Fujii R, Watanabe T, Kikuchi K, Terao Y, Yano T, Yamamoto T, Kawamata Y, Habata Y, Asada M, Kitada C, Kurokawa T, Onda H, Nishimura O, Tanaka M, Ibata Y, and Fujino M. New neuropeptides containing carboxy-terminal RFamide and their receptor in mammals. *Nat Cell Biol* 2: 703-708, 2000.

Honore E. The neuronal background K2P channels: focus on TREK1. *Nature reviews Neuroscience* 8: 251-261, 2007.

Illing N, Troskie BE, Nahorniak CS, Hapgood JP, Peter RE, and Millar RP. Two gonadotropin-releasing hormone receptor subtypes with distinct ligand selectivity and differential distribution in brain and pituitary in the goldfish (Carassius auratus). *Proc Natl Acad Sci U S A* 96: 2526-2531, 1999.

Ishizaki M, Iigo M, Yamamoto N, and Oka Y. Different modes of gonadotropin-releasing hormone (GnRH) release from multiple GnRH systems as revealed by radioimmunoassay using brain slices of a teleost, the dwarf gourami (Colisa lalia). *Endocrinology* 145: 2092-2103, 2004.

Iwamatsu T. *The integrated book for the biology of Medaka*. Okayama: Uniiversity education press Co., Ltd., 2006.

Johnson MA, Tsutsui K, and Fraley GS. Rat RFamide-related peptide-3 stimulates GH secretion, inhibits LH secretion, and has variable effects on sex behavior in the adult male rat. *Hormones and behavior* 51: 171-180, 2007.

Karigo T, Aikawa M, Kondo C, Abe H, Kanda S, and Oka Y. Whole brain-pituitary in vitro preparation of the transgenic medaka (Oryzias latipes) as a tool for analyzing the differential regulatory mechanisms of LH and FSH release. *Endocrinology* 155: 536-547, 2014.

Karigo T, and Oka Y. Neurobiological study of fish brains gives insights into the nature of gonadotropin-releasing hormone 1-3 neurons. *Front Endocrinol (Lausanne)* 4: 177, 2013.

Karten HJ, and Shimizu T. The origins of neocortex: connections and lamination as distinct events in evolution. *J Cogn Neurosci* 1: 291-301, 1989.

Kawai T, Abe H, Akazome Y, and Oka Y. Neuromodulatory effect of GnRH on the synaptic transmission of the olfactory bulbar neural circuit in goldfish, Carassius auratus. *Journal of neurophysiology* 104: 3540-3550, 2010.

Kawai T, Abe H, and Oka Y. Burst generation mediated by cholinergic input in terminal nerve-gonadotrophin releasing hormone neurones of the goldfish. *J Physiol* 591: 5509-5523, 2013.

Kinoshita M, Fukaya M, Tojima T, Kojima S, Ando H, Watanabe M, Urano A, and Ito E. Retinotectal transmission in the optic tectum of rainbow trout. *J Comp Neurol* 484: 249-259, 2005.

Kinoshita M, and Ito E. Roles of periventricular neurons in retinotectal transmission in the optic tectum. *Prog Neurobiol* 79: 112-121, 2006.

Kinoshita M, Kobayashi S, Urano A, and Ito E. Neuromodulatory effects of gonadotropin-releasing hormone on retinotectal synaptic transmission in the optic tectum of rainbow trout. *Eur J Neurosci* 25: 480-484, 2007.

Kinoshita M, Murata K, Naruse K, and Tanaka M. *Medaka: Biology, Management, and Experimental Protocols*. Wiley, 2009.

Kirby ED, Geraghty AC, Ubuka T, Bentley GE, and Kaufer D. Stress increases putative gonadotropin inhibitory hormone and decreases luteinizing hormone in male rats. *Proc Natl Acad Sci U S A* 106: 11324-11329, 2009.

Kiya T, and Oka Y. Glutamate receptors in the terminal nerve gonadotropin-releasing hormone neurons of the dwarf gourami (teleost). *Neurosci Lett* 345: 113-116, 2003.

Kriegsfeld LJ, Mei DF, Bentley GE, Ubuka T, Mason AO, Inoue K, Ukena K, Tsutsui K, and Silver R. Identification and characterization of a gonadotropin-inhibitory system in the brains of mammals. *Proc Natl Acad Sci U S A* 103: 2410-2415, 2006.

Kurt S, Sausbier M, Ruttiger L, Brandt N, Moeller CK, Kindler J, Sausbier U, Zimmermann U, van Straaten H, Neuhuber W, Engel J, Knipper M, Ruth P, and Schulze H. Critical role for cochlear hair cell BK channels for coding the temporal structure and dynamic range of auditory information for central auditory processing. *FASEB J* 26: 3834-3843, 2012.

Lesage F. Pharmacology of neuronal background potassium channels. *Neuropharmacology* 44:

1-7, 2003.

Liu X, Porteous R, d'Anglemont de Tassigny X, Colledge WH, Millar R, Petersen SL, and Herbison AE. Frequency-dependent recruitment of fast amino acid and slow neuropeptide neurotransmitter release controls gonadotropin-releasing hormone neuron excitability. *J Neurosci* 31: 2421-2430, 2011.

Llinas R, and Precht W. *Frog Neurobiology: A Handbook*. Springer Berlin Heidelberg, 2012.

Lloyd JM, and Childs GV. Changes in the number of GnRH-receptive cells during the rat estrous cycle: biphasic effects of estradiol. *Neuroendocrinology* 48: 138-146, 1988.

Maaswinkel H, and Li L. Olfactory input increases visual sensitivity in zebrafish: a possible function for the terminal nerve and dopaminergic interplexiform cells. *J Exp Biol* 206: 2201-2209, 2003.

Maruska KP, and Tricas TC. Gonadotropin-releasing hormone (GnRH) modulates auditory processing in the fish brain. *Hormones and behavior* 59: 451-464, 2011.

Maruska KP, and Tricas TC. Gonadotropin-releasing hormone and receptor distributions in the visual processing regions of four coral reef fishes. *Brain Behav Evol* 70: 40-56, 2007.

Matsumoto S, Yamamoto N, Akazome Y, Yamada S, Tsukamura H, Maeda K, and Oka Y. Possible novel function of metastin neurons as dual neuromodulators in the vertebrate brain. *Program of the 36th Annual Meeting of The Society for Neuroscience* Atlanta, GA, p. 658.656, 2006.

Moenter SM, DeFazio AR, Pitts GR, and Nunemaker CS. Mechanisms underlying episodic gonadotropin-releasing hormone secretion. *Frontiers in neuroendocrinology* 24: 79-93, 2003.

Mollereau C, Mazarguil H, Marcus D, Quelven I, Kotani M, Lannoy V, Dumont Y, Quirion R, Detheux M, Parmentier M, and Zajac JM. Pharmacological characterization of human NPFF(1) and NPFF(2) receptors expressed in CHO cells by using NPY Y(1) receptor antagonists. *European journal of pharmacology* 451: 245-256, 2002.

Nakane R, and Oka Y. Excitatory action of GABA in the terminal nerve gonadotropin-releasing hormone neurons. *Journal of neurophysiology* 103: 1375-1384, 2010.

Naor Z, Shacham S, Harris D, Seger R, and Reiss N. Signal transduction of the gonadotropin releasing hormone (GnRH) receptor: cross-talk of calcium, protein kinase C (PKC), and arachidonic acid. *Cell Mol Neurobiol* 15: 527-544, 1995.

Northmore DP, and Gallagher SP. Functional relationship between nucleus isthmi and tectum

in teleosts: synchrony but no topography. *Vis Neurosci* 20: 335-348, 2003.

Oishi S, Masuda R, Evans B, Ueda S, Goto Y, Ohno H, Hirasawa A, Tsujimoto G, Wang Z, Peiper SC, Naito T, Kodama E, Matsuoka M, and Fujii N. Synthesis and application of fluorescein- and biotin-labeled molecular probes for the chemokine receptor CXCR4. *Chembiochem* 9: 1154-1158, 2008.

Oka Y. Physiology and release activity of GnRH neurons. *Progress in brain research* 141: 259-281, 2002.

Oka Y, and Ichikawa M. Gonadotropin-releasing hormone (GnRH) immunoreactive system in the brain of the dwarf gourami (Colisa lalia) as revealed by light microscopic immunocytochemistry using a monoclonal antibody to common amino acid sequence of GnRH. *J Comp Neurol* 300: 511-522, 1990.

Oka Y, and Ichikawa M. Ultrastructure of the ganglion cells of the terminal nerve in the dwarf gourami (Colisa lalia). *J Comp Neurol* 304: 161-171, 1991.

Oka Y, and Matsushima T. Gonadotropin-Releasing-Hormone (Gnrh) Immunoreactive Terminal Nerve-Cells Have Intrinsic Rhythmicity and Project Widely in the Brain. *J Neurosci* 13: 2161-2176, 1993.

Okubo K, Ishii S, Ishida J, Mitani H, Naruse K, Kondo M, Shima A, Tanaka M, Asakawa S, Shimizu N, and Aida K. A novel third gonadotropin-releasing hormone receptor in the medaka Oryzias latipes: evolutionary and functional implications. *Gene* 314: 121-131, 2003.

Okubo K, Nagata S, Ko R, Kataoka H, Yoshiura Y, Mitani H, Kondo M, Naruse K, Shima A, and Aida K. Identification and characterization of two distinct GnRH receptor subtypes in a teleost, the medaka Oryzias latipes. *Endocrinology* 142: 4729-4739, 2001.

Peng YY, and Zucker RS. Release of LHRH is linearly related to the time integral of presynaptic Ca2+ elevation above a threshold level in bullfrog sympathetic ganglia. *Neuron* 10: 465-473, 1993.

Piekarski DJ, Zhao S, Jennings KJ, Iwasa T, Legan SJ, Mikkelsen JD, Tsutsui K, and Kriegsfeld LJ. Gonadotropin-inhibitory hormone reduces sexual motivation but not lordosis behavior in female Syrian hamsters (Mesocricetus auratus). *Hormones and behavior* 64: 501-510, 2013.

Qiu J, Fang Y, Rnnekleiv OK, and Kelly MJ. Leptin Excites Proopiomelanocortin Neurons via Activation of TRPC Channels. *J Neurosci* 30: 1560-1565, 2010.

Rall W, and Shepherd GM. Theoretical reconstruction of field potentials and dendrodendritic

synaptic interactions in olfactory bulb. *Journal of neurophysiology* 31: 884-915, 1968.

Ramakrishnan S, Lee W, Navarre S, Kozlowski DJ, and Wayne NL. Acquisition of spontaneous electrical activity during embryonic development of gonadotropin-releasing hormone-3 neurons located in the terminal nerve of transgenic zebrafish (Danio rerio). *General and comparative endocrinology* 168: 401-407, 2010.

Ramakrishnan S, and Wayne NL. Social cues from conspecifics alter electrical activity of gonadotropin-releasing hormone neurons in the terminal nerve via visual signals. *American journal of physiology Regulatory, integrative and comparative physiology* 297: R135-141, 2009.

Rasolonjanahary R, Gerard C, Dufour MN, Homburger V, Enjalbert A, and Guillon G. Evidence for a direct negative coupling between dopamine-D2 receptors and PLC by heterotrimeric Gi1/2 proteins in rat anterior pituitary cell membranes. *Endocrinology* 143: 747-754, 2002.

Roumy M, and Zajac JM. Neuropeptide FF, pain and analgesia. *European journal of pharmacology* 345: 1-11, 1998.

Saito TH, Nakane R, Akazome Y, Abe H, and Oka Y. Electrophysiological Analysis of the Inhibitory Effects of FMRFamide-Like Peptides on the Pacemaker Activity of Gonadotropin-Releasing Hormone Neurons. *Journal of neurophysiology* 104: 3518-3529, 2010.

Seo HS, Roidl E, Muller F, and Negoias S. Odors enhance visual attention to congruent objects. *Appetite* 54: 544-549, 2010.

Sikdar SK, McIntosh RP, and Mason WT. Differential modulation of Ca2+-activated K+ channels in ovine pituitary gonadotrophs by GnRH, Ca2+ and cyclic AMP. *Brain Res* 496: 113-123, 1989.

Simonin F, Schmitt M, Laulin JP, Laboureyras E, Jhamandas JH, MacTavish D, Matifas A, Mollereau C, Laurent P, Parmentier M, Kieffer BL, Bourguignon JJ, and Simonnet G. RF9, a potent and selective neuropeptide FF receptor antagonist, prevents opioid-induced tolerance associated with hyperalgesia. *P Natl Acad Sci USA* 103: 466-471, 2006.

Stephenson JF, Partridge JC, and Whitlock KE. Food and conspecific chemical cues modify visual behavior of zebrafish, Danio rerio. *Zebrafish* 9: 68-73, 2012.

Stojilkovic SS, Krsmanovic LZ, Spergel DJ, and Catt KJ. Gonadotropin-releasing hormone neurons: intrinsic pulsatility and receptor-mediated regulation. *Trends Endocrinol Metab* 5: 201-209, 1994a.

Stojilkovic SS, Reinhart J, and Catt KJ. Gonadotropin-releasing hormone receptors: structure and signal transduction pathways. *Endocr Rev* 15: 462-499, 1994b.

Sun Q, and Dale N. Developmental changes in expression of ion currents accompany maturation of locomotor pattern in frog tadpoles. *J Physiol* 507 (Pt 1): 257-264, 1998.

Takahashi A, Islam MS, Abe H, Okubo K, Akazome Y, Kaneko T, Hioki H, and Oka Y. Morphological analysis of the early development of telencephalic and diencephalic gonadotropin-releasing hormone neuronal systems in enhanced green fluorescent protein-expressing transgenic medaka lines. *J Comp Neurol* 2015.

Tsutsui K, Saigoh E, Ukena K, Teranishi H, Fujisawa Y, Kikuchi M, Ishii S, and Sharp JP. A novel avian hypothalamic peptide inhibiting gonadotropin release. *Biochem Bioph Res Co* 275: 661-667, 2000.

Ubuka T, Son YL, and Tsutsui K. Molecular, cellular, morphological, physiological and behavioral aspects of gonadotropin-inhibitory hormone. *General and comparative endocrinology* 2015.

Umatani C, Abe H, and Oka Y. Neuropeptide RFRP inhibits the pacemaker activity of terminal nerve GnRH neurons. *Journal of neurophysiology* 109: 2354-2363, 2013.

Umino O, and Dowling JE. Dopamine release from interplexiform cells in the retina: effects of GnRH, FMRFamide, bicuculline, and enkephalin on horizontal cell activity. *J Neurosci* 11: 3034-3046, 1991.

van den Pol AN. Neuropeptide transmission in brain circuits. *Neuron* 76: 98-115, 2012.

Vanegas H. Basic relationships for visual information processing in optic tectum of fish. *Acta Cient Venez* 25: 98-106, 1974.

Vanegas H, Amat J, and Essayag-Millan E. Postsynaptic phenomena in optic tectum neurons following optic nerve stimulation in fish. *Brain Res* 77: 25-38, 1974a.

Vanegas H, Essayag-Millan E, and Laufer M. Response of the optic tectum to stimulation of the optic nerve in the teleost Eugerres plumieri. *Brain Res* 31: 107-118, 1971.

Vanegas H, Laufer M, and Amat J. The optic tectum of a perciform teleost. I. General configuration and cytoarchitecture. *J Comp Neurol* 154: 43-60, 1974b.

Vanegus H. Organization and physiology of the teleostean optic tectum. In: *Fish Neurobiology: vol 2 Higher Brain Areas and Functions*, edited by Northcutt RG, and Davis RE. Michigan: University of Michigan Press, 1983.

von Bartheld CS, and Meyer DL. Comparative neurology of the optic tectum in ray-finned fishes: patterns of lamination formed by retinotectal projections. *Brain Res* 420: 277-288, 1987.

von Bartheld CS, and Meyer DL. Tracing of single fibers of the nervus terminalis in the goldfish brain. *Cell Tissue Res* 245: 143-158, 1986.

Wallen P, and Grillner S. N-methyl-D-aspartate receptor-induced, inherent oscillatory activity in neurons active during fictive locomotion in the lamprey. *J Neurosci* 7: 2745-2755, 1987.

Waring DW, and Turgeon JL. Ca2+-activated K+ channels in gonadotropin-releasing hormone-stimulated mouse gonadotrophs. *Endocrinology* 150: 2264-2272, 2009.

Watanabe M, Fukuda A, and Nabekura J. The role of GABA in the regulation of GnRH neurons. *Frontiers in neuroscience* 8: 387, 2014.

Watkins DC, Moxham CM, Morris AJ, and Malbon CC. Suppression of Gi alpha 2 enhances phospholipase C signalling. *The Biochemical journal* 299 (Pt 3): 593-596, 1994.

Wirsig-Wiechmann CR, and Oka Y. The terminal nerve ganglion cells project to the olfactory mucosa in the dwarf gourami. *Neurosci Res* 44: 337-341, 2002.

Xiao Z, Deng PY, Rojanathammanee L, Yang C, Grisanti L, Permpoonputtana K, Weinshenker D, Doze VA, Porter JE, and Lei S. Noradrenergic depression of neuronal excitability in the entorhinal cortex via activation of TREK-2 K+ channels. *The Journal of biological chemistry* 284: 10980-10991, 2009.

Yamamoto N, and Ito H. Afferent sources to the ganglion of the terminal nerve in teleosts. *J Comp Neurol* 428: 355-375, 2000.

Yamamoto N, Oka Y, and Kawashima S. Lesions of gonadotropin-releasing hormone-immunoreactive terminal nerve cells: effects on the reproductive behavior of male dwarf gouramis. *Neuroendocrinology* 65: 403-412, 1997.

Yang SN, Lu F, Wu JN, Liu DD, and Hsieh WY. Activation of gonadotropin-releasing hormone receptors induces a long-term enhancement of excitatory postsynaptic currents mediated by ionotropic glutamate receptors in the rat hippocampus. *Neurosci Lett* 260: 33-36, 1999.

Zempo B, Kanda S, Okubo K, Akazome Y, and Oka Y. Anatomical distribution of sex steroid hormone receptors in the brain of female medaka. *J Comp Neurol* 521: 1760-1780, 2013.

Zeng ZZ, McDonald TP, Wang RP, Liu QY, and Austin CP. Neuropeptide FF receptor 2 (NPFF2) is localized to pain-processing regions in the primate spinal of the medulla cord and the lower level oblongata. *J Chem Neuroanat* 25: 269-278, 2003.

Zhang P, Yang C, and Delay RJ. Urine stimulation activates BK channels in mouse vomeronasal neurons. *Journal of neurophysiology* 100: 1824-1834, 2008.

Zhao Y, Lin MC, Farajzadeh M, and Wayne NL. Early development of the gonadotropin-releasing hormone neuronal network in transgenic zebrafish. *Front Endocrinol (Lausanne)* 4: 107, 2013.